Exploring vegetation type, diversity, and carbon stocks in Sundarbans Reserved Forest using high resolution image and inventory data

Md. Mizanur Rahman

2019

Table of contents

Summary

With global climate change, the conservation of mangrove biodiversity and the evaluation of ecosystem services (carbon sequestration) have become foci of concern. This thesis examined the spatial distribution of biodiversity indicators and carbon storage in the Sundarbans Reserved Forest (SRF), Bangladesh, the most diverse mangrove ecosystem worldwide, and modelled their relationship by coupling remote sensing and ground-based data. Carbon storage in the SRF varied by vegetation type and salinity zone. Stands dominated by *Heritiera fomes* within the freshwater zone contained the largest carbon stock (Chapter three). Nine dominant mangrove types with their average canopy height and five non-mangrove types in the Sundarbans East Wildlife Sanctuary (SEWS), as pioneers of large-scale mangrove ecosystems, were mapped with greater accuracy (89.33–89.89%) by combining high-resolution spatial (WorldView2) and vertical (TanDEM-X) imagery (Chapter four). Three dominant species covered 50% of the SEWS: *H. fomes* (44.54%), *Excoecaria agallocha* (3.02%), and *Sonneratia apetala* (1.41%). The finding of *H. fomes* as the dominant species in the SEWS (Chapter four) challenged the previous conclusion that *E. agallocha* was the dominant species. Mangrove species diversity (Shannon index) and canopy height positively influenced the aboveground carbon stock in trunks. Therefore, mangrove stands with high species diversity had high carbon storage (Chapter five). These findings can be used in the monitoring and evaluation of mangrove vegetation and carbon stock changes and formulating policy for Reducing Emissions from Deforestation and Forest Degradation and the Convention on Biological Diversity.

Chapter 1 General Introduction

Mangroves in changing climate

Mangroves refer to the forests found in sheltered coastal zones between the land and sea, of tropical and subtropical countries (Ellison and Zouh, 2012). This unique forest ecosystem has been found in around 120 countries and its total coverage is 83,495 km^2 which represent about 0.1% of the Earth's continental surface (Atwood et al., 2017; Hamilton and Casey, 2016; Kauffman et al., 2014). A total of 70 mangrove species are found globally and these mangrove plants develop specialized morphological and physiological mechanisms to adapt in the adverse costal environment (Kathiresan and Bingham, 2001). Historically, mangrove ecosystems provide various ecosystem services to communities with the economic value estimated to the USD 4185 per hectare per year. But substantial spatial and temporal variations in this value are expected (Friess, 2016). These ecosystem services can be categorized as 4 terms: 1) provisioning services such as food, fuel wood, household materials, sources of traditional and allopathic medicinal materials, and other non-timber forest products (Friess, 2016; Uddin et al., 2013; Walters et al., 2008), 2) regulatory service such as providing protection against tidal surge, tsunami and hurricanes. Mangroves capture and store atmospheric carbon on the ground (Alongi, 2008; Cahoon, 2006; Donato et al., 2011; Komiyama et al., 2008; Pendleton et al., 2012), 3) supportive service of providing breeding ground for diverse flora and fauna both in land and waterbody (Kathiresan and Bingham, 2001), and 4) cultural services, for example, eco-tourism, worship, and educational research (Friess, 2016; Uddin et al., 2013).

Despite these multiple ecosystem services, global mangrove forests have been disappearing and degraded in the last half-century because of anthropogenic activities such as urbanization, agricultural expansion, overharvesting, and upstream fresh water diversion as well as climate changes (Giri et al., 2011; Iftekhar and Islam, 2004; Thomas et al., 2017). Rapid sea-level rise caused by global warming in the twenty-first century has also been cited as a primary threat to mangroves (Ellison, 2015). Due to the rapid rising of sea level, mangrove ecosystem structure would change in terms of reduction of sedimentation rate, increased salinity level, and land erosion which would cumulatively affect the vegetation structure and forest health (dieback of tree, seaward to landward migration of species (Ellison, 2015; Ward et al., 2016). This would result in reduction of forest productivity or complete loss of the mangroves and thereby reduction of carbon sequestration or emission of CO_2 from mangrove ecosystem (Ellison et al., 2005; Pendleton et al., 2012; Woodroffe et al., 2016). As the above-

mentioned causes alter mangrove ecosystem species composition, vegetation dynamics and function, it is imperative to continue monitoring of the mangrove ecosystem for better management.

Mangroves are one of the most productive ecosystems that can sequester atmospheric carbon at a 4 to 7 times higher rate than other tropical forest ecosystems (Donato et al., 2011). Carbon in this ecosystem is stored as aboveground biomass of plant parts (tree trunks, stems and leaves), belowground root system biomass, and as soil organic carbon (Laffoley and Grimsditch, 2009). The global average of mangrove carbon stocks are about 937 t C ha^{-1} , most of which are deposited in soil (Alongi, 2012; Atwood et al., 2017). So, if the mangrove forest is altered to other land uses or changed by the climate change it will become a huge source of greenhouse gases to atmosphere (Atwood et al., 2017). Given this large carbon reserve in the mangroves, other ecosystem services it provides, and its vulnerability to anthropogenic and natural disturbances, protection of mangrove through REDD+ (Reduce emission from deforestation and Forest Degradation) could be a key to conserve the mangrove forest and thereby to mitigate and adapt to the climate change (Herr et al., 2017).

Influence of mangrove zonation on carbon stock

Estimation of spatial distribution of the mangrove is now becoming a fundamental issue for sustainable forest management and conversation of forest resources under the changing global climate (Trettin et al., 2016). Mangrove stands are the part of dynamic coastal ecosystem where different environmental attributes such as topography, climatic conditions, tidal inundation, salinity, geomorphology affect the species distribution and composition (Cruz et al., 2013; Fromard et al., 1998). In response to these factors, mangrove species show a distinctive pattern of zones which leads to spatial variation of species composition, forest structure and productivity and thereby affect their carbon stock capacity (Adame et al., 2013; Ball, 2002; Cruz et al., 2013; Fromard et al., 1998; Twilley and Chen, 1998; Wang et al., 2014). A recent study in Brazil shows that the distribution of *Rhizophora mangle* and *Avicennia germinans* species across an inundation gradient reflects the combined effect of tidal inundation frequency, availability of phosphorus in the sediments and the leaves, and interstitial salinity (Cruz et al., 2013). In Rookery Bay, Florida, Twilley and Chen (1998), found that there was a prominent tradeoff between salinity and distribution of species, and their productivity and growth of mangrove forests. In Bangladesh, Karim and Karim (1993)

investigated two prominent species, *Heritiera forms* and *Avicennia marina* and found that they produced higher biomass at low saline condition than at high saline condition.

Carbon stocks in mangrove ecosystem vary depending on species composition, structure and salinity. In Maxico, Adame et al. (2013), found that higher carbon stocks were associated with law saline areas which is dominant by *Laguncularia racemosa* compared to high saline areas where dwarf mangrove was dominant. In Indian Sundarbans, Mitra et al., (2011), conducted a study on biomass carbon stocks for the three-dominant species, (*Sonneratia apetala*, *Avicennia alba* and *Excoecaria agallocha*). They found that S. *apetala* contained higher level of carbon than other two species. They also inferred that the variation of carbon stocks among the three species was due to the salinity gradient. Even the same species had different carbon stocks depending on the spatial position in Indian Sundarbans (Mitra et al., (2011). The spatial variation in distribution of species, vegetation biomass, and soil organic carbon (SOC) stocks were also found in estuary mangrove in Yingluo Bay, South China (Wang et al., 2014). In that study, they found that both biomass- and soil organic -carbon varied due to topographic variation from upstream to downstream (Wang et al., 2014). SOC stock in mangrove ecosystem, is also influenced by aboveground vegetation, salinity, and tidal elevation (Wang et al., 2014). In Indonesian mangrove forests, Murdiyarso et al. (2010), also found that soil carbon stocks were in association with higher stature of aboveground vegetation. Though a clear zonation exists in Sundarbans Reserved Forest (SRF) with regard to vegetation types and salinity gradient, its effect on carbon stock is still unexplored (Iftekhar and Saenger, 2008).

Remote sensing of mangrove vegetation and structure

Remote sensing is an important method to monitor the earth's surface (Heumann, 2011; Kuenzer et al., 2011). Regular monitoring of tree species, their spatial information on the distribution, composition etc. are the key forest management components for valuation of forest reservation outcome as it has some special targets on protection and conservation of certain inhabiting tree or animal species or to monitor health status of individual trees (Heumann, 2011; Kuenzer et al., 2011; O'Connor et al., 2015; Pereira et al., 2013; Petrou et al., 2015). In inaccessible areas where field surveying is difficult such in many mangrove ecosystems, remote sensing can be a surrogate to field inventory (Kamal and Phinn, 2011). The recent development of both active (LiDAR and SAR) and passive (high resolution imagery e.g., WorldView, Quickbir) remote sensing and analysis methods, can allow description of

vegetation structures such as canopy architecture, height and spacing of individual trees by three dimensional profiles, with a potential to estimate tree species and composition, forest canopy structure and forest cover change at a fine scale with large areas (Fatoyinbo et al., 2018; Heenkenda et al., 2014; Yu et al., 2015; Zhu et al., 2015). As such remote sensing technique is used in global conservation and mitigation actions such as Conservation Biological Diversity (CBD) and REDD+ (O'Connor et al., 2015; Fatoyinbo, 2015). For these types of policy implementation, very high-resolution imagery (under 10 m resolution) provided by commercial satellites like WordView2 (WV2) & 3, Quickbird, and IKONOS have the potential to detect species compositions and fine scale analysis of deforestation or forest cover changes.

Over the last few decades, both multispectral and radar image have been used in mapping regional and global mangrove coverage, measuring mangrove forest composition and structure at local scale, and other biophysical properties at varying spatial resolutions (1 to 30 m; Fatoyinbo et al., 2018; Giri et al., 2008; Giri, 2016; Heumann, 2011; Kamal and Phinn, 2011; Kuenzer et al., 2011, 2014; Lagomasino et al., 2016; Lee et al., 2015; Lee and Fatoyinbo, 2015). However, application of the very high resolution optical imagery (under 10 m resolution) in mangrove species mapping is few. Recently, several studies have identified mangrove species groups using high resolution images following different classification methods. For example, in an artificially restored mangrove in China, Zhu et al. (2015a) separated two mangrove species and other vegetation types using WV2 images. Kamal et al. (2015) identified three *Avicennia* species in Moreton Bay, Queensland Australia. For another region in Australia, five mangrove species were identified in the Northern Territory, using WV2 image (Heenkenda et al., 2014). Neukemans et al. (2008), used Quickbird images for mapping four mangrove species in Gazi Bay mangrove, Kenya. While in another study in Caribbean coast of Panama, Wang et al. (2004), evaluated the performance of IKONOS and Quickbird images in varying combinations for identifying three mangrove *Rhizophora mangle*, *A. germinans*, and *L. racemose.*

The above-mentioned studies based on high resolution imagery were applied in relatively small areas and mostly in restored mangroves and can identify limited number of species in low accuracy. Furthermore, these studies used only optical images and would not attempt their results to relate to some ecological theories such as zonation which is common in almost all mangrove forest globally, either in macro or microscale. However, it has been suggested that inclusion of canopy height layer in vegetation classification that can be derived from active sensor like radar or LiDAR, can improve the overall classification accuracy (van Ewijk et al., 2014) because only optical image-based vegetation index may suffer from

saturation effect and thereby reduce the overall classification accuracy (van Ewijk et al., 2014). Application of the radar and LiDAR-based imagery have also been used in mangrove canopy height measurement recently, for calculating aboveground biomass but its application in species mapping in combination with high resolution optical image is limited (Fatoyinbo et al., 2018; Fatoyinbo and Simard, 2013; Lagomasino et al., 2015; Lee et al., 2015; Lee and Fatoyinbo, 2015). Therefore, application of high resolution optical image such as WorldView2 (WV2) in combination with a radar image such as TanDEM-X (TDX) in classification of species or species composition is needed to extend in natural mangrove ecosystems at large scale for supporting target achievement of environmental policies and sustainable forest management.

Links between carbon and biodiversity

In recent years, scientists have initiated discussions in community ecology on biodiversity and functional diversity whether the latter is the main driver of ecosystem functions or services such as carbon sequestration (Cavanaugh et al., 2014; Mensah et al., 2016; Ruiz-Jaen and Potvin, 2011; Tilman et al., 2014). This emerging research field in community ecology, is now a center of interest in the ecosystems based global climate change mitigation approaches in formulating polices such as in REDD+ and CBD (Murray et al., 2015; Phelps et al., 2012). REDD+ requires a proposed project to have dual roles: climate change mitigation and biodiversity conservation. However, possible concern has been raised in REDD+ activities with high carbon areas (natural forests) might be of potential risk of biodiversity loss from adjacent areas of high biodiversity with low carbon because of land use pressure (Harrison and Paoli, 2012; Murray et al., 2015) and allocation of REDD+ financial support away from high biodiversity areas with low carbon stocks (Murray et al., 2015; Phelps et al., 2012).

Two theories have been established regarding the relationship between greater diversity and greater ecosystem productivity (Tilman et al., 2014). First one is selection effect which is based on the hypothesis that greater productivity is the result of frequent abundance of one or several dominant species, while the other is niche-complementary effect which reveals that greater productivity in a community is contributed by different species that share the same resources (Cavanaugh et al., 2014; Mensah et al., 2016; Ruiz-Jaen and Potvin, 2011; Tilman et al., 2014). Scientists have supported either one of these two hypothesizes or both by relating either species richness as diversity or functional diversity or all of them to biomass or carbon stocks in natural forested ecosystems (tropical, temperate and arid) and in managed landscapes

such different type of agroforestry systems (Homegargen, roadside plantation, cacao agroforests) (Cavanaugh et al., 2014; Kessler et al., 2012; Mensah et al., 2016; Rahman et al., 2015; Rahman et al., 2017; Ruiz-Jaen and Potvin, 2011)

In the forested ecosystems, studies on biodiversity and carbon relationship found positive, negative, or no relationship (Cavanaugh et al., 2014; Islam et al., 2015; Kessler et al., 2012; Kirby and Potvin, 2007; Martinez-Sanchez and Cabrales, 2012; Mensah et al., 2016; Ruiz-Jaen and Potvin, 2011; Sharma et al., 2010; Zhang et al., 2011). Thus, these have led to dispute among ecologists. For example, Sharma, et al. (2010) found that tree diversity is negatively correlated with total carbon density. Kibry and Potvin, (2007) stated that tree diversity has no significant relationship to both aboveground and belowground soil carbon accumulation. However, Sanchez and Cabreles, (2012) found significant positive relationship between species richness and diversity with aboveground carbon mass in Maxican tropical forest. In Subalpine coniferous forest in China, Zhang, et al., (2011) found no significant relationship between the species richness and aboveground carbon storage, but they found a significant negative relationship between diversity and aboveground carbon storage. Ruiz-Jean and Potvin (2010) found positive relationship between species richness and carbon storage in Neotropical Forest in Panama where species richness can explain 19% variation in carbon storage. In different agroforestry systems, positive correlation was also observed between species richness and aboveground carbon storage: in Indonesian cacao agroforestry systems (Kessler et al., 2012), and in homegarden agroforestry system in Srilanka (Mattsson et al., 2015). Similarly, in Bangladesh, Islam et al.(2015) found a positive relation between species richness and SOC content. While the above mentioned studies focus on local vegetation, a regional study covering temperate and boreal forests across Canada found a positive relationship between species diversity and aboveground biomass (Zhang et al., 2017). In the global context which cover tropical forests of Americas, Africa and Asia, a positive relationship was also reported between taxonomic richness and aboveground carbon storage (Cavanaugh et al., 2014). All the above-mentioned reports reveal that the relationship between diversity (in most case species richness) and carbon storage have been widely studied in many forested ecosystems. However, in the mangrove ecosystems only one study in a restored mangrove plantation is available (Kirui et al., 2012), thus it is imperative to investigate this functional relationship in natural mangrove forests as this is one of the most carbon-dense forests in the world.

Research gaps in Sundarbans Reserved Forest, Bangladesh

The Sundarbans Reserved Forest is the world largest mangrove ecosystem (5% of global mangrove 83495 km^2) playing an important role in providing multiple ecosystem services to adjacent communities and saving their lives and properties from tidal surge and cyclone. This forest is a biodiversity hot spot and environmentally it has a global role of mitigating climate change through carbon sequestration. Among the 70 true mangrove species globally, 24 are found in SRF along with 70 other mangrove associates (M. S. Rahman et al., 2015). It is also a home of some endangered species including large population of tigers (Royal Bangle Tiger) and Ganges and Irrawaddy dolphins. Because of its high biodiversity, socioeconomic, and ecological value, this forest was declared a Ramsar Wetlands Site in 1992 and UNESCO world Heritage Site in 1997 (three wildlife sanctuary which cover 52% of the total area of SRF). It contains heterogeneous ecosystems in terms of large area of forest cover (Iftekhar et al 2008), salinity zone (Wahid et al. 2007), dominant mangrove types (Iftekhar et al 2008) and stand structure (basal area, mean tree height, canopy cover etc.), which might influence the above- and below-ground carbon stock and would be of great interest to mangrove ecologists.

In SRF, application of remote sensing in estimating distribution and canopy structure of mangrove species is limited. Several studies in historical forest cover change and vegetation change (mainly mangrove and non-mangrove) have been conducted in SRF which are mainly based on Landsat and radar imagery (Blasco et al., 2001; Cornforth et al., 2013; Emch and Peterson, 2006; Ghosh et al., 2016; Giri et al., 2008; Giri and Shrestha, 1996; Hamilton and Casey, 2016; Islam et al., 1997; Mondal and Debnath, 2017; Thomas et al., 2017b). These previous studies have spatial limitation in terms of image resolution. Details of the vegetation type of SRF have been updated using Aerial photography with manual digitization and *in situ* forest inventory data. The latest detailed vegetation map of the SRF was developed by manual digitization of aerial photos and published by Bangladesh Forest Department in the same year when the three protected areas were declared as World Heritage site, almost in 1997. Since then, the SRF experienced several strong cyclones such as “Sidr” in 2007 and “Aila” in 2009 which caused severe damage in SRF forest structure. Additionally, successional change and forest dynamics may have changed the species composition. Therefore, a detailed species map for SRF is necessary for forest management and policy support. On the other hand, as in SRF huge amount of carbon is stored and this forest is a proposed REDD+ site, the unveiling the

relationships between carbon storage and tree diversity would add value of the SRF ecosystems substantially with regard to payment of ecosystem service and scientific advancement.

Aim and structure of the present study

The present study was based on three main objectives. Firstly, I studied the horizontal variations of carbon stock in SRF (Chapter 3) as this mangrove forest is a heterogeneous ecosystem where species zonation is prominent. Secondly, I evaluated the high resolution optical (WV2) and active imagery (TDX) in vegetation and forest canopy mapping (chapter 4) because both forest parameters are important in ecosystem services assessment such as biodiversity and carbon stock. Finally, I investigated relationships among biodiversity, forest structure and carbon storage (Chapter 5), as it is important in the ecosystem-based climate change mitigation and adaptation standpoint. Finally, I discussed the main findings from my three main chapters and presented its implications to forest management, global environmental policy support and prospective research directions (Chapter 6).

Chapter 2 Study area: Sundarbans Reserved Forest Bangladesh

Sundarbans Reserved Forest

Name and Position

The Sundarbans (literally Sundar means "Beautiful" and Bans means "Forests"). It is the world's largest contiguous mangrove ecosystem (10017 km^2) shared between Bangladesh (62%) and India (38%) and biologically most diverse mangrove forest which was declared a Reserve Forest in 1878 (MOEF, 2010; Rahman et al., 2015). The Bangladesh part of Sundarbans called Sundarbans Reserved Forest (SRF), lies between 21º30´ N and 22º30´ N and 89º 00´ E and 89º55´ E (Fig. 2.1). The total area of SRF is 6,017 km^2; in which; mangrove forests occupy about 69% and the rest is water bodies such as rivers, small streams, and canals. The mangrove extent in SRF accounts for 5 % of global mangrove forests (83495 km^2) (Hamilton and Casey, 2016). It accounts for 4.07% of total area of Bangladesh and 40% of the total forest coverage managed by the Forest Department (FD, 2011). This forest is covered under three southern Administrative districts: Satkhira, Khulna and Bagerhat, where around its periphery there are 2268 villages and 17 Upazilas (subdistricts) (Roy et al., 2012). The eastern boundary of SRF is demarcated by Baleswar River while the western boundary is defined by the Harinbhanga–Raimangal–Kalindi river system (Wahid et al., 2007). The Northern boundary of SRF is defined by small river and canal. The Bay of Bengal is to the south of SRF. So, the whole boundary of SRF is defined by water systems. Because of its multiple ecosystem services and biodiversity value, it is likely to influence regional and global environments under the changing climate (Iftekhar and Saenger 2008; Rahman et al. 2015). This forest was declared as Ramsar Wetlands Sites in 1992 and UNESCO world Heritage Site in 1997 (MOEF, 2010).

Climatic condition

The Sundarbans is located south of the Tropic of Cancer. The four main seasons are pre-monsoon (March-May), monsoon (June-September), post-monsoon (October-November) and the dry winter season (December-January) (Iftekhar and Islam, 2004). In this study, I used climatic data of Bangladesh Meteorological Department, over a 20-year period (1991-2010). There are five weather stations around SRF (Table 2.1). The mean annual rainfall is 2408.50 mm, least at Satkhira (1,749.10 mm) and highest at Khepupara, (2888.4 mm) (Table 2.1).

Again, the rainfall and potential evapotranspiration data of five weather stations around SRF reveal that the wet season includes seven months, February and May to October. During these months rainfall was greater than potential evapotranspiration (Fig.2.2). The mean annual relative humidity over the 20-year period was 82.30%. The relative humidity was found lower in March and higher in July (Table 2.1; Fig. 2.3). The climate of SRF characterized by a long-wet period with very short dry period.

Topography, geology and soil

The SRF is a flat ecosystem, the range of elevation is about 0.9 to 2.11 from the mean sea level (Iftekhar and Islam, 2004). This forest is inundated by sea water two times in a day where the average time difference between the tidal periods is 12 hours, 25 minutes (Chaffey et al., 1985). The maximum tidal height of successive high and low water varies depending on the location and the mean tidal height is about 4 m (Chaffey et al., 1985). During the high spring tides, almost whole of SRF is flooded by sea water (Siddiqi, 2001). The geological formation of the Sundarbans is of comparatively recent origin of which evidence show that it came into existence about 4,000 years ago (Iftekhar and Islam, 2004). Gopal and gosh, (2006) stated that during the 16th century, the Ganga changed its course to shift eastwards and joined the Brahmaputra, which later in the mid-18th century, moved together eastwards to empty into the River Meghna. Thus, the Ganga-Brahmaputra-Meghna river system originated from the Himalayas carried huge amounts of sediments with freshwater into the SRF. Pedologically the soil of SRF is very young, and poorly drained, uncured sediments which have no specific horizon (Iftekhar and Islam, 2004; Siddiqi, 2001). The mineral composition of SRF soil is heterogeneous in nature. The mineral content of the soil in SRF was found higher from east to west wards (Iftekhar and Islam, 2004). The soil pH of SRF varies from 6.8 to 8.4, but across the SRF soil, it is mainly alkaline (pH range between 7.0 and 8.0; MOEF, 2010). Although the Sundarbans soil is in general medium textured, sandy loam, silt loam or clay loam, the grain size distribution is highly variable where silt loam is the dominant textural class (Chaffey et al., 1985). In SRF, the soil contains metals of high alkalinity. The Cation Exchange Capacity in the soil is high which varies between 12-23 meq/100 g (Siddiqi, 2001). The range of Na and Cl content in oven dried soil in SRF, are 5.7–29.8 meq/ 100 g and 5.7–23.2 meq/100 g, respectively (Siddiqi, 2001). The organic matter content varies between 4% and 10% in oven dry soil which appears lower than other mangrove soils in the Indo Pacific region (Rahman et

al., 2015; Siddiqi, 2001). The three distinct salinity zones in SRF, was defined depending on the soil salinity (See, Hydrology and salinity section for details; Fig. 2.4; Siddiqi, 2001).

Hydrology and salinity

In SRF, the hydrological system is complex. Ganga Brahmaputra and Meghna originated from the Himalayas are the main source of freshwater (Wahid et al., 2007). Inside SRF, there are about 450 rivers and canals .Huge amount of freshwater is carried annually by the Baleshwar River in the eastern part of SRF, and most of the discharged water comes from the Brahmaputra and Meghna rivers (MOEF, 2010). However, through Sibsha and Passur rivers the amount of water discharge into SRF, which mainly comes from the Gange river through the Goari river system, is reduced from 4000 to 8880 m^3s^{-1} in the monsoon period to 0.00 to 170 m^3s^{-1} in dry period due to Farakka Barrage (Aziz and Paul, 2015). While in the western side, the main water source is inland water. For this reason, the freshwater flow is limited compared to the middle and eastern parts of the SRF. Being its position in the transition between freshwater from upstream flow and the saline water of the Bay of Bengal, the level of salinity forms a gradient in the SRF (Wahid et al., 2007). Therefore, in SRF, the level of salinity increase from east to west and inland to coast (Wahid et al., 2007). Based on salinity, the SRF is divided into three zones, freshwater (salinity < 5%), moderate saline zone (salinity 5%- 18%) and strong saline zone (salinity 5%- 18%) (Fig. 2.4) (Siddiqi, 2001). During the monsoon time salinity is close to zero while the highest salinity is observed from April to May.

Biological resources

Flora

The floral diversity of SRF is high. It is a home of 528 species of vascular plants which belong to 356 genera and 111 families, where 24 species are true mangroves and 70 species are mangrove associates (Rahman et al., 2015). There are 10 dominant vegetation types in SRF which are composed of varying proportions of *H. fomes*, *Excoecaria agallocha*, *Ceriops decandera* and other species (see Chapter 3, for details).

Fauna

The vertebrate diversity of SRF is also very high. A total recorded number of 1135 species are present, including 315 species of birds (including 84 migratory), 289 terrestrial

species of which 49 species are mammals, including a large population of tigers (Bangle Tiger) and 678 aquatic species including Ganges and Irrawaddy dolphins and saltwater crocodiles which constitute about 35% of the total fauna of Bangladesh (Aziz et al., 2017; MOEF, 2010).

Administrative and forest management

The SRF is a state-owned forest being declared a reserved forest in 1878 under the 1876 Forest Act. during the British colonial period (MOEF, 2010). Bangladesh Forest Department (BFD) is the sole management body of SRF (MOEF, 2010). However, recently Co-Management activities have been adopted in SRF (MOEF, 2010) . Under the Khulna Circle of BFD, headed by the Conservator of Forest, the SRF has been managed by two divisions: Sundarbans East Division (SED) and Sundarbans West Division (SWD) (the Divisional Forest Officer is in charge of forest management) (Fig. 2.1; shapefile source: Center for Environmental and Geographic Information Services, Bangladesh). Additionally, there is another Divisional Forest officer who is in charge of Working Plan Division (BFD, 2018a). Four range offices under two divisions (Sharankhola and Bagherhat under SED, and Khulna and Satkhira under WSD) are headed by four Assistant Conservator of Forests (BFD, 2018a).

In terms of management, the SRF is divided into 8 blocks which consist of 55 compartments (small forest management unit) which are classified according to stand structure and species composition (MOEF, 2010). From the conservation and environmental point of view, SRF has three zones: Ecologically Critical Areas (10 Km buffer around its periphery), Reserved Forest (48 % of total areas) and Protected areas (six wildlife sanctuaries, among which 3 are only water body for protecting Irrawaddy Dolphin) (BFD, 2018b; MOEF, 2010) (Fig. 2.4). Under the co-management approach, there are co-management committees (CMCs) and more than 200 village conservation forums in SRF (MOEF, 2010; Rahman et al., 2017b).

Sundarbans Reserved Forest under different management regimes

Sundarbans has long management history (Table 2.3). Before the Gupta Dynasty (320-415 AD) period, Sundarbans was managed by sustainable manner by local king or empire (Pandit, 2013). During Gupta Dynasty it became deteriorated as forest clearings started for agriculture (Pandit, 2013). Massive forest clearing started from Delhi Sultanate 1204 to Mughal period which continued until 1876 of British Colonial period, when Forest Act was formulated to declare reservation of the Sundarbans (Eaton, 1990; MOEF, 2010; Pandit, 2013). In 1878 part of these forests was declared as reserved forest (MOEF, 2010; Pandit, 2013). After that,

the Sundarbans has been managed in scientific manner under the clear prescriptions through forest management plans (MOEF, 2010; Pandit, 2013). The colonial government had a clear objective of making more revenue by timber exportation (MOEF, 2010; Pandit, 2013). Though the forest was managed by following the management plan prescription, it degraded gradually. This was found in successive forest inventory reports (MOEF, 2010; Pandit, 2013). After partition of the Indian Subcontinent, the Sundarbans was shared between the two-new born countries, India and Pakistan (MOEF, 2010; Pandit, 2013). Name of Pakistan part of Sundarbans was changed to Sundarbans Reserved Forest (MOEF, 2010). In the Pakistan period, several wood-based industries were established in Khulna region, in which raw materials were collected from SRF. This trend continued even after the Independence of Bangladesh in 1971 (MOEF, 2010). Though the management plan prescription was in effect, the SRF became degraded due to over exploitation (MOEF, 2010). In this context, the Bangladesh government declared a moratorium on the harvest of timber from the natural forests in 1989 (except, for fuel wood, NTFPs and *Excoecaria agallocha*) (MOEF, 2010).

After two devastating cyclones in 2007 (Sidr) and 2009 (Aila) damaging the SRF severely, all kinds of forest products extraction was banned except for some NTFPs (Honey, fish, crabs, shell and nypa palm leaves; MOEF, 2010). So, SRF is now managed solely for climate change mitigation and revenue collection from NTFPs and tourism. Outcome of these conservation activities that was adopted after 1989, has a positive effect. The difference of the last two successive forest inventory reports shows that overstory stocking (DBH $\geq$ 15; density, basal area) of the major tree species increased over the 13 year period (1997-2010) and thereby increased carbon accumulation in SRF (Ahmed and Iqbal, 2011).

Resources values of the forest

The SRF provides a multiple ecosystem services to local communities, national economy and to global climate change mitigation. Accurate economic evolution of these ecosystem services is not possible. However, some provisioning such as timber (broken or confiscated timer as commercial timber harvest is officially banned in Bangladesh), fuel wood, fish, thatching materials, honey and waxes, and cultural services such as tourism can be quantifiable. From these two ecosystem services, BFD receives large revenue each year. In a study of ecosystem services evaluation in SRF, Uddin et al. (Uddin et al., 2013) found that over a 10-year period (2001-2010) the provisioning and tourism services provide on an average USD 744,000 and USD 42,000 per year^{-1}, respectively. Another quantifiable service is carbon

sequestration per year which can be credited. The last forest carbon inventory (BFD, 2010) report showed that over the 13-year period (1997-2010), overstory trees (DBH ≥ 15 cm) of the SRF have been sequestering atmospheric carbon at a rate of 4.8 Mega tons CO_2 equivalent per year which can earn USD 72 million per year (@USD 15 per ton CO_{2e}) (Tvinnereim and Røine 2010). If all the carbon pools (prescribed by IPCC) are considered the credited amount would be much more. Thus, SRF has a high potential in contributing national economy through the prospective REDD+ project.

Natural and anthropogenic threats to SRF

Being of its geographic position, the SRF is vulnerable to natural calamity as well as anthropogenic disturbance. Each year several tidal surge and cyclones pass over SRF which damage forest vegetation seriously and cause land erosion. For example, in the first decade of the 21th Century, SRF experienced two server cyclones: Sidr, which hit the area on 11 November 2007, caused massive destruction of forest canopy, breakage and uprooting of trees, increased salinity in the forests' upland areas and in artificial ponds (providing fresh water to wildlife especially deer and tigers). This also raised the death toll of wildlife. Aila, of which land fall was on 15 May 2009, also affected forest vegetation severely and increased salinity inside the SRF (Huq et al., 2015). Another, serious threat is sea level rise which also increase salinity. One island in the transboundary between Bangladesh and India, already submerged due to rise in sea water. It has been predicted that, if the ongoing sea level rise continues from its baseline (2000 for SRF) and increase up to the minimum prediction level (28 cm at the end of 21 century), 96 % SRF will experience a long term waterlogged condition which causes habitat loss and biodiversity decline (Loucks et al., 2010).

Hydrological condition at SRF is determined by the interplay between salinity of sea water and fresh water from upstream rivers where fresh water reduces salinity of the sea water, a natural process (Wahid et al., 2007). However, due to several human activities after 1950 in the vicinity of SRF (Polder making and shrimp farming) and the dam construction in the upstream rivers (and Farakka Barrage at the Indian part of Ganges river), the natural water flow has been interrupted (Rahman and Rahaman, 2017; Wahid et al., 2007). These anthropogenic actives resulted increase in salinity, siltation at river beds and small creaks and channels inside the SRF which had negative effects on forest health; (salinity is one of the causes of top dying of *H. fomes)* (Rahman and Rahaman, 2017). Illegal logging and poaching also caused forest and biodiversity loss. For example, fishermen cut huge numbers of young *H. fomes* trees. Forest

Department confiscates mature logs of *H. fomes* and other species each year; the tiger population is declining seriously in SRF (Aziz et al., 2017; MOEF, 2010).

Table and Figure

Table 2.1 Mean total annual rainfall, mean annual temperature and mean annual humidity over a 20 years period (1990-2010) in SRF.

Weather Station	**Annual mean climate parameters**		
	Rainfall (mm)	Temperature (˚C)	Humidity (%)
Satkhira	1915.50	26.54	80.15
Khulna	1838.72	26.66	81.36
Mongla	2146.05	26.79	82.12
Patuakhali	2839.40	26.38	85.27
Khepupara	3302.85	26.58	82.60
Mean	**2408.50**	**26.59**	**82.30**

Table: Summary of different management periods at Sundarbans Reserved Forest (Eaton, 1990; MOEF, 2010; Pandit, 2013)

Tenure ship	Period	Management	Objective	Impact on ecosystem
Delhi Sultanate	1204-1575	Clearing forest land Bagerhat and Khulna	Rice production	Forest and biodiversity loss
Mughal Empire	(1575-1765)	Clear forest land Barisal and Patuakhali area	Rice production Revenue collection	Forest and biodiversity loss
British colonial	(1765-1854)	Lear forest for cultivation	Rice production Revenue collection	Forest and biodiversity loss
	1855-1875	-Forest Act. 1855 -Land clearing (though suspension forest clearing. -Complete map of Sundarbans	Export timber for revenue generation	Degradation of Forest
	1876	-Forest Act 1876 -Reserved Forest -Forest Management Division in 1879	Timber export revenue generation	Degradation of Forest
	1876-1947	-Some part declared Reserved forest (1876-78) -Scientific Management	Timber export revenue generation	Degradation of Forest
Pakistan	1947-1971	-Wildlife survey -Scientific Management	Raw Material Supply to Wood based Industry	Degradation of Forest
Bangladesh	1971-1988	Scientific Management	Raw Material Supply to Wood based Industry	Degradation of Forest
	1989-2009	-Conservative management -Ban on commercial timber extract (Except, *E. agallocha*)	- Raw Material Supply to Wood based Industry -Recovery of forest naturally	- Degradation of Forest -Forest recovering
	2009-date	Fully conserved except (NTFPs)	-Conservation -Climate change mitigation	-Forest stand recovering -Improve Forest quality

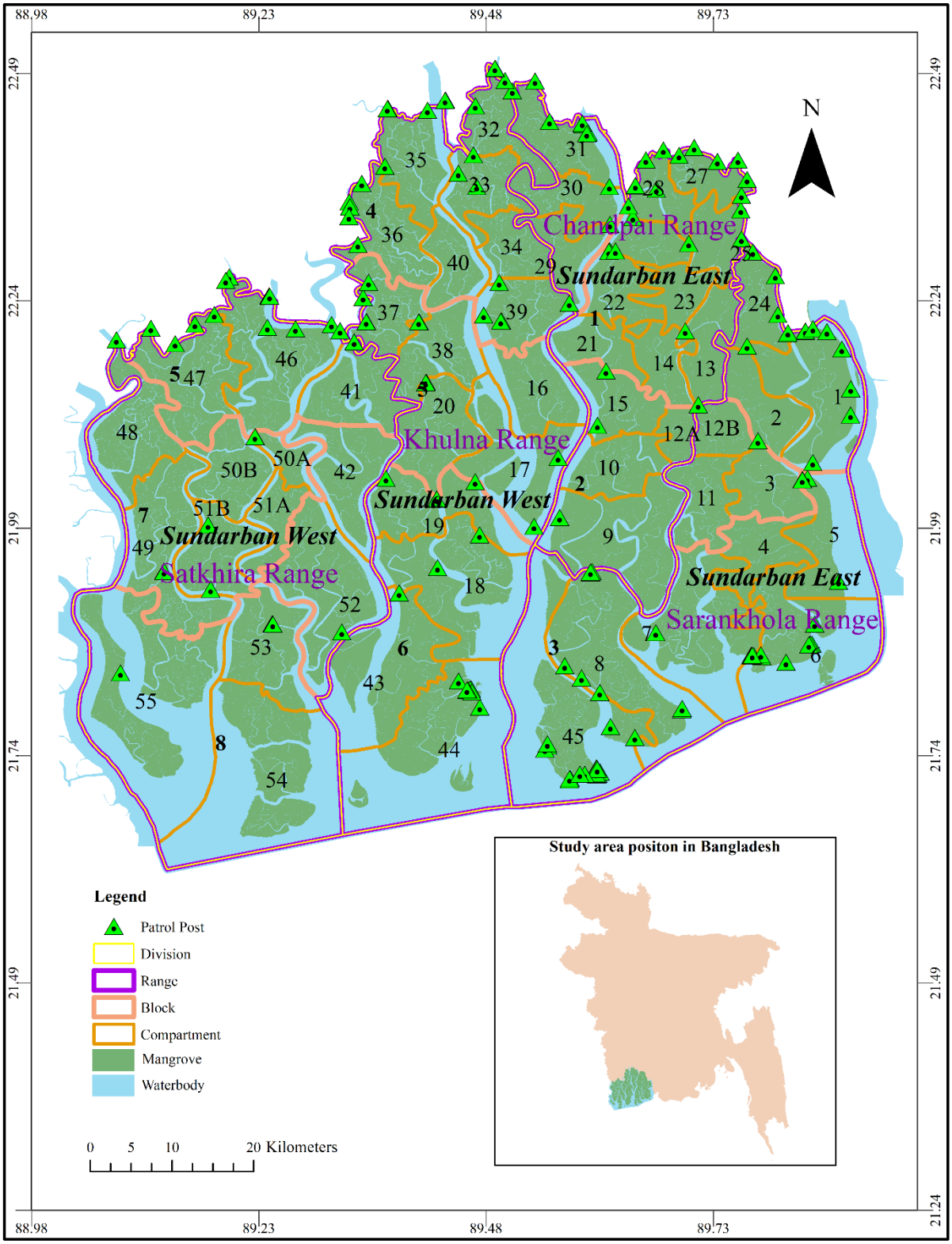

Figure 2.1 Administrative and forest management units in Sundarbans Reserved Forest.

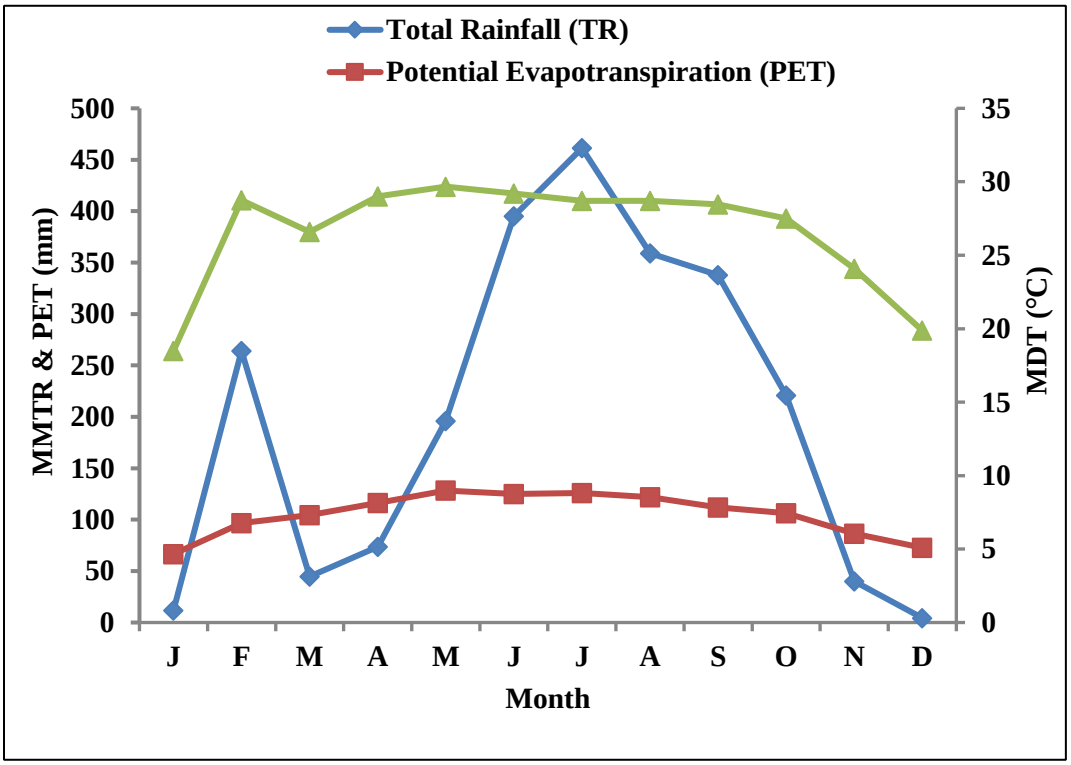

Figure 2.2 Mean climatic parameters in Sundarbans Reserved Forest over a 20-year period (1990-2010) where primary Y axis representing mean monthly total rainfall and potential evapotranspiration while secondary Y axis representing monthly daily average temperature (MDT=Mean Daily Temperature) (MMTR= Mean monthly total rainfall; PET= Potential Evapotranspiration).

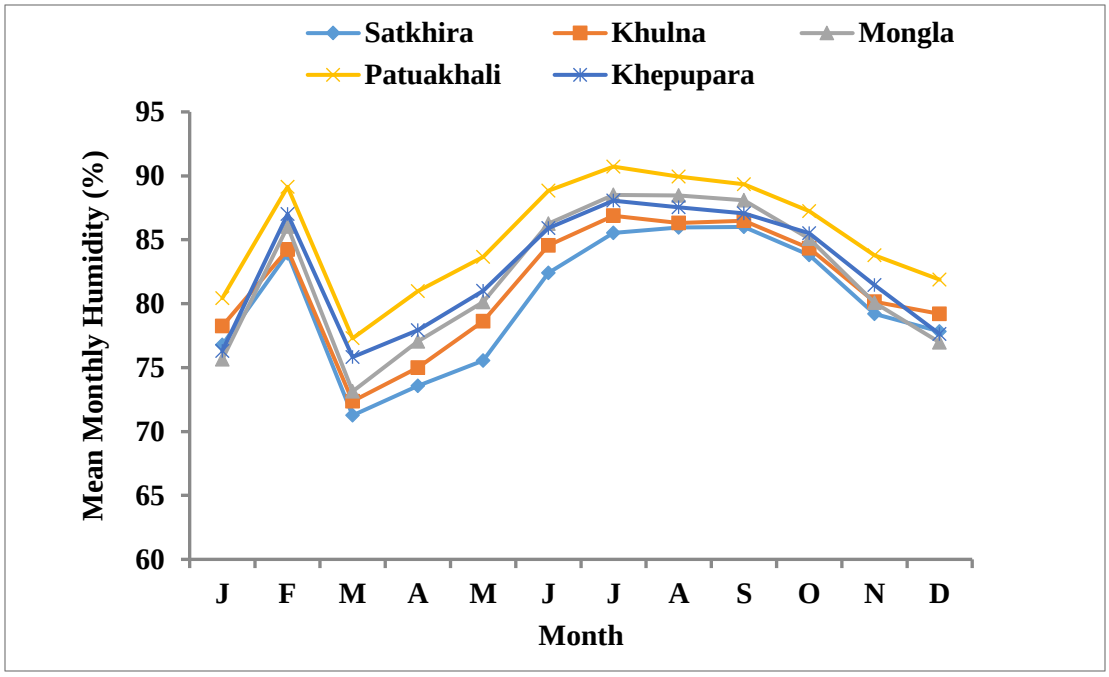

Figure 2.3 Annual relative humidity around SRF over a 20-year period (1990-2010).

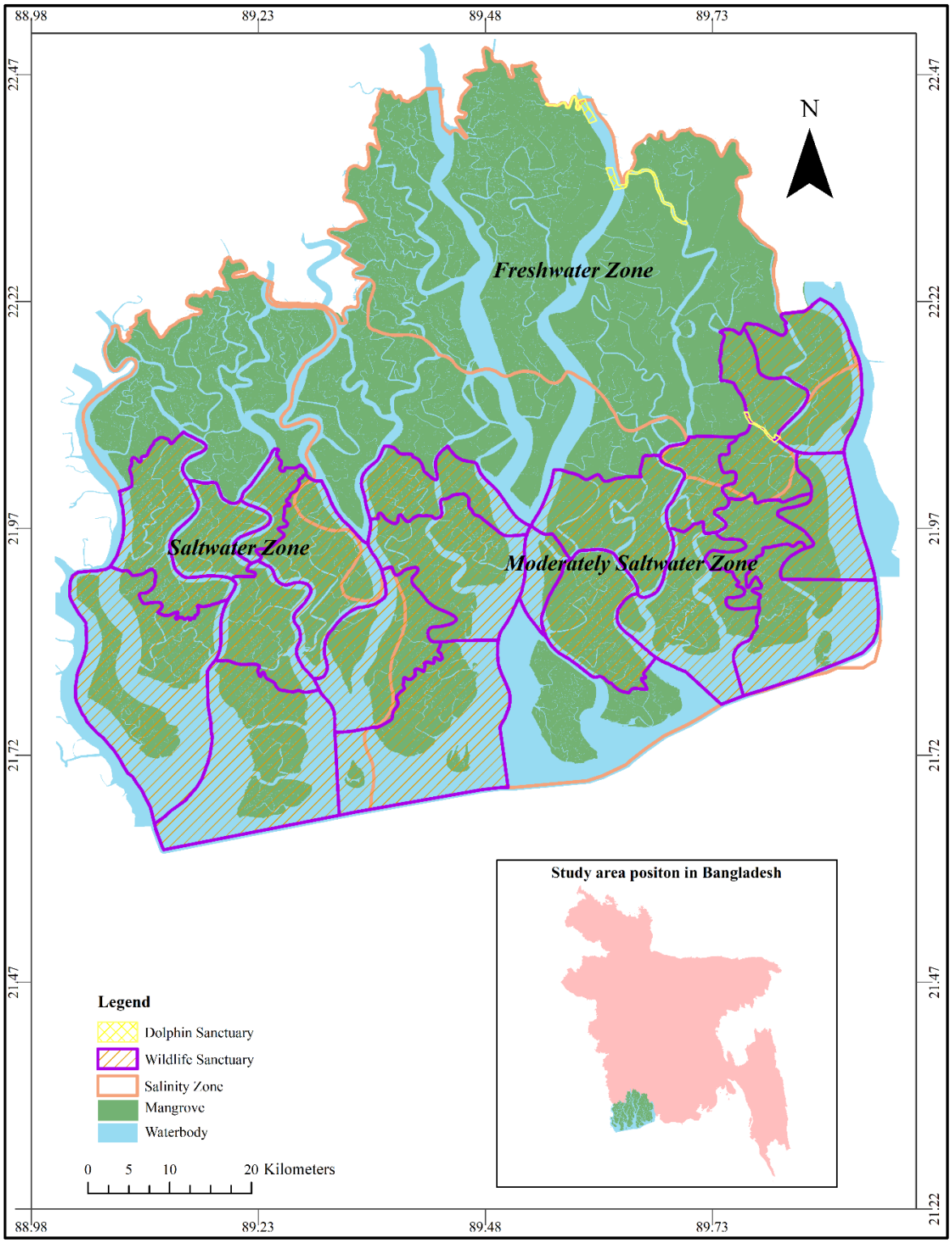

Figure 2.4 Protected area and salinity zone in Sundarbans Reserved Forest.

Chapter 3 Spatial variations of carbon stock among vegetation types and salinity zones in Sundarbans Reserved Forest

Introduction

The World today is facing major challenges caused by increasing atmospheric CO_2 concentration that resulted in global warming (Stocker et al., 2013). Global warming is believed to be mostly due to man-made emissions of greenhouse gases (mainly CO_2) (Stocker et al., 2013). Combustion of fossil fuel and deforestation are two main sources of CO_2 emission to the atmosphere (Detwiler and Hall, 1988; Woodwell et al., 1983). It has been predicted that atmospheric CO_2 will range between 467 and 555 ppm by the year 2050, which was 278 ppm in 1750 and 390 ppm in 2011, and that the average global temperature will increase by 2-4.2^{o}C by the year 2050 (Anderson and Bows, 2011; Pachauri and Reisinger, 2007; Stocker et al., 2013). The global warming of this magnitude could significantly alter the earth's climate, land use, and major vegetation zones and perhaps more importantly melting of polar ice to raise sea level by 5 m causing severe loss of life and property (Detwiler and Hall, 1988; IUFRO, 2009), especially in the developing countries. Bangladesh is among the most vulnerable countries affected by the global warming.

Forests play an important role in mitigating global climate change through sequestering atmospheric carbon (Adame et al., 2013; Donato et al., 2011). Mangroves are particularly efficient sinks, sequestering four times more carbon per unit ground area compared with other terrestrial forests in the tropics (Donato et al., 2011; Khan et al., 2007). However, deforestation of the mangroves, which was widespread in the last few decades (Giri et al., 2011), may render them significant sources of atmospheric carbon (Donato et al., 2011) and policy makers are looking at new ways to save this unique ecosystem through different mitigation approaches such as 'Reducing emissions from deforestation and forest degradation (REDD+)'. So, to participate in UNFCCC's mitigation programs (e.g., REDD+) and thereby generate economic benefit for the country, it is imperative to make a baseline assessment of the ecosystem carbon stock (Adame et al., 2013).

In mangrove forests carbon sequestration (Bouillon et al., 2008; Khan et al., 2007) and organic carbon dynamics (Kristensen et al., 2008; Machiwa and Hallberg, 2002) have been studied

much. Carbon stock in mangrove ecosystems varies with species (Laffoley and Grimsditch, 2009), vegetation type (Adame et al., 2013; Cerón-Bretón et al., 2011; Diloksumpun et al., 2011; Laffoley and Grimsditch, 2009; Mitra et al., 2011), and salinity (Adame et al., 2013a). However, less attention has been paid on the spatial variation of carbon stock among different vegetation types and variation in the above- and belowground carbon.

The Sundarbans is the largest single tract of mangrove forest in the world (6017 km^2 in Bangladesh and 4000 km^2 in India). It is a RAMSAR SITE having three wildlife sanctuaries which are designated as World Heritage by UNESCO in 1997. The forest is, nationally and internationally, of great conservation significance for its environmental services and biodiversity (Iftekhar and Saenger, 2008; Seidensticker and Hai, 1983). To aid in conservation of the forest and to benefit from various global initiatives (e.g., carbon trading), an assessment of the carbon sequestration (above- and below-ground) in Sundarbans is immensely important. Moreover, heterogeneity of the mangrove forest in terms of spatial variation of the forest cover, salinity zone (Wahid et al., 2007), dominant mangrove types and vegetation functional attributes (basal area, mean tree height, canopy cover etc.), which might influence the aboveground and belowground carbon stock would be of great interest to mangrove ecologists. Therefore, objectives of the present study were: i) to estimate the above- and below-ground carbon stock in Sundarbans, ii) to investigate the variation of carbon stock in different vegetation types and salinity zones in the forest and iii) to establish a generalized method for assessing the ecosystem carbon stock in Sundarbans.

Materials and Methods

Description of study area

The study was carried out in the Sundarbans, which lies between 21º30´ N and 22º30´ N and 89º 00´ E and 89º55´ E, in the southwest of Bangladesh (Fig. 3.1). Sundarbans covers an area of 6,017 km^2 (Bangladesh part) of which 4,120 km^2 are the forested areas and the remaining 1,897 km^2 are rivers, canals and creeks of varying width and depth (Islam, 2011). The soil of the Sundarbans is silty clay loam with alternate layers of clay, silt and sand (Gopal and Chauhan, 2006). Trees in the Sundarbans include 22 families representing 30 genera. Important tree species of the Sundarbans along with their life form are presented in Table 3.1 (Iftekhar and Islam, 2004).

In the Sundarbans there are 10 prominent vegetation types (Table 3.2; Fig.1) (Chaffey et al., 1985; Iftekhar and Saenger, 2008).

Sampling design

Through systematic grid sampling method, 155 plots (1570.79 m^2 each) were selected at four-minute intervals of latitude and two-minute intervals of longitude. Of the 155 plots, five plots were fallen over water channels, and the remaining 150 sample plots (total sample area of 23.56 ha) were considered for this study (Fig. 3.1). In each sample plot, five circular plots of 10 m radius were used for data collection (Fig. 3.3). These five subplots were nested and arranged in a cluster manner (Fig. 3.2). The cluster plot designs tend to capture more microsite variation in vegetation, soils, etc., thereby reducing among-plot variation (Pearson, 2005). From the center subplot, the other four subplots (Fig. 3.3) were arranged towards the four cardinal directions with a distance of 50 m (Ahmed and Iqbal, 2011). The vegetation type and salinity zone for each plot were determined from the Sundarbans vegetation map and salinity map developed by Chaffey et al. (1985). The formation of salinity zones in Sundarbans is a recognized phenomenon (Wahid et al., 2007; See Chapter 2 for salinity map) .

Tree inventory

Within 10 m radius from the center of each subplot, diameter of all trees (live or dead with diameter ≥ 10 cm at breast height) was measured. The height of three co-dominant trees (canopy layer tree) within each of the five subplots (Fig. 3.2) was measured with digital range finder. Species name, diameter at breast height (DBH), living status and height in case of dead and broken trees was recorded. For saplings (diameter < 10 cm at BH) data were recorded as it was done for trees but within 3 m radius from the center of each of the five subplots in a sample plot (Fig. 3). The dead trees and saplings with lean below 45^o from true vertical were measured in a similar manner as live tree and sapling. However, for seedlings (trees < 1.3 m high), the number of individuals and the dominant species were recorded. Palms with woody trunks, but not reaching breast height, were counted as seedlings.

Woody debris survey

Mass of dead tree (that lean at an angle > 45^{o} from true vertical) and downed wood materials (twigs, branches or stems of trees or shrubs) that have fallen and lie up to a height of 2 meters above the forest floor, was estimated by using planar intersect technique (Harmon and Sexton, 1996; Van Wagner, 1968). In each subplot (10 m radius), four 10m long transects were laid out; of which first one was directed to 45^{o} from the true north and the other three transects were established at clock wise of 90^{o} off from the previous transect. Woody debris was categorized into 4 size classes according to stem diameter: small (0 - 0.6 cm), medium (0.6 – 2.5 cm) large (2.5 – 7.6 cm), and extra-large (≥ 7.6 cm) (Brown, 1971). Again, the extra-large class was divided into two subclasses: sound (machete bounces off or sinks only slightly when struck) and rotten (hachete sinks deeply and wood is crumbly as its decomposition has been in progress).

An aluminum downed-wood gauge (Fuel Gauge) was used to determine the size class of each piece encountered. Small, medium, and large pieces were tallied as the number of pieces that crossed the transect tape. For extra-large pieces the actual diameter over which the transect line was crossed was measured. Small pieces were only tallied for 2 meters of transect (from meter 10 to meter 8), while medium pieces were only tallied for 5 meters of transect (from meter 10 to meter 5) and the large and extra-large pieces were measured along the 10 meters transect.

In order to quantifying specific gravity and quadratic mean piece diameter (small, medium and large), 21, 22, 20, 19, and 20 pieces of debris were collected respectively for small, medium, large, extra-large rotten, and extra-large sound size classes. The quadratic mean diameter of each of small, medium and large sized classes of woody debris was used to calculate volume of these three classes (Brown, 1971; Kauffman and Cole, 2010).

Non-tree vegetation

Among the non-tree plants, goran (*Ceriops decandra*) and herbaceous plants were measured within 2 m radius from the center of each of the five subplots, while other non-woody palms (e.g., Nypa), pandan, tiger fern and woody shrubs were measured within 4 m radius (Table 1). Groan was tallied by 4 diameter size classes (0-0.6 cm, 0.6-2.5 cm, 2.5-7.6 cm, >7.6 cm). For lianas dbh measurement was taken with the same method use for trees. Herbaceous vegetation was visually estimated and recorded as percent ground cover of herbs and grasses separately (Jain and Fried, 2010). In case of nypa, number of stems rooted in the subplot was counted (not individuals

or clumps, but separate stems), whereas for pandan and tiger fern the number of clumps in the subplot was recorded.

Canopy cover

Canopy cover % was estimated by a spherical crown densitometer standing at the subplot center. To take readings, it was assumed that there are four equi-spaced dots in each of the square blocks and systematically counted the dots equivalent to quarter-square openings. Next the total count was multiplied by 1.04 to obtain percent of overhead area not occupied by canopy. The difference between this and 100 is an estimation of over story density in percent.

Soil sampling

Soil core of 1 m length was pulled out near the subplot center by using a one meter long open face peat auger. Then two soil samples (5 cm length) were collected at positions centered at 15 cm and 65 cm depths from each of the five subplots for determining soil bulk density and organic carbon concentration. Soil samples were air-dried in the field, oven-dried to constant mass at 60°C (to stop microbial decomposition) at the Khulna Integrated Protected Area Co-Management cluster office for determining bulk density, and then sent to Bangladesh Forest Research Institute (BFRI), Chittagong for carbon analysis. Soil carbon analyses were conducted in the laboratory of the soil sciences division of the BFRI. Soil samples were oven dried at 105 °C before homogenizing and organic carbon concentration was determined by following Walkley-Black's wet oxidizing method (Sparks et al., 1996).

Plant mass and carbon computation

Aboveground mass of live trees, poles, saplings and dead ones (decay status 1: having stem, branch and twigs) was estimated by the following general equation (Eqn. 3.1) for mangrove tree species (Chave et al., 2005).

$$AGM\ (kg) = \rho \times \exp\left(-1.349 + 1.980 \times \ln(D) + 0.207 \times (\ln(D))^2 - 0.0281 \times (\ln(D))^3\right) \quad (3.1)$$

where AGM = aboveground mass (kg), ρ = wood density (g cm^{-3}), D = tree DBH (cm), -1.349 = constant, 1.980 = constant, 0.207 = constant, 0.0281 = constant. The wood density data were

obtained from destructive samples supplemented with local literature, World Agroforestry Database (Carsan et al., 2012) and the Global Wood Density Database (Chave et al., 2009; Zanne et al., 2009).

Belowground biomass of trees was computed by using the general mangrove equation (Eqn. 3.2) of Komiyama et al. (2005), while for palms, it was conservatively taking 15% of aboveground biomass (because general mangrove equation for belowground biomass does not apply to palms) (MacDicken, 1997).

$$BGM\ (kg) = 0.199 \cdot \rho^{0.899}\, D^{2.22} \qquad (3.2)$$

where BGM = belowground mass, ρ = wood density, D = DBH.

Pearson et al. (2005) applied an equation for computing the aboveground mass of woody palms that reach breast height. For dead trees having decay status-2 (trees with no twigs/small branches but had large branches or stem only) whose base diameter was smaller than DBH (due to decay at base), the standard calculation would result in artificially large top diameter. Therefore, base diameter for these records (relatively few) was adjusted based on average ratio of DBH: base-diameter, which was 0.82. It was also followed for heavily buttressed trees, for which standard calculations yielded artificially low or even negative top diameters; it was defined heavily buttressed trees as those with a DBH: base-diameter ratio that was two standard deviations below the mean ratio. For small palms not reaching DBH, these were measured as non-tree understory and a destructive harvest was carried out to estimate average mass per understory palm. The short stumps, those not reaching breast height, were simply modeled as a cylinder shape to obtain volume, and then multiplied by species-specific wood density. For belowground biomass of these individuals, the base diameter was used to estimate the projected DBH based on the average ratio of DBH to base diameter (0.82), and then entered this into the equation.

In case of some non-tree vegetation including seedling, subsamples were collected from each destructively harvested individual to determine moisture content. The wet: dry ratios were averaged over the whole sample, then this average value applied to each individual (Table 3.3). Lianas biomass was quantified by using Schnitzer et al.'s (2006), allometric equation.

To calculate the mass of downed wood, it is necessary to know the mean specific gravity of the downed wood in the mangroves as well as quadratic mean diameters for the wood size classes < 7.6 cm diameter (debris diameter greater than 7.6 cm were measured in the field) (Kauffman and Cole, 2010). The quadratic mean diameter for small, medium and large was 0.45

cm, 1.21 cm and 3.17 cm, respectively. The mean specific gravity was 0.59 g cm^{-3}, 0.55 g cm^{-3}, 0.49 g cm^{-3}, 0.25 g cm^{-3} and 0.40 g cm^{-3}, respectively for small, medium, large, extra-large rotten and extra-large sound. By using this specific gravity and mean quadratic data, woody debris biomass was estimated via standard volumetric equations (Brown, 1971).

Conversion of dry mass of trees, understory, and downed wood to carbon mass was done by multiplying 0.5 as tree biomass generally contains half carbon by mass (Gifford 2000). Soil C stock was determined as the product of soil carbon concentration, bulk density, and depth intervals (Donato et al. 2011). The total carbon stock per plot was calculated by adding each of the carbon pool of the 5 subplots.

$$\text{Total C stock } (\frac{\text{Mg}}{ha}) = \text{C}_{\text{tree AG}} + \text{C}_{\text{treeBG}} + \text{C}_{\text{dead tree}} + \text{C}_{SSAG} + \text{C}_{SSBG} + \text{C}_{\text{dead SS}} + \text{C}_{\text{non tree vegetaton}} + \text{C}_{\text{woody debris}} + \text{C}_{\text{soil}} \quad (3.3)$$

AG= Aboveground, BG= Belowground and SS= Sapling Seedling

Statistical analysis

At first, one sample Kolmogorov–Smirnov test (K–S test) was performed to check whether the carbon stock data under the subgroups of vegetation types and salinity zones are normally distributed. The one-way ANOVA was used to test the significance of the differences among the carbon stock in different partitions, vegetation types and salinity zones. In addition, the two-way-ANOVA was performed to investigate the interaction effect with vegetation types nested within salinity zones. For multiple comparisons among the variables Duncan Multiple Range Test (DMRT) was used. Finally, correlation analysis was performed to obtain some generalized regression equations in order to predict above- and belowground carbon stock from vegetation attributes, such as stand basal area or mean tree height. All the statistical and graphical analyses were performed using SPSS version 16 and R version 3.1.0 (R Core Team, 2014).

Results

Vegetation Types and Carbon Stock

(a)Aboveground Carbon

The carbon stock data under the subgroups of vegetation types and salinity zones showed normal distribution as tested with Kolmogorov–Smirnov test (K–S test). Among the vegetation types, VT1 showed significantly higher (P<0.05) tree aboveground carbon (TAGC) stock (152.57 Mg ha^{-1}) than other vegetation types, whereas VT7 showed significantly higher (P<0.05) shrubs and herbs carbon (SHC) stock (61.35 Mg ha^{-1}) than other vegetation types (Fig. 3.4). There was no significant difference (P>0.05) in downed wood carbon (DWC) among the vegetation types (Fig. 4). If the total aboveground carbon stock were considered, the VT1 again showed significantly higher (P<0.05) carbon stock than other vegetation types. The lowest carbon stock of 45.24 Mg ha^{-1} was found in VT8 (Fig. 3.4). The aboveground carbon stock showed no significant interaction effect (P>0.05) between the vegetation types nested within salinity zones as tested with two-way-ANOVA.

(b)Belowground Carbon

As observed in the aboveground carbon, the belowground root carbon (BGRC) stock also showed significant differences among the vegetation types: VT1 showed significantly higher (P<0.05) carbon stock (62.37 Mg ha^{-1}) than other vegetation types (Fig. 3.4). The minimum amount (11.72 Mg ha^{-1}) of BGRC was observed in VT8. Although the belowground soil carbon (BGSC) stock showed significant differences (P<0.05) among the vegetation types, the BGSC stock showed a comparatively high range (90.03 to 134.17 Mg ha^{-1}). If the belowground carbon stock were considered, the vegetation type VT1 showed significantly higher (P<0.05) carbon stock (196.54 Mg ha^{-1}) than other vegetation types and the minimum value (90.83 Mg ha^{-1}) was observed in VT9 (Fig. 3.4). The belowground carbon stock showed no significant interaction effect (P>0.05) between the vegetation types nested within salinity zones as tested with two-way-ANOVA.

Salinity zone and Carbon stock

The fresh water zone (FR) showed significantly higher (P < 0.05) carbon stock among the three major salinity zones (Fig. 3.5). The ecosystem carbon stock increased from strong salinity

zone (ST) to moderate salinity zone (MO) to FR ($P < 0.05$; Fig. 3.5). This trend was observed in all the partitions (tree species, aboveground, BGRC, BGSC, downed wood, ecosystem) except in shrubs and herbs carbon (SHC) stock ($P < 0.05$; Fig. 3.5).

Ecosystem carbon stock

The ecosystem carbon stock ranged from 159.49±6.86 Mg ha^{-1} in Gewa-Goran dominated vegetation type (VT10) to 360.01±22.71 Mg ha^{-1} Sundri dominated VT1 (Fig. 4). VT1 showed significantly higher carbon stock than any other vegetation types (one-way-ANOVA, $P < 0.05$). As tested with DMRT, there was no significant difference in ecosystem carbon stock among the vegetation types VT2, VT3, VT4, VT5 and VT6 ($P > 0.05$; Fig. 4), followed by the next homogenous subset of vegetation types comprising VT7, VT8, VT9 and VT10 ($P>0.05$; Fig. 3.4). The spatial distribution of ecosystem carbon stock was shown in fig. 3.8.

If vegetation type is taken into account, it was found that the minimum proportion of belowground carbon stock constitutes 50.1% of the ecosystem carbon stock in VT9, which reaches upto 75.4% in VT8 (Fig. 3.6). If salinity zone is taken into account, the salinity showed a positive influence with belowground carbon partitioning and it was found that the minimum proportion of belowground carbon stock constitutes 57.2% of the ecosystem carbon stock in fresh water zone (FR), which reaches up to 71.9% in strong salinity zone (ST) (Fig. 3.6). The ecosystem carbon stock showed no significant interaction effect ($P>0.05$) between the vegetation types nested within salinity zones as tested with two-way-ANOVA.

Vegetation functional attributes and carbon stock

The ecosystem carbon stocks were plotted against several vegetation functional attributes such as basal area (BA), mean co-dominant tree height (CDTH), tree density and canopy cover percent (CCP) considering all vegetation types (Fig. 3.7) and all salinity zones (Fig. 3.8). It was found that BA holds a strong positive relationship ($R^2= 0.61$, $P<0.05$), which can be expressed by the following equation:

$$Ecosystem\ C = 135.92 + 0.8292 \times BA + 0.142 \times BA^2 \quad (3.4).$$

The CDTH also showed a strong positive relationship ($R^2= 0.58$, $P<0.05$), which can be expressed by the following equation:

$$Ecosystem\ C = 119.5705\ + 2.1660 \times CDTH + 1.2273 \times CDTH^2 \quad (3.5)$$

However, tree density and CCP did not show significant relationships with ecosystem carbon stock.

Discussion

The richness of mangrove tree species in Sundarbans restricts the use of species-wise allometric equations for biomass estimation. Therefore, in this study we used universal allometric equations (Chave et al., 2005; Komiyama et al., 2005) for estimating the above- and below-ground biomass of tree species using trees DBH and wood density, in order to avoid destructive sampling of trees.

The results of this study suggest significant differences (P<0.05) in carbon stock among different mangrove vegetation types. However, no significant interaction effect (P>0.05) of the vegetation types and nested within salinity zones was detected, which indicates that the variations of carbon stock are caused independently by vegetation types or salinity. Among the vegetation types, *Heritiera fomes* dominated forest contained the highest amount of ecosystem (above- and belowground) carbon (360.0 Mg ha^{-1}) per unit area followed by *Heritiera fomes -Excoecaria agallocha*, *H. fomes – Xylocarpus mekongensis - Bruguiera sexangula*types, and so on (Fig. 3.4). The reason behind this variation could be aboveground vegetation stature as the carbon stock was found strongly correlated with the size of the trees (height and diameter) and basal area. Klimešová et al. (2008), Westoby et al. (2002), Westoby (1998), also observed that trees attaining greater height out competing their neighbors accumulate more carbon. In natural ecosystems, the diameter of a tree is often a determinant of aboveground biomass (Chave et al., 2004). The dominant species in each vegetation type may have an effect on aboveground biomass depending on their basal area (Ruiz-Jaen and Potvin, 2010), as observed in this study (Figs. 3.7 and 3.8). While canopy cover is a weak indicator of carbon stock as canopy cover is formed by all the sizes of trees in natural forests. Similarly, tree density forms a weak indicator of ecosystem carbon stock (Figs. 3.7 and 3.8), which is a general phenomenon, because a young forest with high density may show lower biomass than in a low density mature forest. However, tree density may be a strong indicator of ecosystem carbon stock when seedlings and saplings are few or absent (Gross et al. 2014). So, vegetation types with higher canopy height, trees having larger diameter and thus more basal area,

contain more ecosystem carbon. It is important to note that *H. fomes* is among the tallest tree species in the Sundarbans (height 15 to 21 m) (Karim, 1988) and comparatively large diameter (except *Avicennia officinalis* and *Sonneratia apetala*). Therefore, vegetation types with fewer *H. fomes* have lower carbon stock.

Significant differences in ecosystem carbon stock were also observed in different salinity zones in the Sundarbans. The fresh water zone contained the highest amount of carbon followed by moderately saline zones. The strongly saline zone contained the least carbon (Fig. 3.5). As salinity increases plants become dwarfed in the Sundarbans. Here, salinity is highly dependent on the fluctuating volume of freshwater coming from upstream (Wahid et al., 2007) and literally absence of fresh water flow creates a strongly saline condition. There is also spatial variation of nutrients in tidal water (Wahid et al., 2007). Therefore, the variation of carbon stock in different salinity zones in the Sundarbans could be due to adverse impact of increased salinity on biomass productivity and due to spatial variation of nutrients in fresh water (Wahid et al., 2007). Generally, in mangrove ecosystems especially in riverine mangrove forests experiencing incursion of larger amount of freshwater with fluvial nutrients (Kathiresan and Bingham, 2001), there is a prominent tradeoff between salinity and distribution of species, productivity and growth of mangrove forests (Twilley and Chen 1998), and thus on carbon stock (Crooks et al., 2011). In the mangrove ecosystems, vegetation is more abundant in lower salinity zones where productivity is higher which is associated with higher biomass and higher carbon stock (Ball, 1998, 2002; Crooks et al., 2011; Kathiresan and Bingham, 2001).

In this study it was found that, contribution of soil carbon (up to 1 meter) to total ecosystem carbon stock was similar to that of total aboveground carbon both among vegetation types and salinity zones. These patterns reveal that mangroves can store larger amount of organic carbon in the sediment (Bouillon et al., 2003; Donato et al., 2011; Khan et al., 2007). When soil carbon and root carbon are considered together, contribution of belowground carbon in ecosystem carbon stock was more than that of aboveground carbon like in other mangrove forest (Adame et al., 2013; Donato et al., 2011; Kauffman et al., 2011). This is due to high root-shoot ratios in mangrove forests (Fujimoto et al., 1999; Khan et al., 2007; Komiyama et al., 2008, 2000; Page et al., 2002), which means that mangroves store a larger amount of carbon in soil at several meters depth (Bouillon et al., 2003).

Variation of the estimated carbon stock for vegetation types and salinity zones was similar

to that of Indian Sundarbans and mangrove ecosystems in Northwestern Madagascar (Table 3.4). However, comparing with Indo Pacific region and Mexican Caribbean mangroves (soil carbon up to 1m), our results are lower than those at the *Sonneratia alba* dominated Mangrove in Yab, Micronesia, the *Rhizophora apiculata* dominated Mangrove in Babeldoab (Republic of Palau), the *Rhizophora apiculata* and *Bruguiera gymnorrhiza* dominated Mangrove in Kalimatan, Indonesia and the *R. mangle* mangroves of the Sian Ka'an Biosphere Reserve, Mexico (Table 3.4). This difference in mangrove carbon stock would develop due to difference in the amount of peat soil (Crooks et al., 2011; Siikamaki et al., 2012; Smith, 1983; Smith, 1983), mineral sediment (Crooks et al., 2011; Siikamaki et al., 2012), stature of aboveground vegetation (Daniel Murdiyarso et al., 2010), wood density (Baker et al., 2004), forest age (Cerón-Bretón et al., 2011; Kridiborworn et al., 2012), disturbance history (Goodale et al., 2002), dominant species (Kasawani et al., 2007), depth of the organic soil, salinity, available soil phosphorus, etc. (Adame et al., 2013).

For a gross estimation of ecosystem carbon stock, the generalized regression equations (Eqn. 3.4, 3.5) with variables, such as 'basal area' or 'mean tree height' could be very useful not only for Sundarbans mangrove forests but also for other mangrove ecosystems as the results were obtained from a wide variety of mangrove vegetation types and from sample of large spatial scales. Rahman et al. (2017), applied the basal area based general equation that developed in this study, for estimating the ecosystem carbon sequestration in the three protected areas in the Sundarbans Reserved Forest Bangladesh. In that study, Rahman et al. (2017) estimated that yearly ecosystem carbon sequestration was equivalent to 1.31 million-ton CO_2 (from 1997 to 2010) in the three protected areas (90,747 ha). Similarly, this basal area-based equation can be applied to the other mangrove ecosystems for estimating ecosystem carbon sequestration.

In conclusion, this study presents estimates of ecosystem carbon stock of the mangrove forest at the Sundarbans using data sets covering widely distributed samples. The results suggest existence of significant variations of carbon stock in different mangrove vegetation types and variable salinity regimes. The vegetation attributes (basal area and height) of the dominant mangrove species in each vegetation type are the key indicator of determining nature of ecosystem carbon stock. The results also reveal that no matter whether the mangroves are tall or dwarf, significant amount of carbon is stored the sediment, which is a characteristic feature of mangrove ecosystems. For a gross estimation of ecosystem carbon stock, the generalized regression equations (Eqn. 3.4, 3.5) with variables, such as 'basal area' or 'mean tree height' could be very

useful not only for Sundarbans mangrove forests but also for other mangrove ecosystems as the results were obtained from a wide variety of mangrove vegetation types and from sample of large spatial scales. The results of this study may be of use for policy makers to develop suitable adaptive measures to cope with the trends of sea level rise (Loucks et al., 2010; Stocker et al., 2013). Future studies should focus on the driving forces other than salinity of the so called 'salinity zones' in the Sundarbans, which might influence differences in vegetation patterns as well as in carbon sequestration patterns in these zones.

Figure and Tables

Table

Table 3.1 Life form characteristics of main flora in the SRF.

Local name	Scientific name	Life form
Amoor	*Amoora cucullate*	small tree
Baen	*Avicennia officinalis*	large tree
Bola	*Hibiscus tiliaceous*	small tree and semi climbing liana
Dhundul	*Xylocarpus granatum*	small tree
Gewa	*Excoecaria agallocha*	fair sized tree
Golpata	*Nypa fruticans*	palm with soboliferous stem
Goran	*Ceriops decandra*	shrub with coppice like growth
Hantal	*Phoenix paludosa*	small gregarious palm
Hargoza	*Acanthus ilicifolius*	small prickly leaved shrub
Hodo (Tiger fern)	*Acrostichum aureum*	rigid tufted fern under growth
Kankra	*Bruguiera sexangula*	medium sized tree
Keora	*Sonneratia apetala*	large tree generally with spreading habit
Kewa Kanta	*Pandanus ordoratissimus*	gregarious screwpin under-growth
Passur	*Xylocarpus mekongensis*	fair sized tree
Sundri	*Heritiera fomes*	fair sized tree

Source: (Siddiqi 2001)

Table 3.2 Major vegetation types in the Sundarbans with distribution and area. See table 3.1 for species scientific and local names.

Code	Vegetation type	Distribution in Saline zone	Area %
VT1	Sundri	FR	21.0
VT2	Sundri-Gewa	FR, MO and ST	25.8
VT3	Sundri- Passur- Kankra	FR, ST	1.7
VT4	Gewa Mathal, Passur-Kankra-Baen, Sundri-Passur-Keora,	FR, MO and ST	2.9
VT5	Gewa	MO	5.2
VT6	Gewa-Sundri	MO, ST	18.4
VT7	Non- Tree Vegetation (NTV)	FR, ST	1.2
VT8	Goran-Gewa	MO, ST	13.7
VT9	Goran	ST	1.6
VT10	Gewa-Goran	MO, ST	8.4

Note: FR = Fresh water zone, MO = Moderate saline zone, and ST = Strong saline zone
Source: (Chaffey et al. 1985; Ifthekhar and Saenger, 2008)

Table 3.3 Average aboveground mass of species developed by destructive harvest (30 individuals for each species). See table 3.1 for species scientific and local names.

Species name	Average mass (kg)
Golpatta (per frond)	2.00
Tiger fern (Per clump)	0.30
Hargoza (Per stem)	0.05
Pandan	0.29
Goran (Small)	0.0048
Goran (Medium)	0.37
Goran (Large)	3.64
Goran (Extra-large)	10.55

Table 3.4: Comparison of ecosystem carbon stock (Above- and belowground; soil carbon up to 1m depth) of current study to other mangrove ecosystems of the world.

Source	Site	Ecosystem Carbon stock (Mg C ha^{-1})
Present study	Vegetation types, Sundarbans Reserved Forest	159.5 -360.0
Present study	Salinity zones Sundarbans Reserved Forest	170.1 - 336.1
Donato et al. 2011	Indian Sundarbans	~212.5-312.5
Kauffman et al. 2011	Mangrove in Yab, Micronesia	897.8
Kauffman et al. 2011	Mangrove in Babeldoab, Republic of Palau	618.3
Murdiyarso et al. 2010	Mangrove in Kalimatan, Indonesia	488
Adame et al. 2013	Sian Ka'an Biosphere Reserve, Mexico	631.33
Jones et al. 2014	Mangrove Ecosystems in Northwestern Madagascar	443.2

Figure

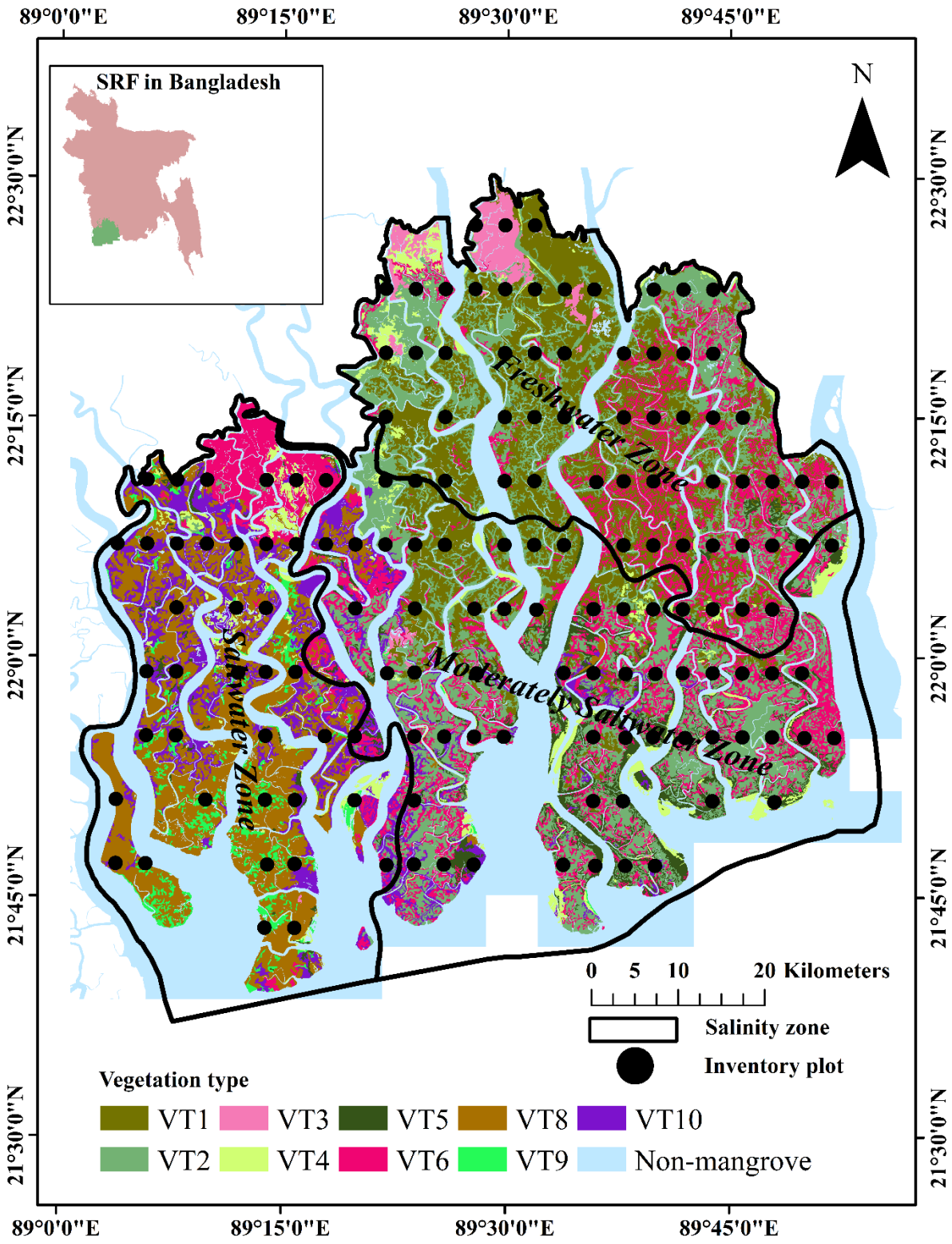

Figure. 3.1 Location of sample plots (black circles) in Sundarbans mangrove forest, Bangladesh.

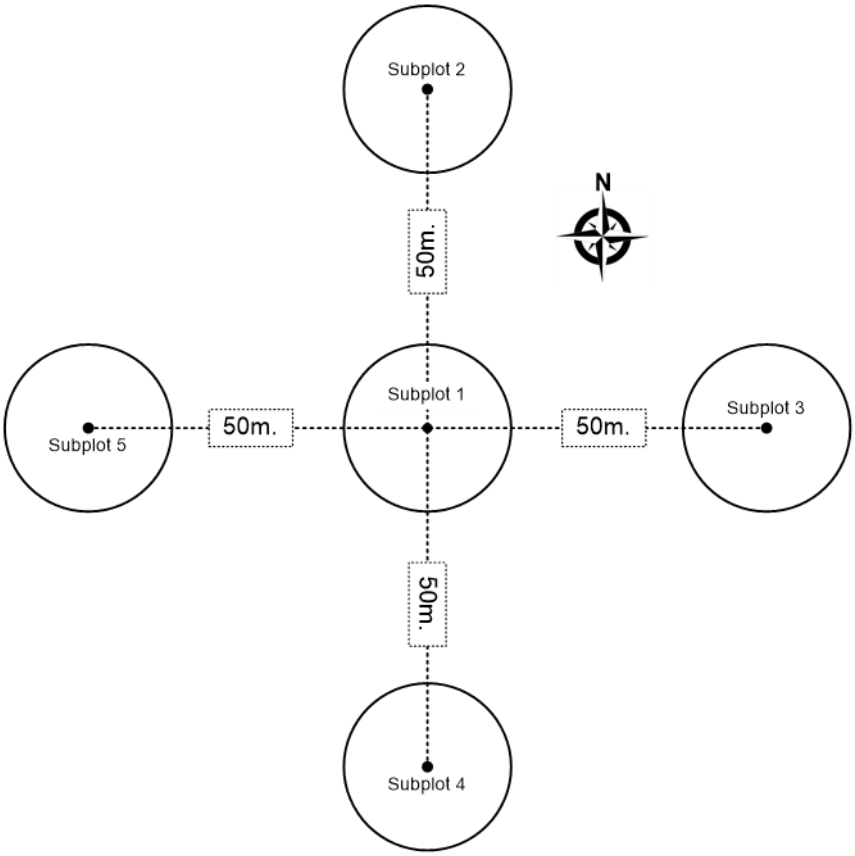

Figure. 3.2 Cluster plot composed of five nested subplots in a main plot.

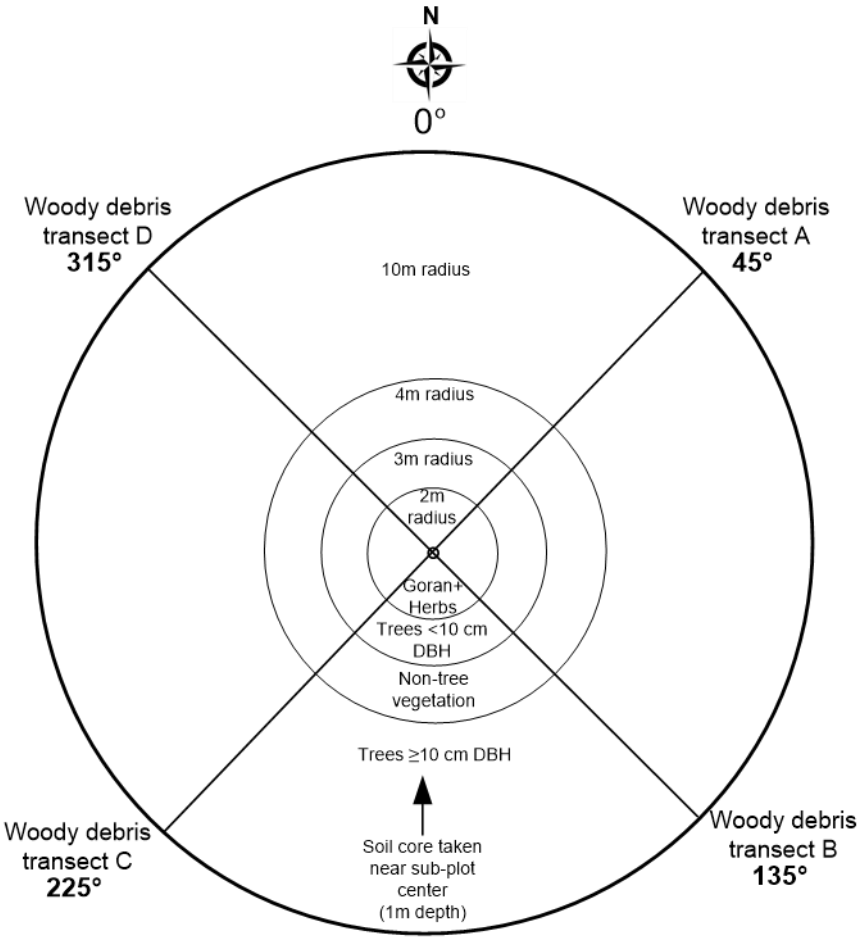

Figure.3.3 Layout of a nested subplot.

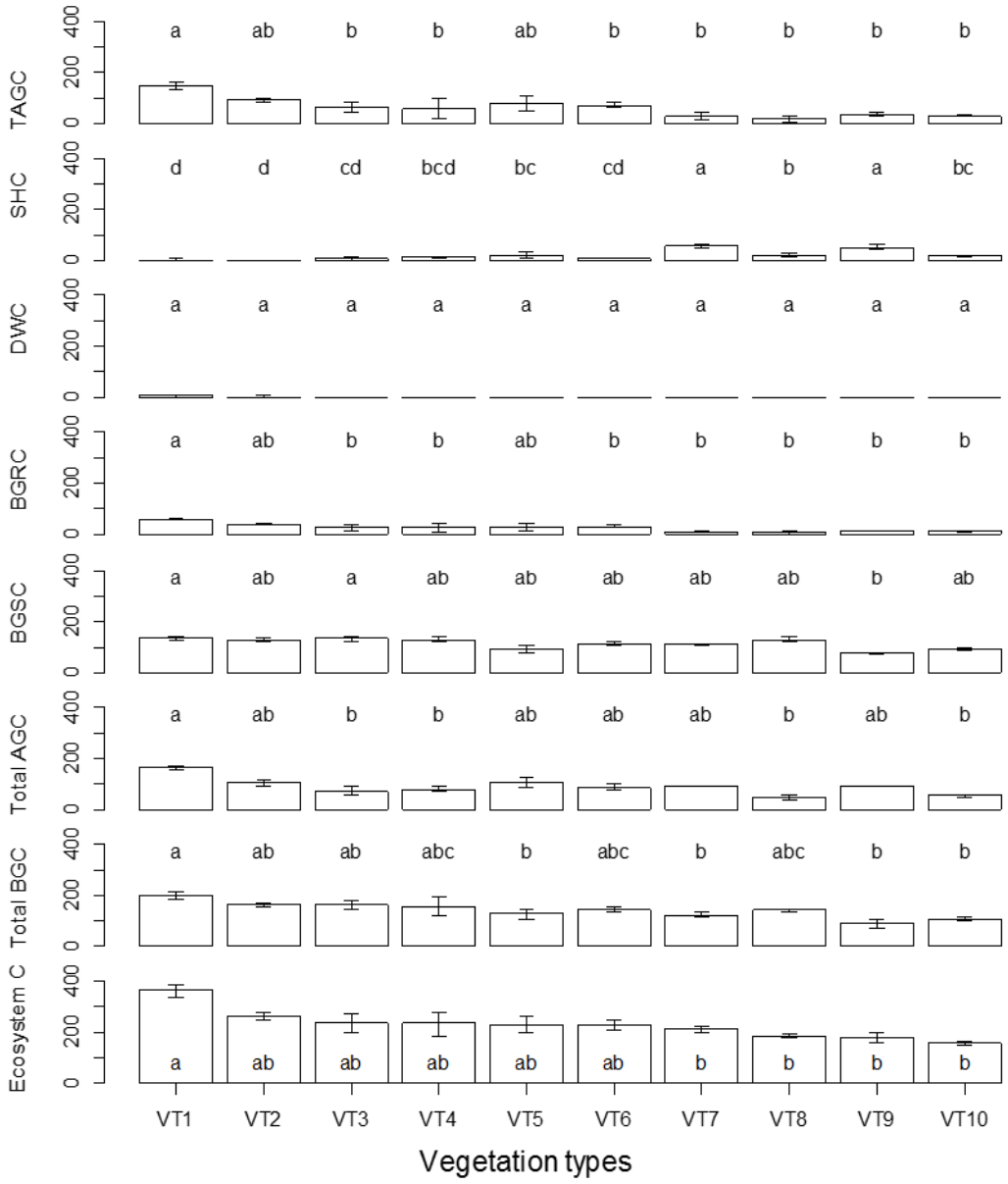

Figure. 3.4 Carbon stock (Mg ha^{-1}, Megagram per hectare ± SE) in different partitions (TAGC = Tree Aboveground carbon, AGC = Aboveground Carbon, SHC = Shrubs and Herbs Carbon, DWC = Downed Wood Carbon, BGRC = Belowground Root Carbon, BGSC = Belowground Soil Carbon), in vegetation types (VT1= Sundri, VT2 = Sundri-Gewa,VT3 = Sundri–Passure-Kankra, VT4 = others (Gewa Mathal, Passur-Kankra-Baen,Sundri-Passur-Keora), VT5 = Gewa, VT6 = Gewa-Sundri, VT7 = Non tree vegetation, VT8 = Goran-Gewa, VT9=Goran, VT10= Gewa-Goran). The same letter(s) among vegetation types are not significantly different (P> 0.05) as tested with Dancun Multiple Range Test.

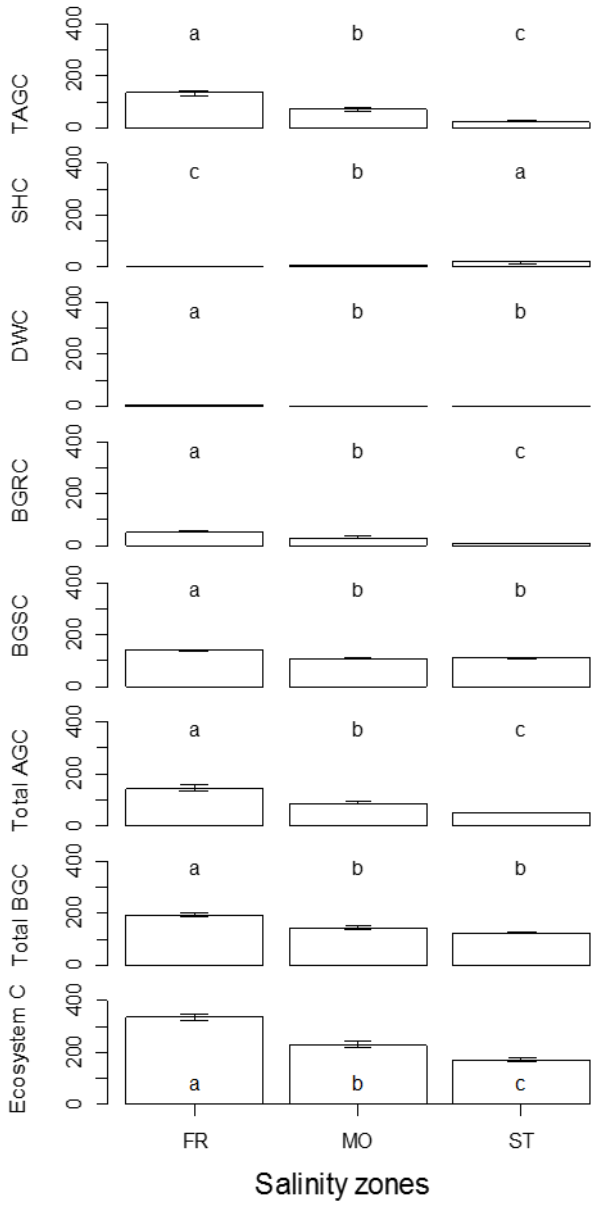

Figure. 3.5 Carbon stock (Mg ha^{-1} ± SE) in different partitions (codes are same as Fig. 2) in the three salinity zones (FR = Fresh water zone, MO = Moderate Saline zone, and ST = Strong Saline Zone). The same letter(s) among salinity zones are not significantly different (P> 0.05) as tested with Dancun Multiple Range Test.

Figure. 3.6 Proportions of aboveground (purple colored), belowground root (orange colored), belowground soil (orange colored) carbon stock in relation to vegetation types (codes are same as Figure 3.4) and salinity zones (codes are same as Figure 3.5)

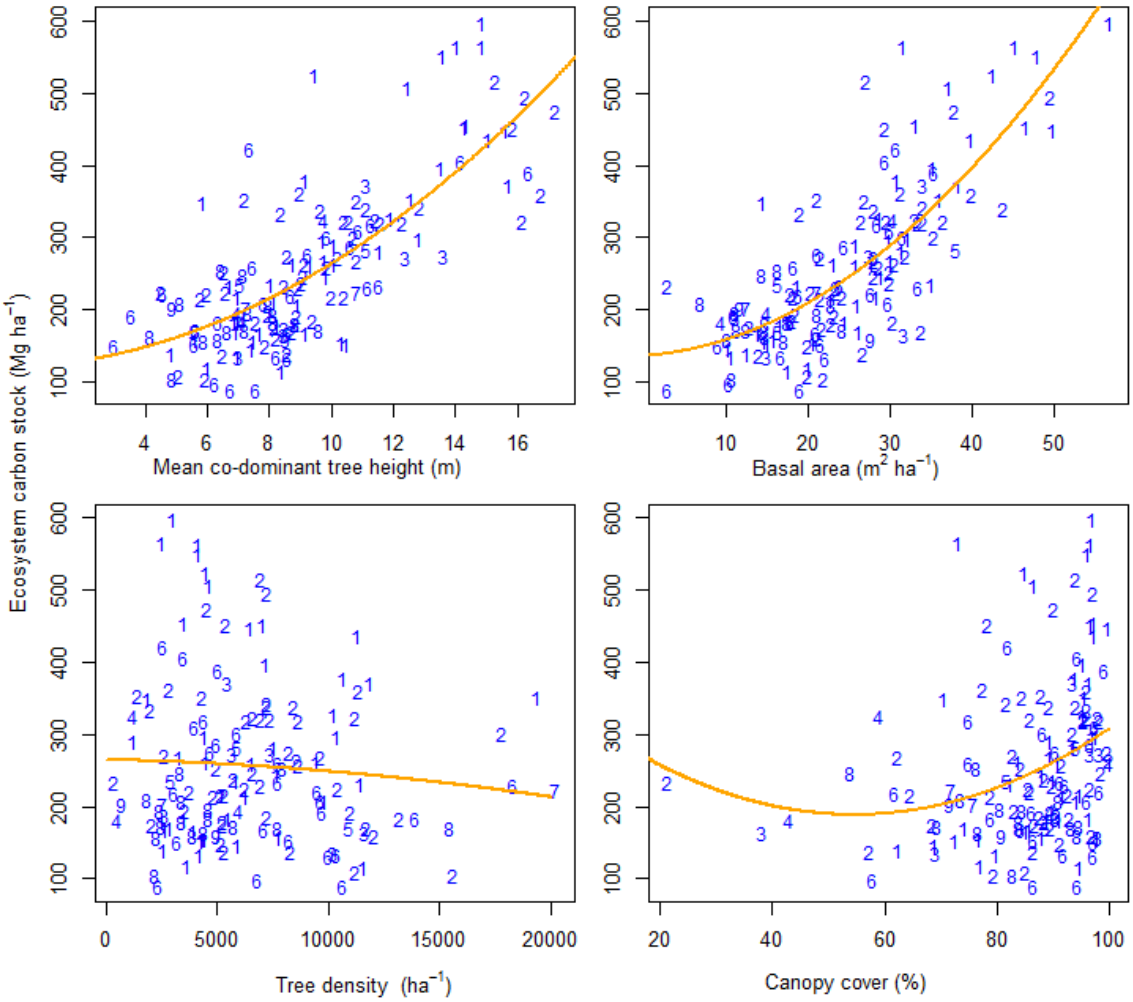

Figure. 3.7 Relationships between ecosystem carbon stock (Mg ha^{-1}) and mean co-dominant tree height (m) (R^2= 0.58, P<0.05), basal area (m^2 ha^{-1}) (R^2= 0.61, P<0.05), tree density (ha^{-1}) (R^2= 0.01, P>0.05) or canopy cover (%) (R^2= 0.09, P>0.05). Data points (plot) represent vegetation types (VT1=1, VT2= 2, VT3 = 3, VT4 = 4, VT5 = 5, VT6 = 6, VT7=7, VT8 = 8, VT9=9, VT10= 10; codes are the same as Fig. 4). The curves were fitted using quadratic equations (Eqns. 4, 5).

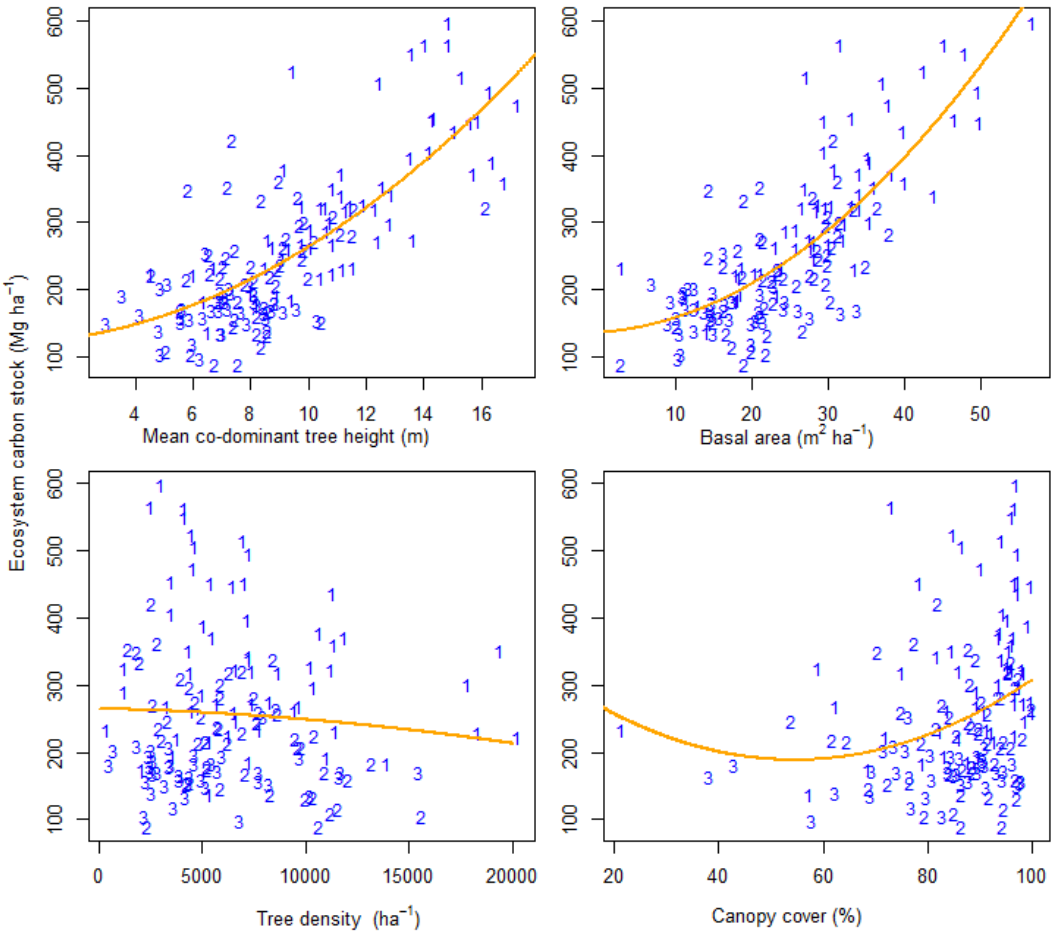

Figure. 3.8 Ecosystem carbon stock in relation to mean co-dominant tree height, basal area, tree density, or canopy cover among different salinity zones. Data points (plot) represent salinity zone (1= Fresh water zone, 2= Moderate Saline zone and 3= Strong Saline Zone). The curves were fitted using quadratic equation (Eqns. 4, 5).

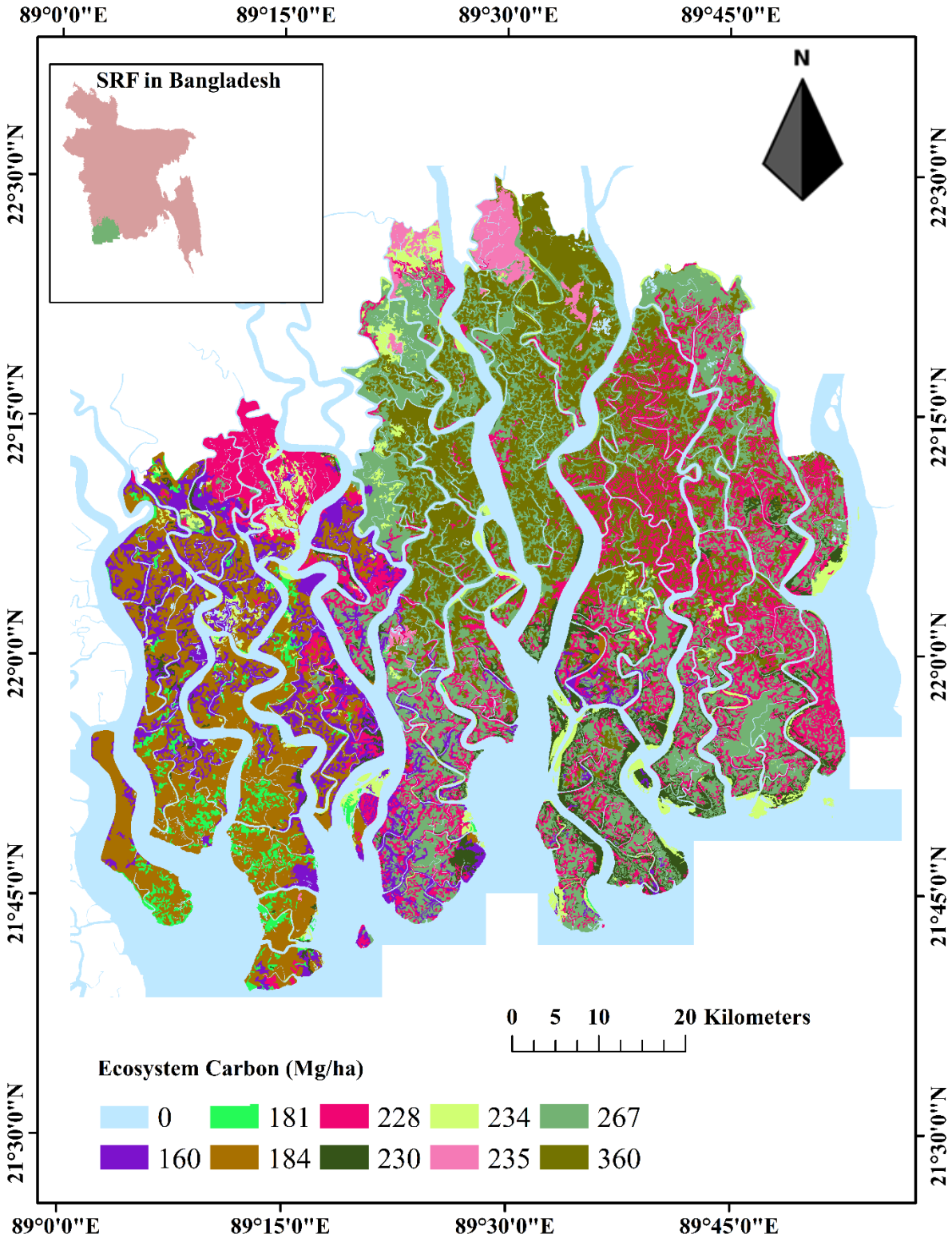

Figure. 3.8 Spatial distribution of ecosystem carbon stock in Sundarbans Reserved Forest (vegetation map 1997 and carbon census 2010).

Chapter 4 High resolution mangrove assessment using optical and radar imagery in Sundarbans East Wildlife Sanctuary.

Introduction

The coastal ecosystems, recently termed as Blue Carbon ecosystems are most carbon dense ecosystems which play an important role in mitigating global climate change by sequestering significant amounts of carbon into sediments and plant biomass (Alongi, 2012b; Donato et al., 2011; Fatoyinbo et al., 2017; Herr et al., 2017; Lagomasino et al., 2015). These ecosystems also provide diverse other ecosystem services to coastal communities including saving their lives and properties of the citizens at the time of cyclones (see chapter 1). (Alongi, 2008; Kathiresan and Bingham, 2001; Kathiresan and Rajendran, 2005; Thant et al., 2010; Uddin et al., 2013). Conservation of these mangrove ecosystems against anthropogenic and natural threats is now a main focus on climate change mitigation programs such as REDD+, because due to these threats mangrove ecosystems may alter in stand structure and species composition (See chapter 1; Giri et al., 2008; Hamilton and Friess, 2018). For effective conservation planning, updated vegetation or species map with horizontal and vertical distribution is necessary which can also be used as the baseline data for evaluation of conservation programs and monitoring of forest dynamics (Heumann, 2011; Kuenzer et al., 2011; O'Connor et al., 2015; Pereira et al., 2013; Petrou et al., 2015).

A traditional approach to assess the mangrove resources has been a field-based inventory. This type of assessment is the most desired, but it requres substantial economic and logistical costs (Kamal and Phinn, 2011). This is a result of remote environment settings, difficult terrain, dangerous conditions, and daily tidal flooding. Considering these constraints, remote sensing has been playing an important role in augmenting field inventories, by increasing spatial and temporal mapping of mangrove areas at the level of species or composition of species which can be of help to sustainable forest management and formation of regional and national policies (O'Connor et al., 2015).Remote sensing (RS) is also useful in fulfilling international biodiversity conservation targets such as Aichi Biodiversity Targets 2020 (O'Connor et al., 2015). Commercial satellites like WordView2 (WV2) & 3, Quickbird, and IKONOS can provide very high-resolution imagery and have the potential to detect species compositions (See details in chapter 1).

Several studies have identified mangrove species using high resolution images (mainly optical) in small areas of natural or plantation mangrove with limited accuracy or few number of species detection (Heenkenda et al., 2014; Kamal et al., 2015; Kamal and Phinn, 2011; Neukermans et al., 2008; Wang et al., 2004; Zhu et al., 2015). However, the vertical structure of

forests e.g. canopy height, can also contribute in improving classification accuracy which can be mapped using radar and LiDAR images (See chapter 1). Thus, application of the high-resolution imagery by incorporating both multispectral and radar images (less costly than LiDAR and have large spatial coverage) to a large natural mangrove area like Sundarbans Reserved Forest (SRF) will generate new knowledge in remote sensing of mangrove species. Furthermore, in the view point of REDD+, monitoring of biodiversity is necessary to safeguard biodiversity as REDD+ has dual objective, climate change mitigation as well as biodiversity co benefit (Imai et al., 2014). In monitoring of biodiversity indicators, remote sensing can play an important role, particularly very high resolution imagery because some essential biodiversity indication of CBD can directly or indirectly be monitored by remote sensing such as species, species composition and canopy structure (Imai et al., 2014; O'Connor et al., 2015; Pereira et al., 2013; Petrou et al., 2015).

In this study, thus, for making a high-resolution species or vegetation type map, using WV2 and TanDEM-X (TDX) image, I selected Sundarbans East Wildlife Sanctuary (SEWS) as a pilot study site because of its proximity to three salinity zones because salinity is one of the major determining factors of species composition in SRF and high biodiversity (Rahman et al., 2015b). The objectives of my study were 1) to produce a high-resolution vegetation maps in SEWS, 2) to quantify vegetation canopy height map using TDX image and 3) Combine multispectral and canopy height data to test the improvements of classification methods in SEWS.

Methodology

Study area

In the SRF in Bangladesh, there are three protected areas under the World Heritage Site, which was declared by UNESCO in 1997; Sundarbans West Wildlife Sanctuary (SWWS), Sundarbans South Wildlife Sanctuary (SSWS), and Sundarbans East Wildlife Sanctuary (SEWS). The three sanctuaries are situated along the coast of SRF and cover a total of 139,699 ha (23% of the entire SRF; Rahman et al., 2017). In 2017, the country of Bangladesh increased the size of the three wildlife sanctuaries and it has now a total area of 317,950ha (52% of the whole SRF; BFD, 2107). The main purpose of the expansion of the protected areas was to a provide free breeding ground for wildlife and help enhance the biodiversity conservation, especially for the Bengal tiger. The SWWS is in the high saline zone, which is mainly dominated by *Ceriops decandra* and *Excoecaria agallocha* (Rahman et al., 2017). The SSWS falls between a moderate saline and strong saline zones which make the region more diverse. It is mainly dominated by *Heritiera fomes, E. agallocha*, and *C. decandra* forest type. The SEWS is the closest to the freshwater zone and is mainly dominated by *H. fomes* (Rahman et al. 2017; Fig. 4.1). In this study, we concentrated

on SEWS within the old sanctuary boundary that covers 40,768 ha as delineated by the Bangladesh Forest Department. The mean annual maximum and minimum temperatures vary between 32 and 20°C. Mean annual relative humidity varies from 77 to 80 %. The mean annual rainfall ranges between 1900 and 2500 mm. In 2010, under the financial support of USAID, Forest Department of Bangladesh conducted a forest carbon inventory at 150 plots. Out of these 150 plots, nine fall in the SEWS which were used in this study as field data (Rahman et al., 2015). As each plot composed of five nested circular (10 m radius) subplots, the 45 subplots (9 x 5) wise species data were used in this study. The stand structural parameters of these nine plots were given in table 4.1 and 4.2.

Remote sensing data processing

For the classification of mangrove species in SEWS, I used two types of earth observations: (1) passive sensor high resolution (2 m pixel) from WV2 and (2) active sensor e.g., TDX SAR images (12 m pixel). The WV2 imagery provides multispectral information about land cover types, while the TDX imagery is used to produce accurate canopy height models for mangrove forests (Lagomasino et al., 2016; Lee et al., 2015). WV2 imagery is comprised of 8 multispectral bands that cover wavelengths between 430 and 1050 nm. The spectral range of these 8 multispectral (MS) bands are coastal blue (400–450 nm), blue (450–510 nm), green (510–580 nm), yellow (585–625 nm), red (630–690 nm), red edge (705–745 nm), NIR1 (770–895 nm) and NIR2 (860–1040 nm) (Rapinel et al. 2014). Three images from December 26, 2015 and one from January 15, 2016 were acquired from Digital Globe through the NextView License Agreement (Neigh et al., 2013). Each image was radiometrically corrected in ENVI image analyzing software and passed on to Fast Line-of-sight Atmospheric Analysis of Hypercubes (FLAASH) to account for atmospheric effects. After corrections, the three images were mosaicked, and several normalized band ratios were determined from the multispectral data to provide supplemental information into the classification. Band ratios can be helpful in reducing errors associated with land type classification modeling. The band ratios used are:

1. Normalized Difference Vegetation Index

   (NIR 1 band - Red band) / (NIR 1 band + Red band) (Eq. 4.1)

2. Normalized Difference Vegetation Index (Green)

   (NIR 1 band - Green band)/ (NIR 1 band + Green band)

   (Eq. 4.2)

3. Normalized Difference Vegetation Index (Red Edge)

(NIR 1 band - Red Edge band)/ (NIR 1 band + Red Edge band)

(Eq. 4.3)

4. Normalized Difference Vegetation Index (NIR)

(NIR 1 band - NIR 2 band)/ (NIR 1 band + NIR 2 band)

(Eq. 4.4)

For this classification scheme, we combined information about the land cover types (multispectral and band ratios) and forest structure (TDX canopy height) to help distinguish generalized mangrove species types. The forest canopy height data generated from TDX (originally at a 12 m spatial resolution), by following a novel inversion approach, Random Volume over Ground (RVoG; see Lee and Fatoyinbo, 2015 for details). This process was done by using single-polarization TDX yielded top canopy height maps of mangrove forests by taking an advantage of flat underlying topography (i.e. water surface) in mangrove environments (Lee et al., 2016; Lee and Fatoyinbo, 2015). The 12 m pixel image was resampled to the same spatial resolution as the WV2 imagery (approximately 2 m). In total, there were 13 different map layers that were used in the unsupervised classification scheme; 8 multispectral, 4 band ratios, and 1 height layer.

Unsupervised classification

All the 13 different layers (multispectral, band ratios, and canopy height) were used in an unsupervised classification scheme (Fig. 4.2). We used the Iso Cluster Unsupervised Classification algorithm in ArcMap 10.2.1. The ISODATA algorithm is the method of iteration that makes clusters of similar groups into one by measuring the Euclidean distance between cluster center and similar groups or data (Dhodhi et al., 1999). In the classification, we set three parameters: Number of classes = 50, Minimum class size = 10, and Sample interval = 5. The classification tool returns a 1-band image with numbered land cover types.

Class assigning and filtering

I assigned the vegetation or species and other land cover type in each of 50 classes that were produced in the unsupervised image classification step. The assignment of vegetation was done mainly by hand using field inventory data based on the overstory basal area or abundance. For some classes, cover types were assigned based on field photos, expert knowledge and Google Earth image visual interpretation because those classes were not found in the 45 subplots (Fig. 4.3.1 and 4.3.2). Those classes were occupied by *Sonneratia apetala*, *Nypa fruticans*-mixed and other non-mangroves such as shrubs, grass waterbody, and mudflat. Once land cover classes were

identified, those classes that were similar were then combined into one class except the canopy gaps and shadow classes which are more frequent in fine resolution image. Also, to remove noise associated with edge effects of standing water we applied two majority filters. The majority filter selected the highest occurrence of class values within a 3-pixel x 3-pixel kernel for removing small shadows or canopy gaps, while for removing bigger canopy gaps or shadows I set kernel size of 11-pixel x 11-pixel only for the canopy gap classes. The bigger kernel sized filter added the shadows or canopy gap to neighboring dominant class. After application of these two filters, some canopy gaps or shadows were found particularly within the dominant class of *H. fomes* which then added to this class. The class assignment and filtering were performed using ENVI (Version 5.2).

Accuracy assessment

I randomly generated 356 point following multinomial probability theory as the dominant class (*H. fomes*) in my study covering close to 50% (45%) of the whole SEWS. This procedure allows me to assess accuracy of the approach with 95% Cl (Congalton and Green, 2009). The reference point class type was confirmed by visual interpretation of Google Earth images in the same year of image acquisition, hand captured photo visualization, and expert field knowledge (Congalton, 2001; Rahman et al., 2015; Rahman et al., 2017; Yu and Gong, 2012).

Results

Land cover type

A total of 14 land cover classes were identified at SEWS using two datasets: WV2 with and without TDX. Of the 14 classes, nine were covered by trees, shrubs, and palms (TSP; 65.01-65.02 %), two were herbs and grasses (HG; 1.17-1.18 %) and three were sandbars, mudflats, and waterbodies (SMW; 33.80-33.80%; Table 4.3). Three classes were separated at the species level e.g. HEFO (*H. fomes*), EXAG (*E. agallocha*), and SOAP (*S. apetala*), while four classes were identified as mixed species types where the first species listed was the dominant species within the class (Table 4.3). A mixed class also identified which was composed of multiple species (NYFR MIXED: *Nypa fruticans, Sonneratia caseolaris, S. apetala, Phoenix paludosa, Hibiscus tiliaceous and Avicennia officinalis*). This mixed type was mainly found along rivers and canal banks. The spatial distribution of these land cover classes is shown in Fig. 4.4. The total areas of the SEWS mapped in this study was 32.930.77 ha where 67.7% was land and the remaining 32.3% was water according to WV2 and TDX image classification. I did not find any significant difference between the two classification maps, WV2 and WV2-TDX. The total difference was

0.10% of the total area (Table 4.3). The most dominant vegetation type in terms of area was HEFO which covered 44.76-44.82% of the total area of SEWS based on WV2 and WV2-TDX classification maps, while the other three dominant types EXAG-HEFO, HEFO-EXAG and EXAG covered, 6.84%, 6.34%, and 3.02%, respectively (Table 4.3).

There was clear zonation found in SEWS, where in most cases, stands became more monospecific with increasing distance from the shore (Fig. 4.6). For example, from the canal bank to inland the presence of vegetation types was, NYFR-MIXED followed by EXAG-NYFR, then either followed by EXAG-HEFO or HEFO-EXAG, followed by HEFO or EXAG (Fig. 4.6). Several other zones were also found (big canal and river side) such as SOAP or EXAG or EXAG-HEFO followed by HEFO or EXAG-HEFO and then followed by EXAG or HEFO.

Accuracy assessment

The overall classification showed a strong agreement between the WV2 and WV2-TDX classification maps and the reference points, yielding an overall accuracy and the Kappa Coefficient were 89.89% and 0.89, and 89.33% and 0.88, respectively for WV2 and WV2-TDX based classifications (Table 4.4 and 4.5). The specific land cover accuracy, also revealed that there was strong agreement between most of the land cover types of WV2 and WV2-TDX and random reference points (Table 4.4 and 4.5). The SANDBARS had higher producer's and user's accuracy. The most dominant tree species HEFO, had similar producer's accuracy in both WV2 and WV2-TDX based classification but slightly lower user 's accuracy in WV2 than WV2-TDX (Table 2 and 3). While EXAG showed the best User's and Producer's accuracy in both WV2 and WV2-TDX classification among the tree species (Table 4.4 and 4.5). In both WV2 and WV2-TDX classification, SOAP and NYFR MIXED had lower producer accuracy (Table 4.4 and 4.5).

HEFO dominant vegetation type had higher canopy height (12.30±2.93 m) than other 8 vegetation types, while SHRUBS dominated forest has lowest canopy height (7.37±3.95m; Fig. 4.5).

Discussion

In this study, I applied a hybrid classification scheme for separating vegetation at the community level in a complex natural mangrove in SRF by combining high resolution optical (WV2) and radar (TDX) imagery. The classification was performed using the ISODATA Algorithm and showed a strong agreement with Google Earth visual interpretations and field inventory data. Both classifications could separate mangrove from non-mangrove, here we termed it as TSP which covered more than two-thirds of the total areas of SEWS (Table 4.3). Any

significant difference was found between the two classifications (WV2 and WV2-TDX) in land cover identification which suggesting that the inclusion of TDX in classification has almost no contributions in vegetation classification within the area of study (Table 4.3). So, high resolution WV2 bands along with the four vegetation indices (used in this study), can separate dominant mangrove species and communities with higher accuracy. Though I did not find any significant contribution of canopy height in species identification in the current study, it may have some contribution if the whole SRF is considered, because the canopy height in SRF tends to increase from seaward to landward and east to west direction (M. M. Rahman et al., 2015b). Furthermore, tree height can be useful in biomass carbon assessment upon coupling with field data (Aslan et al., 2016). Also, here I noticed that the canopy height of dominant species (*H. fomes*) becomes shorter when it has found in mixed stands, for example in case of HEFO-EXAG and EXAG-HEFO classes. The reason behind this difference may be due to the variation of site conditions between monospecific and mixed stand (Fig. 4.6). However, further field-based study may explore the actual causes of this height difference.

The dominant class (HEFO) in SEWS was identified as *H. fomes*, among the 14-land cover types in this study which were also reported by Rahman (2003). However, Islam et al. (2014) reported that *E. agallocha* was more dominant than *H. fomes* in SEWS based on Importance Value Index (IVI-average value of relative -abundance, -frequency and -dominance of species; *E. agallocha* = 35.932 and *H. fomes* =35.656) which means that both *H. fomes* and *E. agallocha* should be about equal coverage in the SEWS. They laid out 12 transects of 200 m long with two plots (20m x 50m): one at 0-50m (stream side) and another at 150-200 m (inland side; they called it "forest proper") from river or canal bank in SEWS. Within this distance, I found NYFR MIXED class (stream side of canal) and EXAG, HEFO or EXAG-HEFO or HEFO-EXAG (forest proper). The spatial distribution of species or groups of species in this study reveals,that *H. fomes* stands are mainly found in the inner -most parts of almost all islands (Fig. 4.4). Islam et al. (2014) reported that the near shore site was the most diverse which I also found in my study. However, their report suggested that the protected areas were dominated by *E. agallocha*. My findings suggest that ~45% of the total area in the SEWS was covered by *H. fomes* while *E. agallocha* covered only 3% (Table 4.3 and Fig. 4.4). Thus, the current approach can overcome some of the spatial limitations and potential biases of field plot-based studies and represents the spatial distribution of species or group of species more accurately with the use of high resolution satellite imagery.

Both the error matrix and visual interpretation reveal that the produced map in the present study matched well with randomly sampled ground truth points and inventory plots (Table 4.4

and 4.5; Kamal et al., 2015; Kamal and Phinn, 2011; Neukermans et al., 2008; Wang et al., 2004; Zhu et al., 2015). The overall accuracy of both data sets (WV2 and WV2-TDX; 89.33% and 89.89%) in my study, were similar to that of Zhu et al. (2015b) that report an overall accuracy of 89% in mapping mangrove species in Lingding Bay of the Pearl River Estuary, Guangdong Province, China using WV2 image. Heenkenda et al. (2014) also found in Northern Territory, Australia a high accuracy (89%) where they also used WV2 image for mapping mangrove at species level following a supervised classification method. While in my study the overall accuracy was much higher than Kamal et al. (2015), another study in Moreton Bay mangrove in Queensland, Australia using WV2 image for mapping three *Avicennia species*, (overall accuracy of 54%). The above-mentioned studies, followed a supervised classification method in separating mangrove species in relatively small areas of either natural or restoration sites with clear homogeneous patches where there was a limited number of species identified. However, in my study, I used unsupervised method in a large complex natural mangrove ecosystem in SRF (32930.76 ha) and produced maps with representative dominant and mixed species.

The spatial distribution of species in my study, suggested that there is clear zonation in the SEWS. This was because I separated big homogeneous patches of three species (*H. fomes*, *E. agallocha* and *S. apetala*). Also, the six other vegetation types showed a distinct zonation where in most cases, transition started from shore to inland. For example, from the bank of small river or canal, we found either *Nypa fruticans* or mixed stand of *N. fruticans, P. paludosa, S. apetala,* and *A. officinalis,* followed by mixed stands of *E. agallocha* and *N. fruticans*, or *E. agallocha* and *H. fomes* or *H. fomes* and *E. agallocha,* which ended up with a monospecific zone of either *E. agallocha* or *H. fomes* (Fig. 4.4). While the seaward or big river bank forest margin was formed with either *S. apetala* or *E. agallocha* followed by monospecific stands of either *E. agallocha* or *H. fomes,* then followed by mixed stands of *E. agallocha* and *H. fomes, A. officinalis* and *E. agallocha* or *H. fomes* and *E. agallocha* and ended up with monospecific zone of *H. fomes* (Fig. 4.4 and 4.6). My findings contrasted with the field-based study on zonation patterns in Sundarbans Reserved Forest (Ellison et al., 2000) . Ellison et al. (2000). where they examined at 11 blocks by randomly laying out three random 200-m transects at each block in the whole SRF and concluded with no specific zonation exist in SRF. Limited number of transects (at two blocks with six transects within 32930.76 ha) in SEWS, may not be enough for observing species zonation or the traditional sampling method of sequential quadrats which may not be in line with natural distribution or species zoning. Further study, may be necessary to explore the reason behind this zonation. For example, it may occur either by different geomorphology or plant physiology or climate change or sea level rise or their combined effects.

Visual interpretation with Google Earth showed that there was minor misclassification between mudflat, SOAP, EXAG, and GRASS1, and NYFR MIXED especially in open or sparsely-dense areas. This may be a result of the complicated mangrove environment, where the spectral reflectance values measured by WV2 over the mangrove vegetation can be affected by wet soils and water and atmospheric vapor (Adam et al., 2010; Chauvaud et al., 1998; Heenkenda et al., 2014). SOAP was misclassified mostly by HEFO (12%), followed by GRASS1, EXAG-HEFO, NYFR MIXED, and WATERBODY MUDFLATS type which also confirmed by Google earth visual interpretation and expert knowledge (Table 4.4 & 4.5). *S. apetala* is a pioneer species in Sundarbans and primarily found in a newly colonized land and along the bank of canals and creeks, whereas the *H. fomes* is the climax species and primarily located in the more stable and high land. However, visually it was found that in some cases, especially in newly formed areas, the *S. apetala* was misclassified as *H. fomes* (Fig. 4.4). This may have been a result from shadow effects or because of similar height structure or similar spectral signature (Adam et al., 2010). In its mature state, *S. apetala* is taller than *H. fomes*, but at earlier life stages its height is similar to *H. fomes.* But, as it was found in both WV2- and WV2-TDX, new methods or further research is needed to improve the separability to better distinguish *S. apetala* and *H. fomes*.

Two more species such as *A. officinalis* (very large tree with wide spread canopy) from EXAG-AVOF class and *N. fruiticans* (usually grows along the canal bank as big clear patches) from NYFR MIXED class should be separated which was also confirmed by visual interpretation and expert knowledge that both species appeared as unique at one place but, in another place, they appeared as combined. However, in ISODATA unsupervised classification in both datasets (WV2- and -TDX) they appeared in their respective class. In the case of NYFR MIXED, misclassification was mainly between EXAG-HEFO (13.04%-17.39 %) and EXAG-NYFR (7.41 %- 8.70%; Table 4.4 & 4.5). The misclassification between NYFR MIXED and EXAG-HEFO may have happened due to the presence of common liana or vines (usually found along the canal bank or streamline in SEWS) over the canopy of these species which was difficult to be separated by both WV2 and WV2-TDX. Similarly, this liana and *H. tiliaceus* may also misclassified as *A. officinalis* as their appearance was quite similar and could not be separated in my study.

RS based monitoring of biodiversity indicators has been recognized to global biodiversity forum such as Convention of Biological Diversity (CBD), as RS has been playing an important role in cost effective measurement of spatiotemporal distribution of forest species composition or functional type as biodiversity indicators (Kuenzer et al., 2014; O'Connor et al., 2015; Petrou et al., 2015). To achieve the Aichi Biodiversity Targets 2020, Pereira et al. (2013) synthesized 22 essential biodiversity variables (EBVs) for monitoring global biodiversity. Out of these 22 EBVs,

14 can be assessed directly or indirectly by remote sensing (O'Connor et al., 2015). In REDD+, it is necessary to report even at fine scales deforestation and forest degradation in Monitoring Reporting and Verification section which can be possible if fine resolution satellite imagery is used (Herold et al., 2011). Very High Resolution (VHR) satellites e.g. WorldView can be useful in mapping at the species level or at tree community level (Petrou et al., 2015). Using WV2, I was able to separate three vegetation types at the species level, while six and other classes were a combination of two and more species. I mapped these mangrove classes with a high level of accuracy (Table 4.4-4.5) which directly matched the EBV's variables such as species abundance and distribution, ecosystem composition, functional type and ecosystem extent (O'Connor et al., 2015). The mangrove and non-mangrove were also separated at certain level of accuracy in my study.WV2 can also be used in monitoring of deforestation and forest degradation and thereby contribute to REDD+ MRV. Furthermore, the canopy height (a structural biodiversity indicator) maps can be coupled with *in situ* data (see Rahman et al. 2015) for assessing the level of ecosystem service such as carbon storage, which one of the major requirements of REDD+ MRV. It is also related to the EBVs: trends in distribution, condition, and sustainable ecosystem services for equitable human well-being (Petrou et al., 2015). So, WV2 and radar imagery can be instrumental in future monitoring of mangrove biodiversity indicators, deforestation and forest degradation which would be helpful for monitoring, reporting, and evaluation of CBD targets and REDD+.

Conclusion

In this study, I combined both high resolution optical WV2 and TDX canopy height imagery to classify mangrove species and land cover types following an ISODATA unsupervised approach. The result of my study, showed a strong agreement with field referenced data and photography, visual interpretation with Google Earth, and expert knowledge. The overall classification accuracy was 89.89-89.33 % with a kappa coefficient range of 0.89-0.88. I could not find any significant difference between the land cover classifications with the inclusion of height layer with WV2 data set. Three species separated at the species level along with six other mixed classes where *H. fomes* (44.54%), *E. agallocha* (3.02 %) and *S. apetala* (1.41-1.46 %) covered 49.24 % of total land area of the SEWS. So, *H. fomes* is the most dominant species in SEWS not *E. agallocha* as previously thought. I found clear species zonation in SEWS, though more information is needed to identify the factors responsible for this zonation. Finally, my study suggested that mangrove biodiversity indicators (either in the form of species level or functional type, forest cover and carbon stock change) can be monitored by using WV2 imagery, which could be supported in policy formulation of REDD+ and CBD.

Table and Figure

Table

Table 4.1: Plot level species composition and forest characteristics across the SEWS

Species	Number tree	Basal area (m^2 ha^{-1})	Relative abundance (%)	Relative dominance (%)	Mean DBH (cm)	Canopy Cover %	Canopy height (m)
1024							
HEFO	123	13.98	70.69	48.51	14.47±0.39		
EXAG	42	4.13	24.14	14.34	13.58±0.56	94.12±2.04	11.13±0.38
SOAP	9	10.70	5.17	37.15	46.79±4.91		
Total	174	28.81	100.00	100.00	15.93±0.67		
1075							
HEFO	88	7.54	52.07	57.34	12.88±0.26		
EXAG	80	5.54	47.34	42.12	11.65±0.20	92.46±3.69	7.58±0.37
AVOF	1	0.07	0.59	0.55	12.00		
Total	169	13.15	100.00	100.00	12.29±0.17		
1076							
HEFO	90	14.05	76.92	76.49	16.37±0.71		
EXAG	14	1.69	11.97	9.19	15.10±1.02		
XYME	6	1.81	5.13	9.84	21.25±5.51	89.18±6.15	9.67±0.46
XYGR	4	0.57	3.42	3.08	16.38±2.26		
AMCU	3	0.26	2.56	1.39	12.87±1.58		
Total	117	18.36	100.00	100.00	16.38±0.63		
1078							
HEFO	97	14.03	61.01	65.67	16.33±0.49		
EXAG	62	7.34	38.99	34.33	14.72±0.58	84.30±3.71	6.58±0.10
Total	159	21.37	100.00	100.00	15.70±0.38		
1080							
HEFO	172	21.90	82.69	82.18	15.25±0.36		
XYME	18	3.07	8.65	11.51	17.75±1.24	97.30±1.57	10.86±0.27
EXAG	18	1.68	8.65	6.30	13.43±0.61		
Total	208	26.64	100.00	100.00	15.31±0.33		
1082							
HEFO	101	16.44	71.13	74.56	17.44±0.47		
EXAG	36	5.13	25.35	23.29	16.40±0.69		
AMCU	4	0.39	2.82	1.76	13.73±1.45	81.96±5.42	11.57±0.30
UNSP	1	0.08	0.70	0.38	13.00		
Total	142	22.04	100.00	100.00	17.04±0.38		
1135							
HEFO	187	21.17	84.62	86.32	14.66±0.25		
EXAG	32	3.24	14.48	13.21	13.86±0.59		
XYME	1	0.06	0.45	0.26	11.40	95.32±1.45	7.39±0.19
AMCU	1	0.05	0.45	0.21	10.20		
Total	221	24.53	100.00	100.00	14.51±0.23		
1137							
HEFO	99	10.20	64.29	63.67	13.86±0.38		
EXAG	51	5.15	33.12	32.15	13.71±0.53		
XYME	2	0.52	1.30	3.23	21.85±6.35	95.53±1.04	9.16±0.17
CYRA	1	0.05	0.65	0.31	10.00		
EXIN	1	0.10	0.65	0.64	14.30		
Total	154	16.01	100.00	100.00	13.89±0.32		
1138							
HEFO	148	22.44	79.14	87.05	16.47±0.47		
EXAG	39	3.34	20.86	12.95	12.93±0.34	92.01±1.32	16.17±0.21
Total	187	25.78	100.00	100.00	15.74±0.39		

HEFO = *Heritiera fomes*, EXAG =*Excoecaria agallocha*, SOAP = *Sonneratia apetala*, AVOF= *Avicennia officinalis*, XYME = *Xylocarpus mekongensis*, EXIN = *E. indica*, CYRA = *Cynometra ramiflora* XYGR = *Xylocarpus granatum*, XYME = *X. mekongensis*, UNSPP = Unknown species

Table 4.2: Structural composition and mean DBH (± S.E.) of mangrove species in the SEWS

Species	Number of tree	Basal area (m^2 ha^{-1})	Relative abundance (%)	Relative dominance (%)	Mean DBH (cm)
HEFO	1105	15.75	72.18	72.06	15.30±0.14
EXAG	374	4.14	24.43	18.93	13.65±0.19
XYME	27	0.61	1.76	2.77	18.60±1.51
SOAP	9	1.19	0.59	5.44	46.79±4.91
AMCU	8	0.08	0.52	0.35	12.9±60.95
XYGR	4	0.06	0.26	0.29	16.38±2.26
UNSP	1	0.01	0.07	0.04	13.00
AVOF	1	0.01	0.07	0.04	12.00
CYRA	1	0.01	0.07	0.03	10.00
EXIN	1	0.01	0.07	0.05	14.30
Total	1531	21.86	100.00	100.00	15.12 ±0.14

Table 4.3. Comparison of land cover areas between WV2- and -TDX in SEWS.

Landcover type	WV2 (E1)		WV2-TDX (E2)		E1 -E2/E1 (%)
	Area (ha)	Percentage	Area (ha)	Percentage	
HEFO	14761.14	44.82	14741.15	44.76	0.00
EXAG	993.09	3.02	996.02	3.02	0.00
SOAP	465.92	1.41	479.50	1.46	-0.03
HEFO-EXAG	2086.76	6.34	2090.71	6.35	0.00
EXAG-HEFO	2251.32	6.84	2251.38	6.84	0.00
EXAG-NYFR	200.26	0.61	200.63	0.61	0.00
AVOF-EXAG	483.61	1.47	485.52	1.47	0.00
NYFR-MIXED	145.84	0.44	146.25	0.44	0.00
SHRUBS	19.81	0.06	20.40	0.06	-0.03
GRASS 1	180.20	0.55	181.70	0.55	-0.01
GRASS2	203.52	0.62	205.90	0.63	-0.01
SANDBAR	54.77	0.17	54.58	0.17	0.00
WBSBMF	433.21	1.32	439.28	1.33	-0.01
WATERBODY	10651.32	32.34	10637.73	32.30	0.00
Total	32930.76	100.00	32930.77	100.00	-0.10

HEFO = *Heritiera fomes*, EXAG =*Excoecaria agallocha*, SOAP = *Sonneratia apetala*, AVOF= *Avicennia officinalis,* NYFR MIXED: *Nypa fruticans, Sonneratia caseolaris, S. apetala, Phoenix paludosa, Hibiscus tiliaceous,* and *A. officinalis, GRASS1= Grasss-Tigerfern,* GRASS1= Grasss, WBSBMF= Waterbody, Sandbars and Mudflat

Table 4.4. Error matrix between WV2 derived land cover class and ground truth point. Elaboration of land cover type code is the same as that in table 4.3.

WV2 classes	Google Earth observation classes														Total	User %	Commission%
	1	2	3	4	5	6	7	8	9	10	11	12	13	14			
1	26	0	3	1	2	0	0	0	0	0	0	0	0	0	32	81.25	18.75
2	0	27	0	1	1	0	1	0	0	0	0	0	0	0	30	90	10
3	1	0	17	0	0	0	0	0	1	0	0	0	1	1	21	80.95	19.05
4	0	2	0	26	0	0	0	0	0	0	0	0	0	0	28	92.86	7.14
5	1	0	1	1	20	1	0	3	0	0	1	0	1	0	29	68.97	31.03
6	0	0	0	0	1	23	1	2	0	0	0	0	0	0	27	85.19	14.81
7	0	0	0	0	0	2	19	0	0	0	0	0	0	0	21	90.48	9.52
8	0	0	1	0	1	0	1	18	0	0	0	0	0	0	21	85.71	14.29
9	0	0	0	0	0	0	0	0	23	0	0	0	0	0	23	100	0
10	0	0	0	0	0	0	0	0	0	24	0	0	0	0	24	100	0
11	0	0	2	0	0	0	0	0	0	1	21	0	0	0	24	87.5	12.5
12	0	0	0	0	0	0	0	0	0	0	0	25	0	0	25	100	0
13	0	0	1	0	0	0	0	0	0	0	0	0	24	0	25	96	4
14	0	0	0	0	0	0	0	0	0	0	0	0	1	25	26	96.15	3.85
Total	28	29	25	29	25	26	22	23	24	25	22	25	27	26	356		
Producer %	92.86	93.1	68	89.66	80	88.46	86.36	78.26	95.83	96	95.45	100	88.89	96.15		Overall Accuracy	89.33
Omission %	7.14	6.9	32	10.34	20	11.54	13.64	21.74	4.17	4	4.55	0	11.11	3.85		Kappa	0.88

1 = HEFO, 2 = EXAG, 3 = SOAP, 4 = HEFO-EXAG, 5 = EXAG-HEFO, 6 = EXAG-NYFR, 7 = AVOF-EXAG, 8 = NYFR-MIXED, 9 = SHRUBS, 10 = GRASS1, 11 = GRASS2, 12 = SANDBAR, 13 = WBSBMF, 14 = WATERBODY

Table 4.5. Error matrix between WV2-TDX derived land cover class and Google Earth observation point. Elaboration of land cover type code is the same as that in table 4.3.

WV2 classes	Google Earth observation point classes														Total	User %	Commission%
	1	2	3	4	5	6	7	8	9	10	11	12	13	14			
1	26	0	1	1	2	0	0	0	0	0	0	0	0	0	30	86.67	13.33
2	0	27	0	1	1	0	1	0	0	0	0	0	0	0	30	90	10
3	1	0	19	0	0	0	0	0	1	0	0	0	1	1	23	82.61	17.39
4	0	2	0	26	0	0	0	0	0	0	0	0	0	0	28	92.86	7.14
5	1	0	1	1	20	1	0	4	0	0	0	0	0	0	28	71.43	28.57
6	0	0	0	0	1	23	1	2	0	0	0	0	0	0	27	85.19	14.81
7	0	0	0	0	0	2	19	0	0	0	0	0	0	0	21	90.48	9.52
8	0	0	1	0	1	0	1	17	0	0	0	0	0	0	20	85	15
9	0	0	0	0	0	0	0	0	23	0	0	0	0	0	23	100	0
10	0	0	0	0	0	0	0	0	0	24	0	0	0	0	24	100	0
11	0	0	2	0	0	0	0	0	0	1	22	0	2	0	27	81.48	18.52
12	0	0	0	0	0	0	0	0	0	0	0	25	0	0	25	100	0
13	0	0	1	0	0	0	0	0	0	0	0	0	24	0	25	96	4
14	0	0	0	0	0	0	0	0	0	0	0	0	0	25	25	100	0
Total	28	29	25	29	25	26	22	23	24	25	22	25	27	26	356		
Producer %	92.86	93.1	76	89.66	80	88.46	86.36	73.91	95.83	96	100	100	88.89	96.15		Overall Accuracy	89.89
Omission %	7.14	6.9	24	10.34	20	11.54	13.64	26.09	4.17	4	0	0	11.11	3.85		Kappa	0.891

1 = HEFO, 2 = EXAG, 3 = SOAP, 4 = HEFO-EXAG, 5 = EXAG-HEFO, 6 = EXAG-NYFR, 7 = AVOF-EXAG, 8 = NYFR-MIXED, 9 = SHRUBS, 10 = GRASS1, 11 = GRASS2, 12 = SANDBAR, 13 = WBSBMF, 14 = WATERBODY

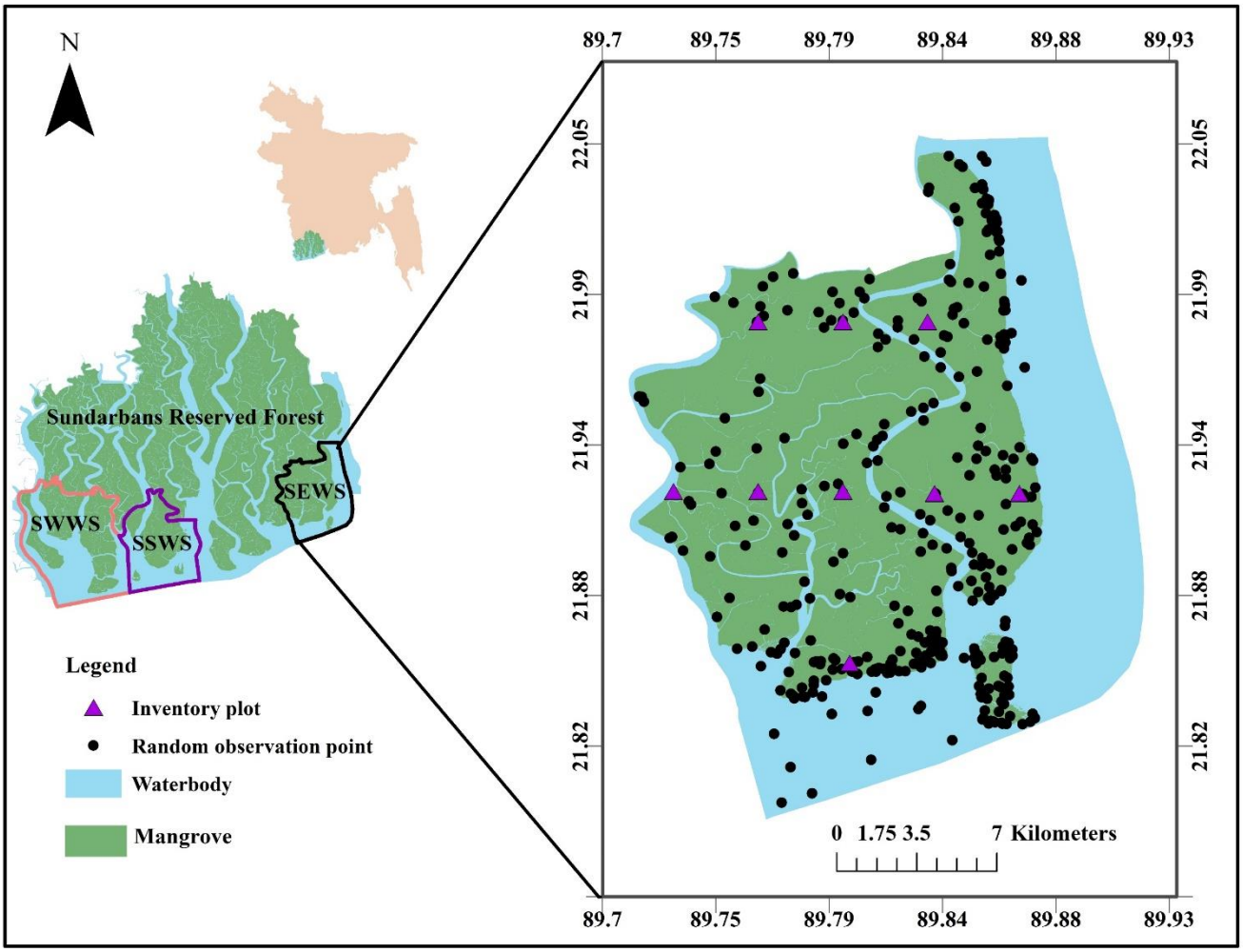

Figure 4.1: Positions of field inventory plot and ground truth point in Sundarbans East Wildlife Sanctuary.

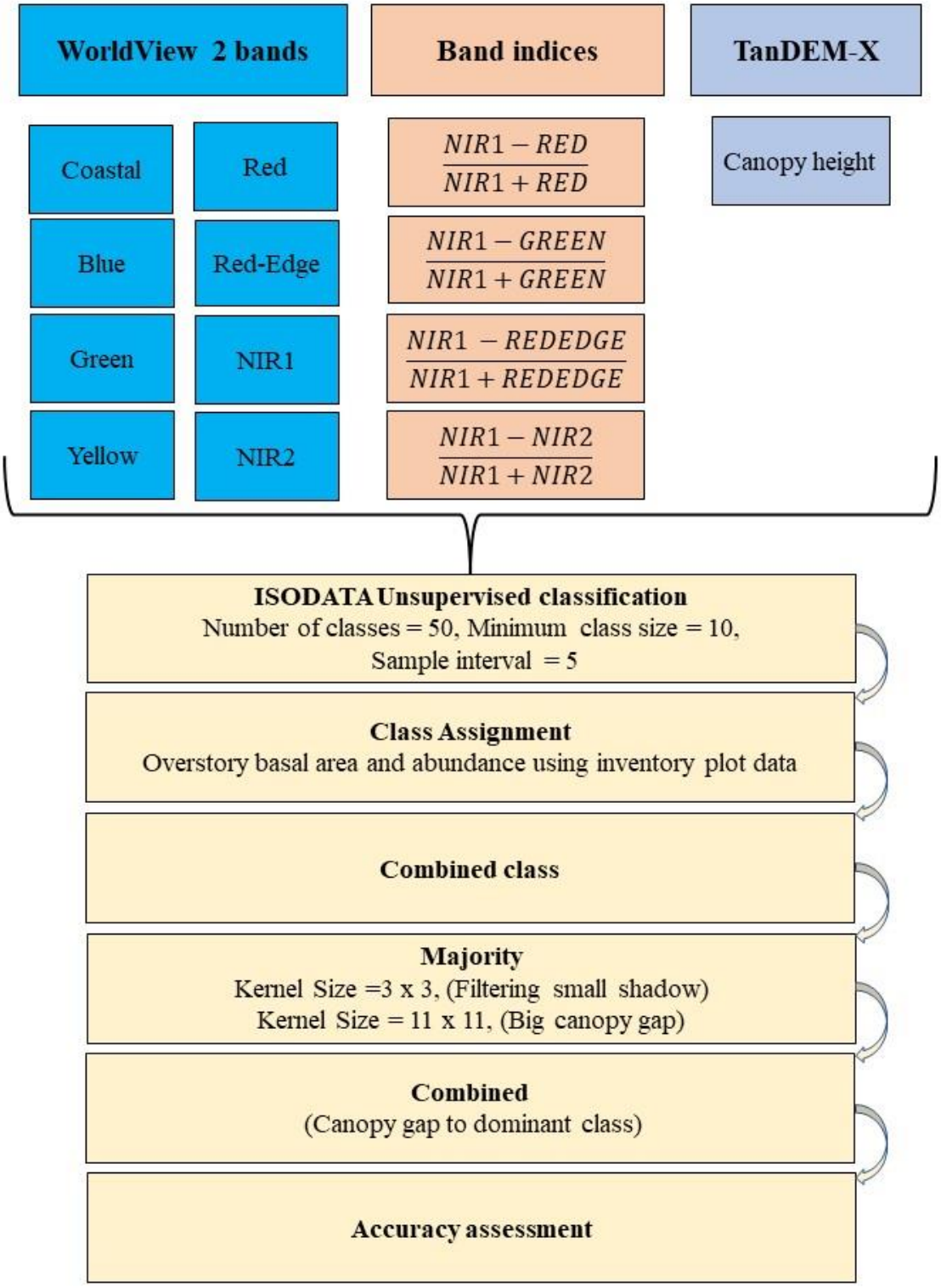

Figure. 4.2: Flowchart of classification method

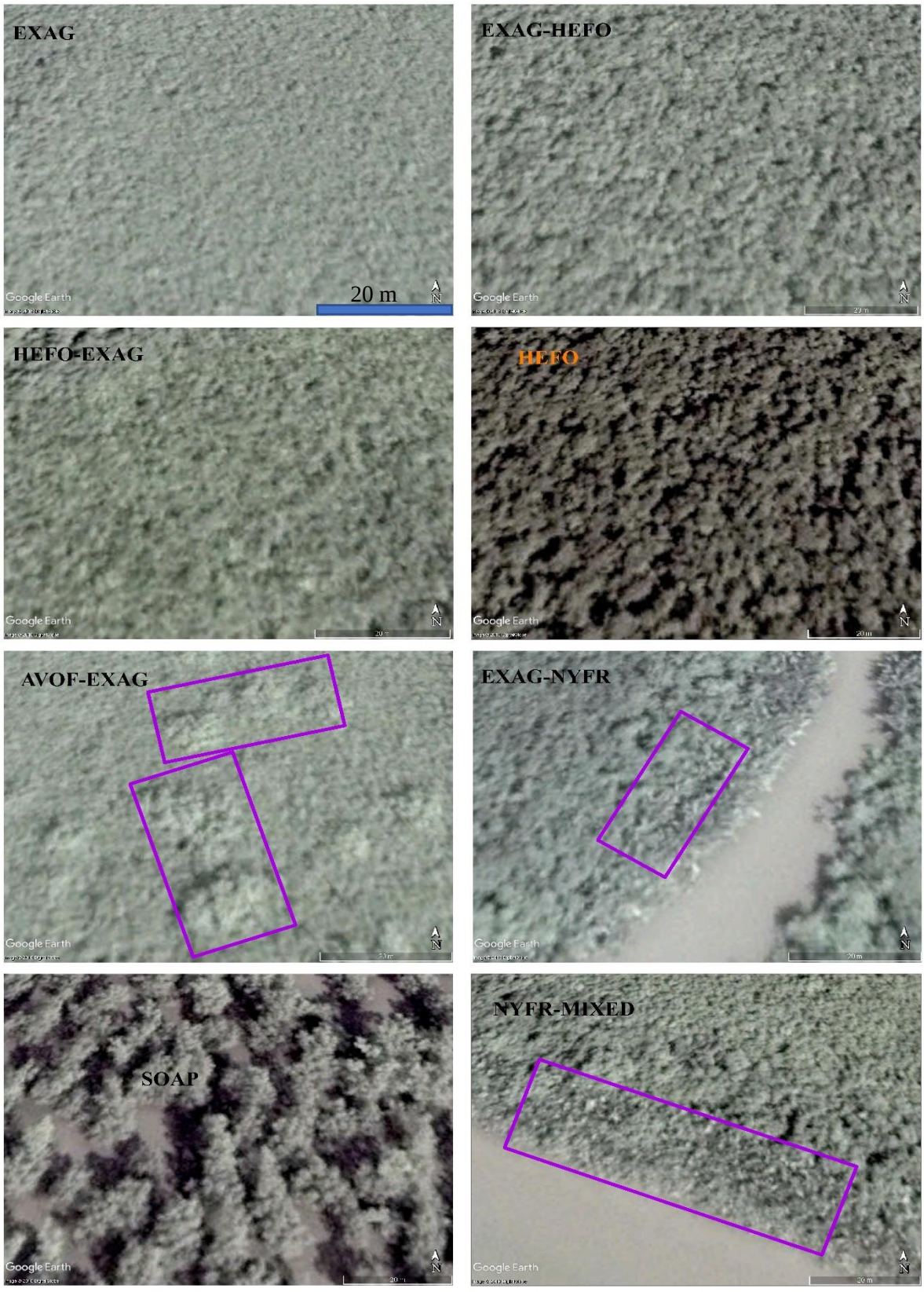

Figure 4.3.1 Google Earth@ visual interpretation (Image@ 2018, DigitalGlove; imagery date 11/05/2014), HEFO = *Heritiera fomes*, EXAG =*Excoecaria agallocha*, SOAP = *Sonneratia*

apetala, AVOF= *Avicennia officinalis*, NYFR MIXED: *Nypa fruticans*, *S. caseolaris*, *S. apetala*, *Phoenix paludosa*, *Hibiscus tiliaceous*, and *A. officinalis*,

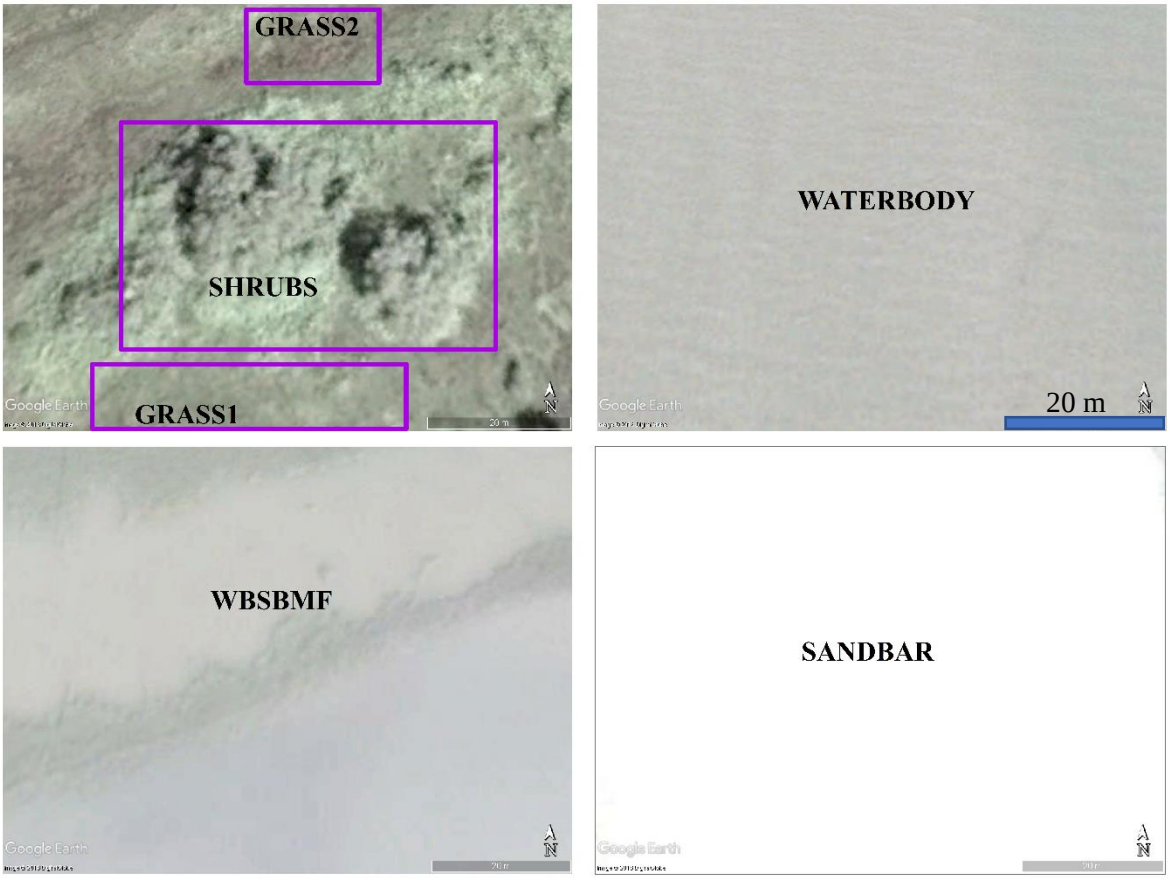

Figure 4.3.2 Google Earth@ visual interpretation (Image@ 2018, DigitalGlove; imagery date 11/05/2014). GRASS1 = Grasss-Tigerfern, GRASS2 = Grasss, WBSBMF = Waterbody, Sandbars and Mudflat

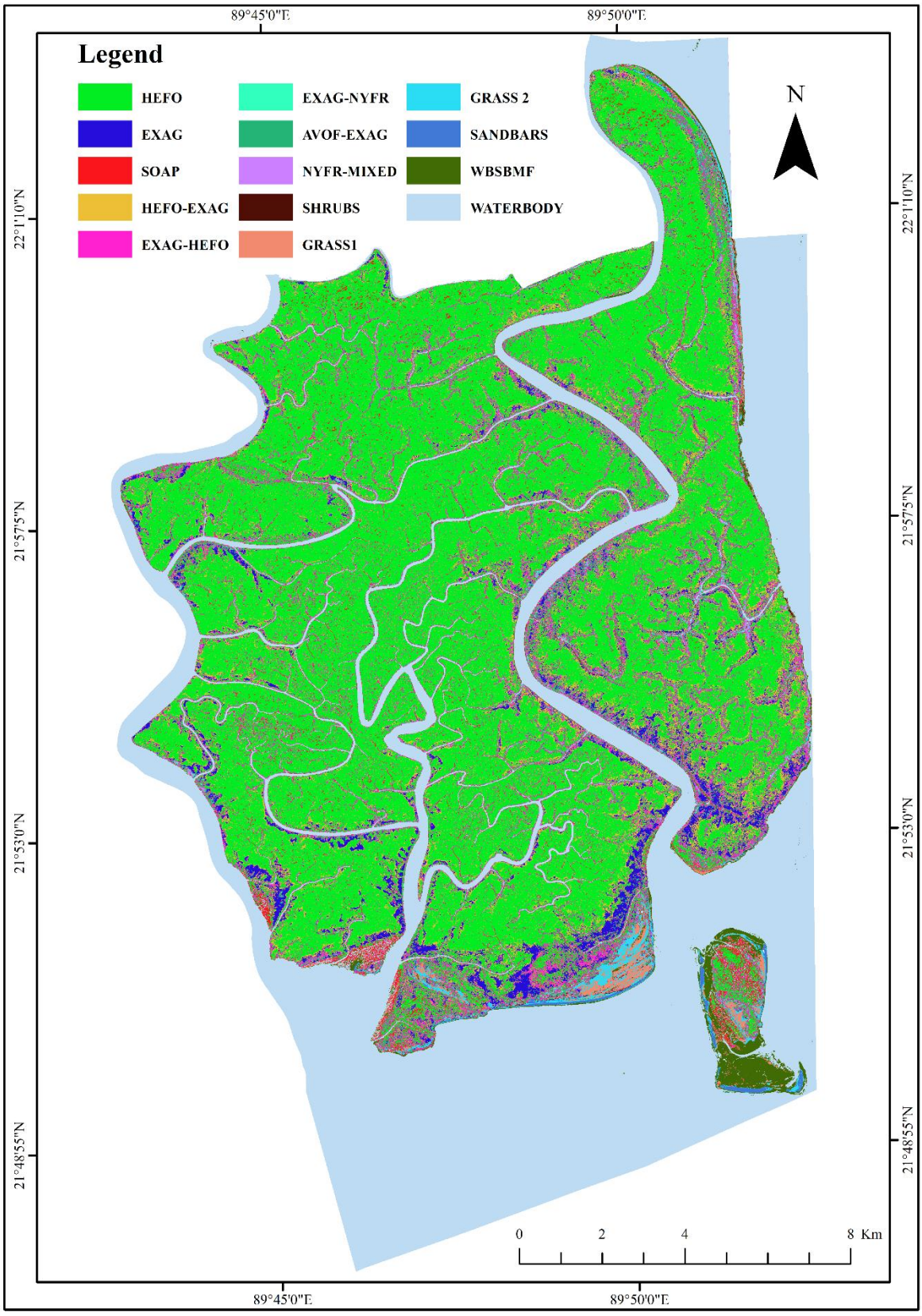

Figure 4.4. Spatial distribution of land cover types of Sundarbans East Wildlife Sanctuary based on WV2. HEFO = *Heritiera fomes*, EXAG =*Excoecaria agallocha*, SOAP =

Sonneratia apetala, AVOF= *Avicennia officinalis*, NYFR MIXED: *Nypa fruticans*, S. *caseolaris, S. apetala, Phoenix paludosa, Hibiscus tiliaceous*, and *A. officinalis*, GRASS1= Grasss-Tigerfern, GRASS2= Grasss, WBSBMF= Waterbody, Sandbars and Mudflat

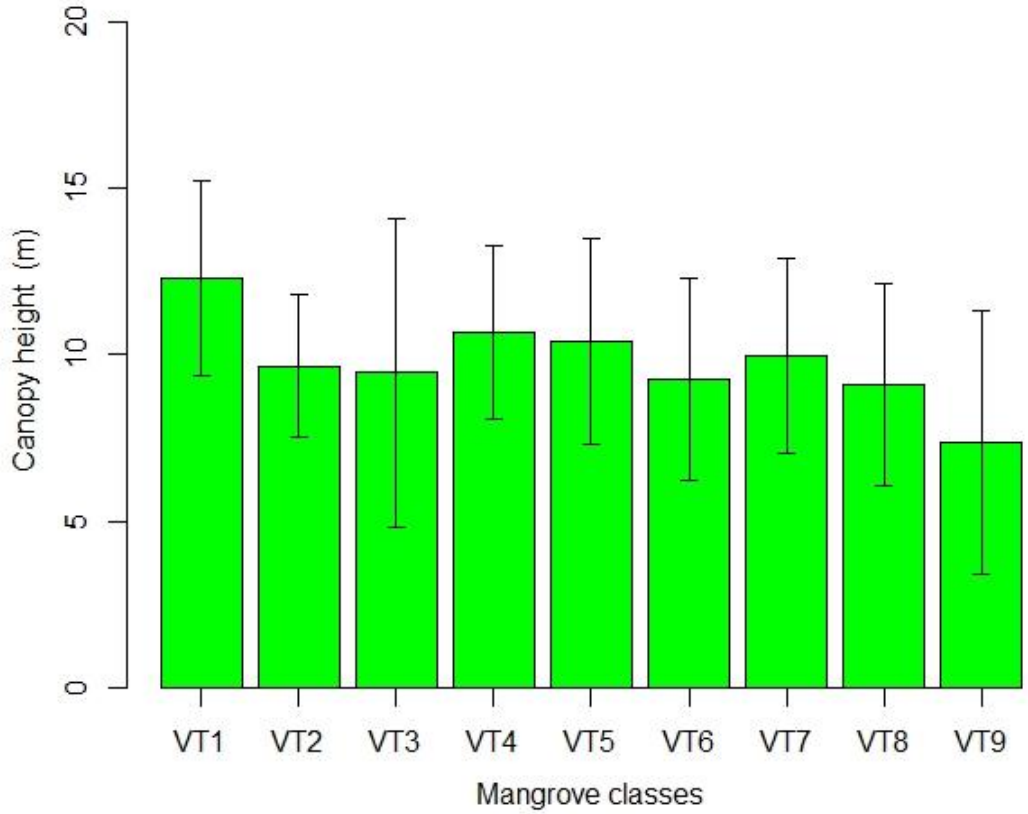

Figure 4.5. TanDEM-X derived mean canopy height (±SD) across the nine mangrove vegetation types in SEWS. VT1=HEFO, VT2=EXAG, VT3=SOAP, VT4=HEFO-EXAG, VT5=EXAG-HEFO, VT6=EXAG-NYFR, VT7=AVOF-EXAG, VT8=NYFR-MIXED and VT9=SHRUBS

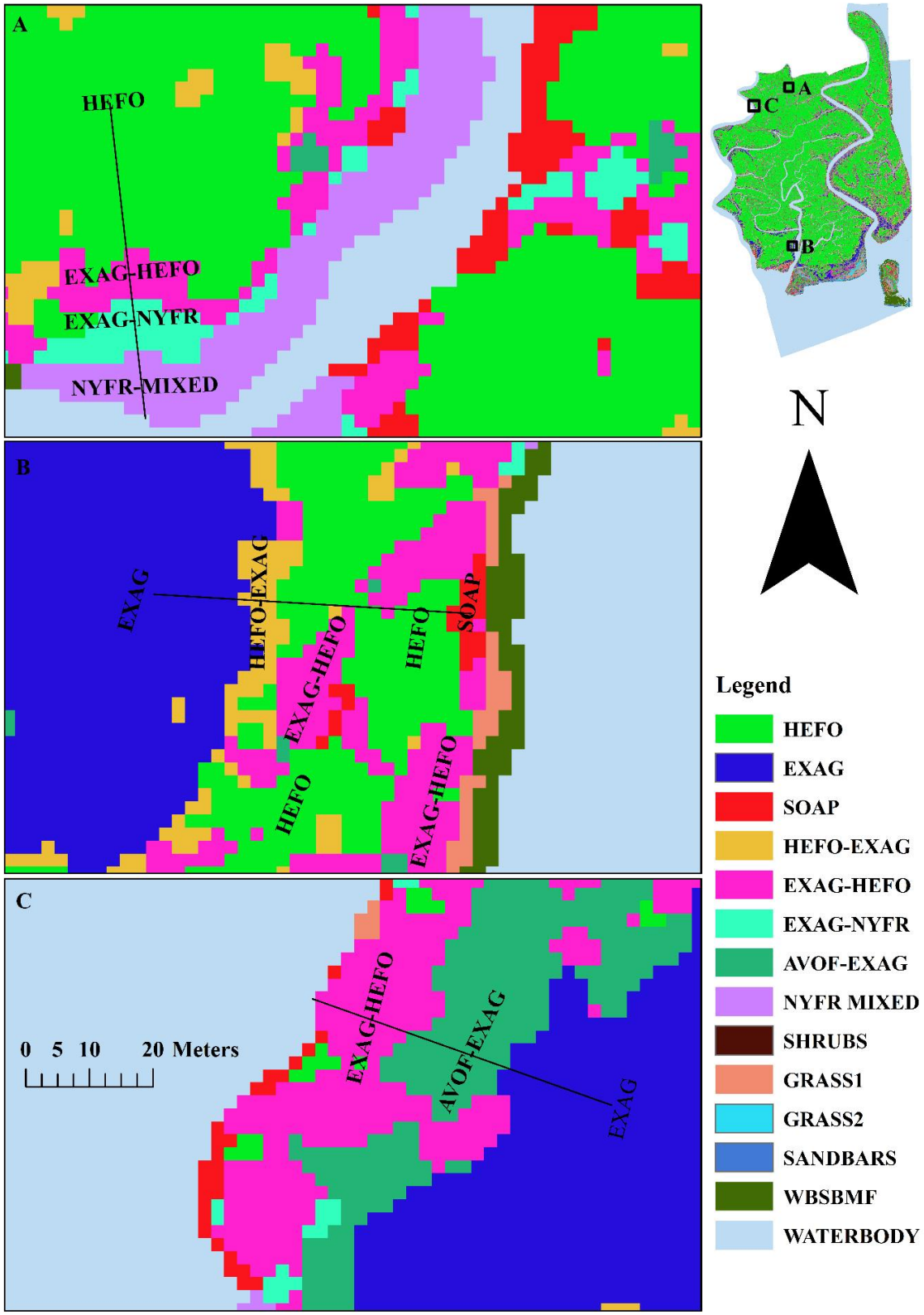

Figure 4.6. Species zonation in SEWS within 50 m transect: (A) from canal bank to inland side; (B) from big river bank to inland side; (C) from big river bank to inland side. Species code same figure 4.4.

Chapter 5 Aboveground carbon stock in relation to tree diversity in Sundarbans Reserved forest Bangladesh.

Introduction

Climate change and biodiversity loss are the two-serious threats to human being (Werf et al., 2009). These two issues have arisen mainly from fossil fuel burning and large-scale deforestation in tropical countries (Werf et al., 2009). Among the forested ecosystems in the tropics, mangroves have been facing severe anthropogenic distraction such as agricultural expansion, shrimp farming, landfilling, urbanization, upstream fresh water diversion and sea level rise (Ellison, 2015; Giri et al., 2011). Though the rate of mangrove deforestation per year has reduced in the recent decades (0.38%) compared to late 20^{th} Century (1-2%) due to awareness and global conservation effort, still it is a threatening cause of global warming and biodiversity loss, because mangrove forests store about four to six times higher carbon than other terrestrial forests in the tropics and the presence of mangrove species is directly correlated to forest coverage (Duke et al., 2007; Ellison et al., 2005; Hamilton and Friess, 2018). For combating these two threats under the same platform, payment for ecosystem-based approach was adopted in 2009 under the United Nation Framework Convention on Climate Change (UNFCCC) after a decade's discussion between developed and developing countries e.g., Reducing Emissions from Deforestation and forest Degradation, plus the sustainable management of forests, and the conservation and enhancement of forest carbon stocks (REDD+; Phelps et al., 2011).

Another international program of the United Nations for conserving global biodiversity is the Convention of Biological Diversity (CBD) which develops a 10 years' strategic plan (2011–2020) where all the 196 signatory countries of CBD, came to a consensus to protect and enhance their biodiversity (known as The Aichi Biodiversity targets; CBD, 2010). So, almost all tropical countries (where more than 90 % of the mangrove forests is found) are committed to both REDD+ and CBD to achieve their climate change mitigation and biodiversity targets through conservation of biodiversity and thereby enhancement of carbon sequestration (Turnhout et al., 2017). However, potential for protection of carbon-rich forest such as mangrove forests with biodiversity co-benefit needs to understand the relationship between carbon pool and tree diversity, on local and regional scales which can be contributed to formulate REDD+ policy.

In community ecology, it is suggested that ecosystem with greater diversity ensures optimum use of resources resulting in greater productivity and ecosystem services such carbon stock (Cavanaugh et al., 2014; Isbell et al., 2015; Tilman et al., 2014; Zhang et al., 2012; Zhong et al., 2017). Standing tree biomass is the dominant portions of total aboveground biomass in mangrove ecosystem. This biomass is treated as one of the indicators of forest stand productivity. Thus, the relationship between tree diversity and aboveground biomass carbon can be a representative part of biodiversity and ecosystem function (Lasky et al., 2014, Manesh et al 2016).

In most of the biodiversity and carbon relationship studies, species richness has been mainly used as biodiversity measure (See chapter 1 for details). However, species richness alone is not a surrogate for actual diversity as it would not consider the special roles of common and rare species in the community, the evenness of species distribution, species coexistence, and species-habitat associations (Isbell et al., 2015; Zhang et al., 2012; Zhong et al., 2017). Therefore, for quantifying the biodiversity and ecosystem function relationship, both species richness and evenness should be considered which can be accomplished if the Shannon-Wiener index is used as diversity measure because it involves both richness and evenness (Zhang et al., 2012; Zhong et al., 2017).

Canopy height in forested ecosystems, plays a pivotal role in figuring forest biomass, site quality, species richness, and diversity and other ecosystem processes (Moles et al., 2009). Thus, in modeling the diversity-carbon relationship, incorporation of height information is necessary (Mensah et al., 2016). Previous studies, considered maximum tree height as it is an indicator of light uses opportunity among species (Ruiz-Jaen and Potvin, 2011). However, in the mangrove forests where species usually show zonation or homogeneous patches, mean canopy height is important rather than maximum tree height as this layer is formed by the codominant and dominant trees (Ellison et al., 2005; Rahman et al., 2015).

Abiotic factors such as soil properties influence species distribution in natural forests, which may affect ecosystem functions (aboveground biomass, productivity and carbon storage) (Cavanaugh et al., 2014; Isbell et al., 2015; Tilman et al., 2014; Potter et al. 2015; Zhong et al., 2017). Thus, in biodiversity and ecosystem function relationship this site factor may play an important role which can be explored by setting the random 'site' effect in the mixed model (Manesh et al. 2016). In the mangrove ecosystem, higher net primary productivity (NPP) and biomass accumulation are associated with freshwater areas compared to hypersaline areas. Thus, spatial variation of salinity in mangrove forest, determine species distribution, growth

productivity and carbon sequestration capacity which may also influence the relationship between tree diversity and aboveground carbon (Rahman et al. 2015; Komiyama et al. 2008)

The aims of this study were 1) to explore the stand structure and diversity in Sundarbans Reserved Forest, and 2) to quantify the relationship between aboveground carbon stock, tree diversity forest canopy height and salinity.

Method

Study area

This study was conducted in Sundarbans Reserved Forest (SRF) in Bangladesh which remain unchanged or not deforested like other mangrove ecosystems (Figure 5.1). This forest represents 5% of global mangrove coverage and is a biodiversity hot spot. This unique mangrove ecosystem is a secure habitat of 528 species of vascular plants including 24 true mangrove species and 70 mangrove associates (Rahman et al., 2015). The faunal diversity of SRF is also very rich: total recorded species is 1135 including the large community of tigers (Royal Bangle Tiger), Ganges and Irrawaddy dolphins and saltwater crocodiles which represents about 35% of the total fauna of Bangladesh (Aziz and Paul, 2015). This forest provides livelihood support to neighboring people and save their lives and properties from tidal surge and cyclone. With its higher biodiversity, ecological, and socioeconomic value, 52 % of SRF has been declared as protected areas in 2017, for providing free breeding ground of diverse flora and fauna. From its reserved part (48%) only four types of nontimber forest products are allowed to be extracted for providing the livelihood support to the adjacent community: 1) Fish, 2) Crabs, 3) Honey and 4) Nypa leaves.

Data source and analysis

In 2009-2010, with the financial and technical support from USAID and US Forest Service, Bangladesh Forest Department had conducted a forest carbon Inventory in SRF following a systematic grid sampling (M. M. Rahman et al., 2015b). A total 150 cluster plots were laid out where tree (DBH ≥ 10cm) was census within five 10 m radius circle (See Chapter 3). Here I used the live tree data of 133 plots for linear mixed effect model (17 plots were excluded because some subplots were under water or subplots with water body, and plots with dominated by *Ceriops decandra* (a shrub species in SRF), for examining the relationship between tree diversity (Shannon, 1948), richness (Margalef, 1958), evenness (Pielou, 1969), canopy height (Co-dominant tree height) and aboveground biomass carbon (AGC) (Rahman et al., 2015). Previous study in SRF, showed that basal areas was highly correlated with carbon

storage. Biomass also has a strong correlation with carbon storage, so I did not use them as a weight factor in diversity calculation. Rather I used species abundance as weight factor (Cavanaugh et al., 2014; Rahman et al., 2015). I used co-dominant tree height as a structural predictor of forest biomass carbon as in mangrove ecosystem. Where species show a clear zonation, the canopy height tree (co-dominant) plays an important role in ecosystem process (Ellison et al., 2005; Rahman et al., 2015). Because they act as a foundation species and their architectural, functional and physiological characteristics control forest structure and ecological function e.g., alter microclimates, biomass flow and chemical process (Ellison et al., 2005).

Tree diversity parameters were computed using Vegan Package in R program (R Core Team, 2018). For estimating AGC I used Hossain et. al.'s (2015) allometric equation for *Excocaria agallocha* and for other species, Chave at al.'s (2005) common allometric equation for mangrove as species specific allometric equation was not available. The wood density data were collected from Bangladesh Forest Research Institute and the Global Wood Density Database (Yakub et al., 1972; Zanne et al., 2009). AGC biomass were converted to carbon mass by multiplying 0.5 as it is assumed that biomass contains 50% carbon of its dry weight (Penman et al., 2003).

In this study, two types of models were employed for observing the effect of tree diversity, evenness and canopy height on AGC : multiple linear model because of its simplicity, and linear mixed effect model as it incorporates multilevel hierarchies in data such as cluster or spatially correlated data (Nakagawa and Schielzeth, 2013). Here, I considered salinity zone as a random effect because plots within a given zone may have different carbon stocks due to salinity gradient, while tree diversity and canopy height were treated as fixed variable. The variation explained by fixed and random effects was assessed by Marginal and Conditional R^2, respectively using 'MuMin' package of Program R (Nakagawa and Schielzeth, 2013). The normality of AGC was checked by performing one sample Kolmogorov–Smirnov test (K–S test) before performing the model calculation. Outlier was checked by cook's distance where in general use those observations that have a cook's distance greater than 4 times the mean may be classified as influential (Fig. 5.3). Four outliers were identified and removed from modeling as these plots had some large sized trees which results more carbon stock. By using bivariate correlation between the predictors, the multicollinearity was tested while homoscedasticity was tested by plotting standardized residuals against fitted value in-R program and model diagnostics were shown in Fig. 5.4-8. The fitted models performance were assessed by following commonly used fit statistics such as Akaike information criterion (AIC) (Nakagawa

and Schielzeth, 2013). The accuracy of the coefficients of multiple linear regression model was assessed using bootstrap analysis method with 1000 times random resampling in Statistical Package for the Social Science (SPSS).

Results

A total of 17758 individuals of live trees (DBH≥ 10 cm) were found in the study plots at SRF which belong to 17 species (excluding 9 unidentified species) and 14 families. In the SRF, the top three dominant species were *Heritiera fomes Excoecaria agallocha* and *Xylocarpus mekongensis* where their relative abundance were 53.15, 40.78 and 2.44 %, respectively (Table 5.1). The number of species in freshwater, moderate and strong saline zone were 16, 14 and 11, respectively (Table 5.1). According to relative abundance *H. fomes* was most dominant species in the freshwater and moderate saline zone, while in the strong saline zone the it was *E. agallocha* (Table 5.1).

Stand level AGC varied highly across the whole SRF (2.59 to 263.09 Mg ha^{-1}) with a mean value of 64.43 (Table 5.2). The mean stand level species diversity was 0.97 across the whole SRF (Table 5.2) which was varied from 0 to 2.47. The canopy height was varied between 4.90 m to 17.25 m with a mean of 9.49 m with (Table 5.2). In case of salinity zones, the freshwater zone had highest AGC and canopy height while at strong saline zone AGC and canopy height were found least (Table 5.2). The Margalef richness of freshwater zone was significantly different from moderate and strong saline zones ($p < 0.05$; Table 5.2) but it was not significantly diffident between moderate and strong saline zones ($p > 0.05$; Table 5.2). Shannon diversity of freshwater zone were significantly different from strong saline zone ($p < 0.05$; Table 5.2). There were no signification differences found in case of Pielou evenness and Shannon diversity between freshwater and moderate saline zone ($p > 0.05$). However, the strong saline zone had significantly lower Pielou evenness and Shannon diversity compared to the other two saline zones ($p < 0.05$; Table 5.2).

In multiple linear model both Shannon diversity and canopy height had positive effect on AGC ($\beta = 11.90$ and 11.46, respectively for Shannon diversity and canopy height; Table 5.2). In this model the combined effects of Shannon diversity and canopy height can significantly explain 66% variation in AGC ($P < 0.5$; Table 5.2). However, I did not find any significant effect of Magalef species richness and Pielou evenness when both diversity parameters coupled separately with canopy height for finding their effect on AGC in multiple linear models ($P > 0.5$). At the three different levels of Shannon diversity (0, 1 and 2), AGC increased with canopy height (Fig. 5.2).

A total of three multivariate linear mixed effect models were tested where canopy height was combined separately with Shannon diversity, Margalef richness and Pielou evenness and treated as fixed factors. Salinity zones was used as random factor in all the three models. In these three models canopy height showed significantly positive relationship AGC ($p < 0.05$), while none of these three biodiversity parameters showed significant relation with AGC ($p > 0.05$; Table 5.3). In both models, the conditional R^2 values (explain the combined effect of both fixed and random variables) were same but they were higher than Marginal R^2 values (explain the effect of fixed variables; Table 5.3).

Discussion

Comparison of stand structure with other studies needs a unified sampling method as diversity and species richness are sensitive to plot size and sampling design which was the limitation to compare finding of the present study to other mangroves. The result of this study reveals that overstory tree diversity is lower in SRF compared to Islam et al. (2016). The reason of this lower diversity in my study may be the difference of sampling design and plot size. Most of the plots were laid out following systematic grid sampling with nested circular in study, and fell in the inland side. However, Islam et al. (2016), laid out 200 m long transect with two plots from rivers or canals bank and this zone is more diverse than the inland side. Furthermore, low diversity can be explained by relative abundance of the species as I found, two species (*Heritiera fomes* and *Excoecaria agallocha*) covers 94% of the total individuals recoded in this study (17758 individual; Table 5.1). The canopy height in SRF showed an increasing trend from strong saline zone to freshwater zone which may have occurred due to the salinity difference. In the mangrove ecosystem, stand becomes more dwarf in association with high saline areas than low saline areas (Ball et al. 2002; Rahman et al. 2015)

The positive relationship between diversity, and AGC carbon in multiple linear model in this study, reveals that in the mangrove ecosystems with higher biodiversity promote aboveground biomass carbon (Fig. 5.2; Table 5.3). The finding of my study similar to different terrestrial forests that can be categorized as local (Kessler et al., 2012; Martinez-Sanchez and Cabrales, 2012; Mattsson et al., 2015; Mensah et al., 2016; Ruiz-Jaen and Potvin, 2011; Ruiz-Jaen and Potvin, 2010), regional (Zhang et al., 2017) and global (Cavanaugh et al., 2014) where these studies found positive relationship between species richness and diversity and aboveground biomass carbon. This is the implication of optimum utilization of resources by diverse species at stand level which is fundamental in the niche complementary theory in

community ecology (Cavanaugh et al., 2014; Mensah et al., 2016; Ruiz-Jaen and Potvin, 2011; Tilman et al., 2014).

On the other hand, canopy height was also positively related with aboveground biomass carbon stock. This result in my study was analogues to previous studies in tropical forests (Cavanaugh et al., 2014; Mensah et al., 2016; Ruiz-Jaen and Potvin, 2011; Tilman et al., 2014). The canopy layer in the mangrove, is usually formed by large sized trees with dominant or fundamental species. Thus, it can be inferred that ecosystem function in the mangrove forests is also supported by species dominance or selection hypothesis (Cavanaugh et al., 2014; Mensah et al., 2016; Ruiz-Jaen and Potvin, 2011; Tilman et al., 2014). In mangrove ecosystems, therefore, ecosystem functioning, niche complementarity and selection effect are mutually inclusive which means ecosystem function (carbon storage) is the result of their product. These findings therefore, suggest that mangrove tree diversity can positively affect carbon pool size and consequently contribute to mitigation of global climate change which should be treated as a key part in payment for ecosystem services policy making like tropical forests (Poorter et al., 2015).

Forest canopy height is an important parameter for predicting aboveground biomass which can be used in estimating carbon pools stored in the vegetation (Balzter et al., 2007). This forest canopy height can be measured by using remote sensing technology with higher accuracy (Aslan et al., 2016; Balzter et al., 2007; Fatoyinbo et al., 2018; Lagomasino et al., 2016; Lee and Fatoyinbo, 2015). The positive relationships between canopy height and AGC in the mangrove ecosystem, also indicate that AGC can be monitored by means of remote sensing techniques either by LiDAR or SAR imaging where one can map AGC by coupling RS based canopy height with *in situ* data calculated from height based allometry (Aslan et al., 2016; Fatoyinbo et al., 2018; Feliciano et al., 2017; Lagomasino et al., 2015). Thus, accurate Monitoring, Reporting and Verification (MRV) of spatiotemporal variation of mangrove AGC can be possible by making a synergy between remote sensing and field inventory data, with efficient cost and less labor input which are essential for mangrove-based REDD+ as field-based measurement of mangrove carbon stock is challenging and more time consuming.

The conditional R^2 (explained the combined effect of canopy height, diversity and salinity zone on aboveground carbon) in linear mixed models in this study was greater than marginal R^2 (explained the fixed effect of canopy height and diversity on aboveground carbon) (Nakagawa and Schielzeth, 2013). These findings suggest that modeling the relationship between carbon storage and canopy height in mangrove forests should consider salinity which is an environmental factor in case of mangrove forest and controls species distribution and

richness, tree growth, forest productivity and thereby affects the carbon sequestration capacity (Adame et al., 2013; Rahman et al., 2015). Thus, for maintaining tree growth, size and ecosystem function (carbon storage) in SRF, freshwater flow should be ensured during the dry season. Because due to upstream water removal, freshwater flow significantly decreased in SRF during this season which increases salinity in SRF. The diversity parameters in SRF had no significant effect on the AGC ($p > 0.05$; Table 5.4) because among the three salinity zones at least two had similar diversity parameters ($p > 0.05$; Table 5.1). However, further study on direct soil salinity measurement may unveil what the effect of soil salinity on AGC and diversity relationship in SRF.

Mangrove tree diversity and mitigation of global warming

Mangrove forest is a store house of carbon most of which are deposited in soil (Donato et al., 2011). In a recent global mangrove carbon study, Hamilton and Fries (2018) have showed that 70.65 % of global mangrove carbon are stored in soil while 30% carbon are stored as biomass (Aboveground and belowground root carbon). Thus, mangrove ecosystems can be a source or sink of atmospheric carbon dioxide depending on land use change or alteration of these ecosystems to other land use (Hamilton and Friess, 2018). Protection of mangrove diversity, is therefore necessary for permeance of this carbon reserve and keeping continuous carbon flow to sediment from living parts of the mangrove vegetation. Because globally, mangrove is the most threating ecosystem from anthropogenic distraction point of view. Payment for Ecosystem Services based mitigation approaches can be effective to conserve this unique ecosystem such REDD+.

Over the last decades REDD+ was the most debated climate change mitigation program which aimed at a win–win solution for climate change mitigation, rural development and biodiversity conservation (Phelps et al., 2012). Several mangrove countries already selected mangrove ecosystem as a key REDD+ site such as Indonesia, Madagascar, Costa Rica, Ecuador (Herr et al., 2017). SRF in Bangladesh, also a proposed REDD+ site. However, for gaining financial rewards from REDD+, parties need to satisfy certain standard (Herr et al., 2017). The widely accepted standard is Climate Community and Biodiversity (CCB), which main principle for REDD+ based project is to avoid biodiversity harm and generate positive environmental impacts (Herr et al., 2017). As in my study, I also found that carbon storage increases with increased species diversity (Table 5.3 and fig. 5.2) in mangrove, by conserving mangrove REDD+ objective. Therefore, a participatory REDD+ program either in natural mangrove or

in restored mangrove forests with mixed species would be created a triple win situations where conservation of mangrove biodiversity would be ensured through climate change mitigation and livelihoods support for adjacent forest -dependent community from the non-timber forest products including fishery and carbon credit (Turnhout et al., 2017). This triple win REDD+ concept would help tropical mangrove countries achieve their targets of two other UN driven programs:1) Aichi Biodiversity Targets 11 of CBD, part of which directly related to conservation of mangrove ecosystems aimed at conserving at least 10 per cent of coastal and marine areas, especially areas of particular importance for biodiversity and ecosystem services by 2020 (CBD, 2010), and 2) two Sustainable Development Goals : i) climate change mitigation (Goal 13) which aimed at taking urgent action to combat climate change and its impacts, and ii) biodiversity conservation for better environment (Goal 15) a part of which aimed at adopting sustainable forest management and halting deforestation and biodiversity loss by 2020 (SDG, 2015).

Figures and Tables

Table 5.1 Relative abundance of species in the three salinity zones and whole SRF

Salinity zones		Number tree	Relative abundance
Freshwater			
Heritiera fomes		5003	63.69
Excoecaria agallocha		2137	27.21
Xylocarpus mekongensis		266	3.39
Bruguiera sexangula		244	3.11
Avicennia officinalis		71	0.90
Amoora cucullata		54	0.69
Sonneratia apetala		17	0.22
Intsia bijuga		12	0.15
S. caseolaris		12	0.15
Unknown		8	0.10
X. granatum		8	0.10
E. indica		7	0.09
Cynometra ramiflora		6	0.08
Aegiceras corniculatum		4	0.05
Pongamia pinnata		4	0.05
Hibiscus tiliaceous		2	0.03
	Total	7855	100.00
Moderate saline zone			
Heritiera fomes		4021	62.36
Excoecaria agallocha		2247	34.85
Xylocarpus mekongensis		80	1.24
Xylocarpus granatum		37	0.57
Avicennia officinalis		19	0.29
Amoora cucullata		18	0.28
Sonneratia apetala		12	0.19
Lumnitzera racemosa		4	0.06
Pongamia pinnata		3	0.05
Aegiceras corniculatum		2	0.03
Rhizophora mucronata		2	0.03
Cynometra ramiflora		1	0.02
E. indica		1	0.02
Unknown		1	0.02
	Total	6448	100
Strong saline zone			
Excoecaria agallocha		2857	82.69
Heritiera fomes		414	11.98
Xylocarpus mekongensis		88	2.55
Avicennia officinalis		37	1.07
Xylocarpus granatum		30	0.87
Bruguiera sexangula		9	0.26
Sonneratia apetala		7	0.20
Rhizophora mucronata		5	0.14
Aegiceras corniculatum		3	0.09
Cynometra ramiflora		3	0.09
Amoora cucullata		2	0.06
	Total	3455	100
SRF			
Heritiera fomes		9438	53.15
Excoecaria agallocha		7241	40.78
Xylocarpus mekongensis		434	2.44
Bruguiera sexangula		253	1.42
Avicennia officinalis		127	0.72
X. granatum		75	0.42
Amoora cucullata		74	0.42
Sonneratia apetala		36	0.20
Intsia bijuga		12	0.07
S. caseolaris		12	0.07
Cynometra ramiflora		10	0.06
Aegiceras corniculatum		9	0.05
Unknown		9	0.05
E. indica		8	0.05
Pongamia pinnata		7	0.04
Rhizophora mucronata		7	0.04
Lumnitzera racemosa		4	0.02
Hibiscus tiliaceous		2	0.01
	Total	17758	100.00

Table 5.2 Descriptive statistics of Margalef species richness (D), Pielou species evenness (J'), Shannon species diversity (H'), canopy height and aboveground carbon (AGC). 95% confidence intervals derived from 10,00 bootstrap resamples of the data (sampling with replacement) are shown in parentheses.

Stand structure	Salinity zones			SRF
	Freshwater (n=48)	Moderate saline (n=47)	Strong saline (n=34)	
Margalef richness (D)	0.65 (0.55-0.75) [a]	0.50 (0.42-0.58) [b]	0.40 (0.31-0.51) [b]	0.53 (0.47-0.58)
Pielou evenness (J')	0.62 (0.55-0.67) [a]	0.63 (0.58-0.67) [a]	0.44 (0.33-0.55) [b]	0.57 (0.53-0.61)
Shannon diversity (H')	1.17 (1.03-1.30) [a]	1.01 (0.93-1.10) [a]	0.66 (0.48-0.86) [b]	0.98 (0.89-1.06)
Canopy height (m)	11.99 (11.24-12.73) [a]	8.68 (8.18-9.24) [b]	7.23 (6.80-7.71) [c]	9.53 (9.03-10.00)
Aboveground Carbon (Mg ha^{-1})	98.48 (88.67-108.39) [a]	59.75 (50.81-68.55) [b]	22.83 (19.30-26.44) [c]	64.43 (57.46-71.73)

Table 5.3: Result of multiple linear model in assessing the effect of canopy height Shannon diversity (H') on Above Ground Carbon (AGC).

Model	Estimated coefficients	Bootstrap (1000 times resampling)		R^2	Adjusted R^2	AIC
		95% Confidence Interval	P value			
Intercept	-56.426	±17.4	0.001			
H'	11.90	±10.21	0.023	0.66	0.65	1242.90
Canopy height	11.46	±1.88	0.001			

Table 5.4 Combined linear mixed effect of Margalef richness (D), Pielou evenness, Shannon species diversity (H') and canopy height on aboveground carbon (AGC).

Parameters	**Fixed effect**		**p value**	**Random effect**	**RMSE**	**Marginal R^2**	**Conditional R^2**	**AIC**
	Estimated coefficients	SE		Salinity zone				
D & Canopy Height								
Intercept	-27.61	14.53	0.05	15.62	24.29	0.47	0.64	1179.43
D	3.23	4.67	0.4906					
Canopy Height	9.14	0.99	0.0000					
J' & Canopy Height								
Intercept	-27.43	14.69	0.06	15.93	24.36	0.46	0.64	1178.147
J'	6.02	9.01	0.5052					
Canopy Height	9.08	0.98	0.0000					
H' & Canopy Height								
Intercept	-27.61	14.53	0.05	17.02	24.60	0.44	0.64	1179.16
H'	3.23	4.67	0.4906					
Canopy Height	9.14	0.99	0.0000					

Figure

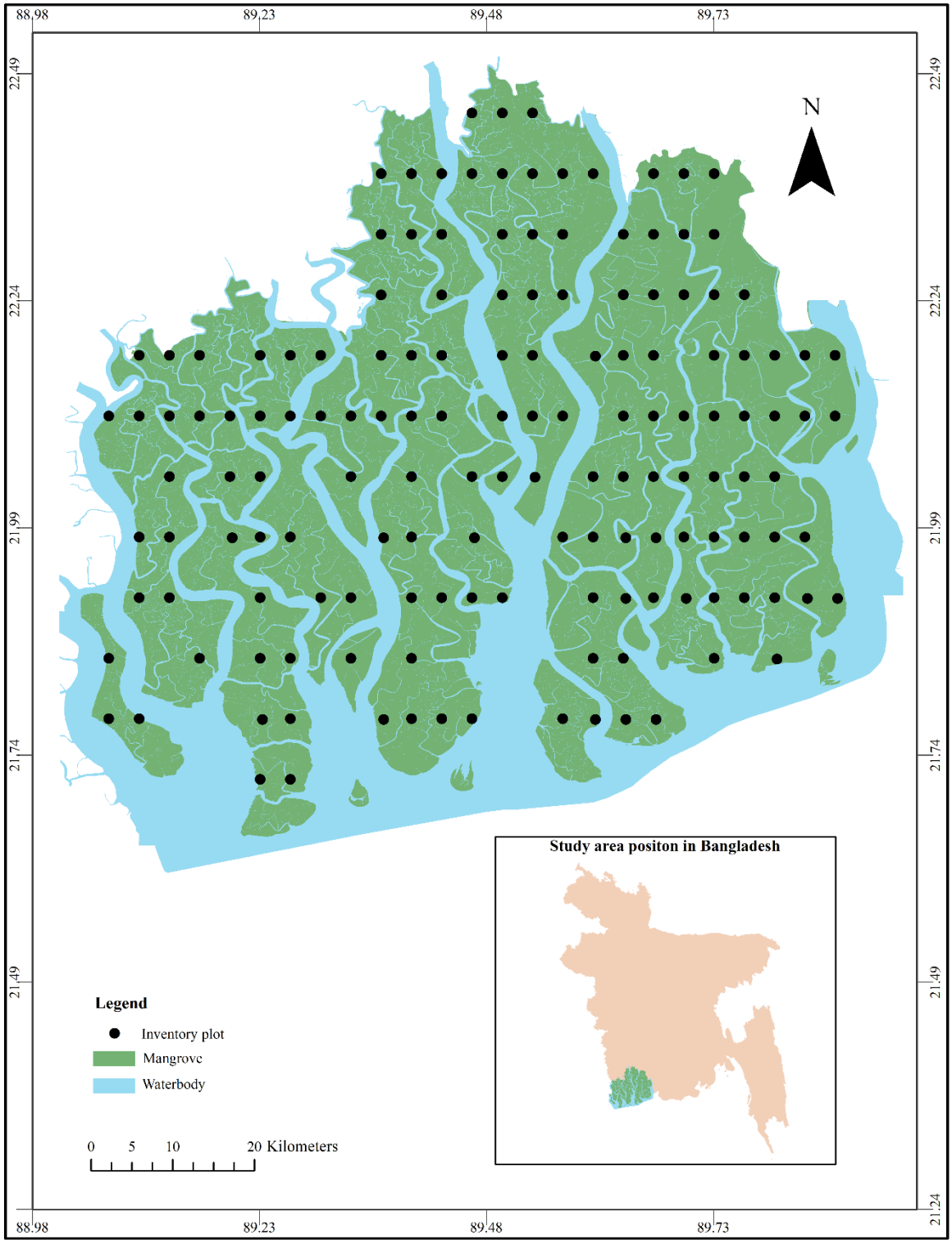

Figure 5.1 Distribution of sampling plots in Sundarbans Reserved Forest**.**

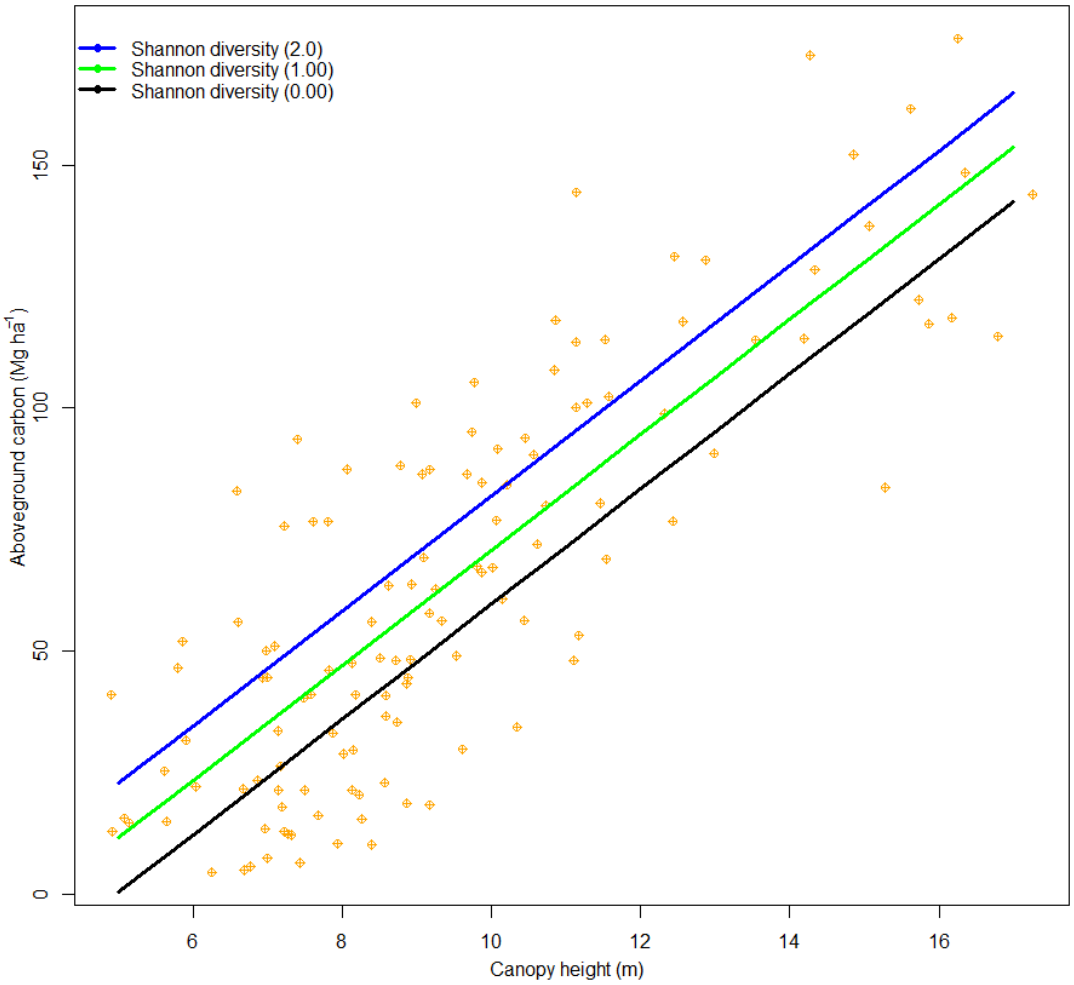

Figure 5.2 Interaction of Shannon diversity in aboveground carbon and canopy height. The three lines were generated at three fixed diversity level using fitted multiple linear regression (Table 5.3).

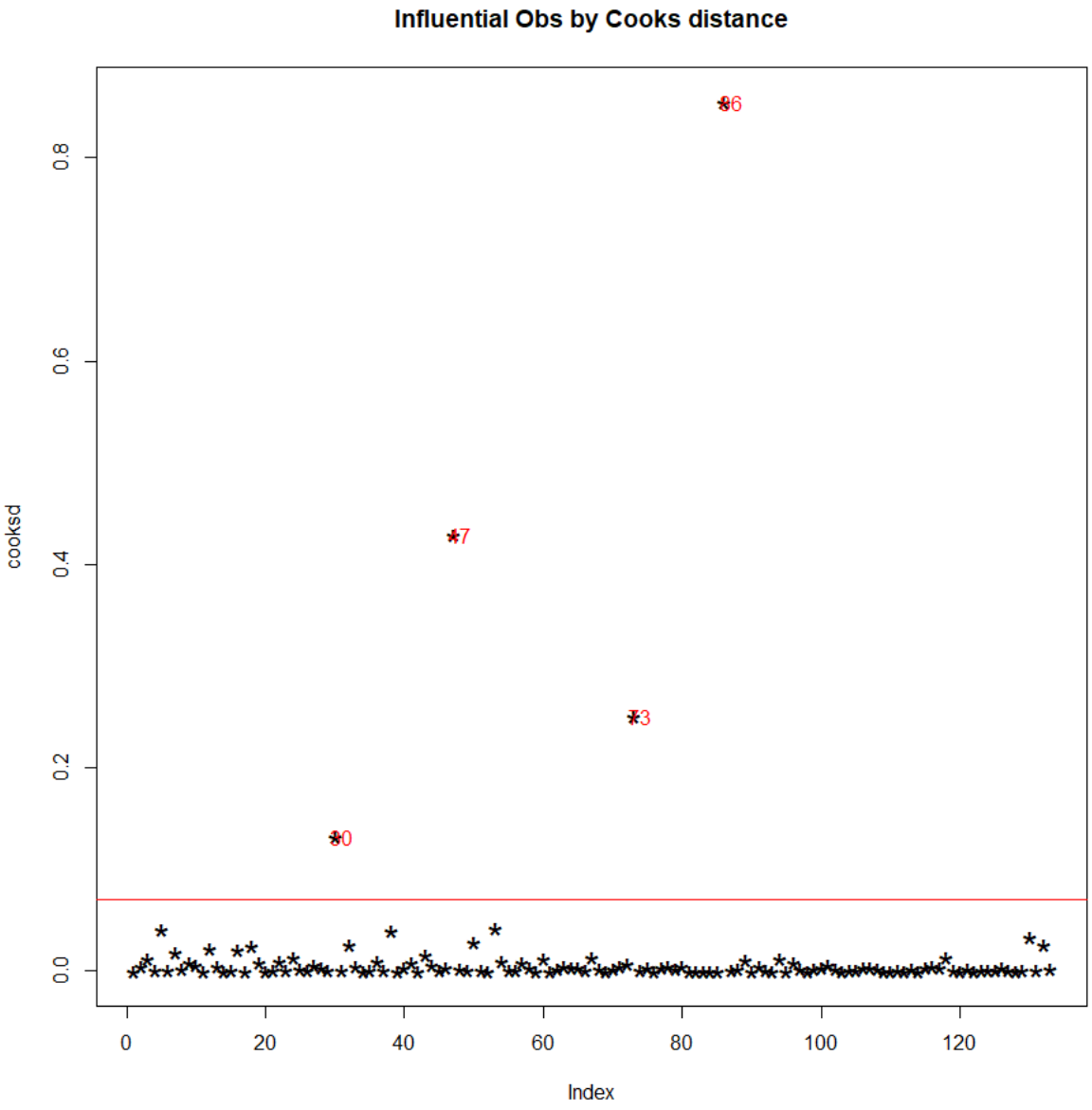

Figure 5.3 Detection of influential observations based on cook distance: the four numbered observations (red) above the redline were the outliers.

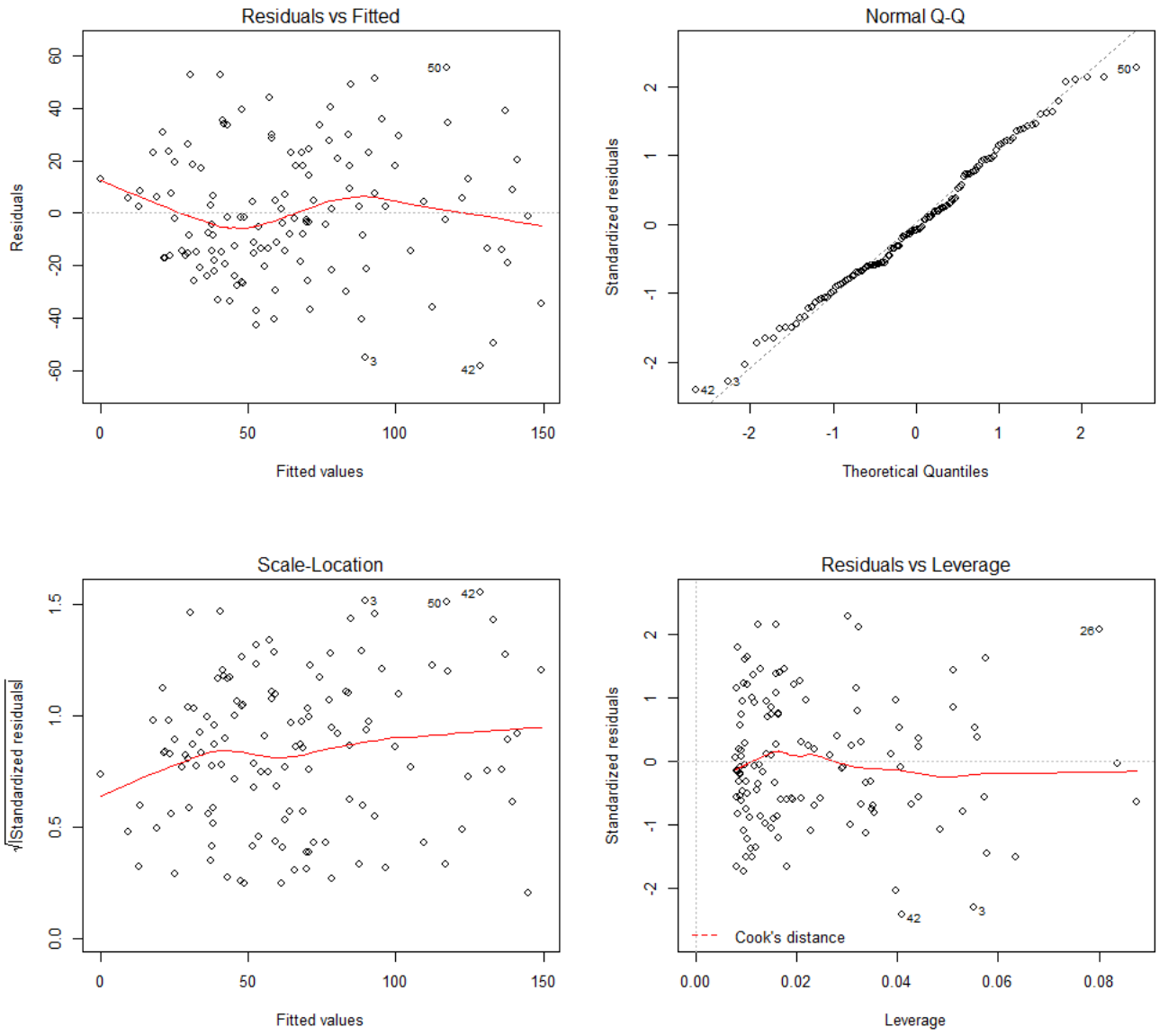

Figure 5.4 Diagnostic plots for multiple linear regression (Table 5.3)

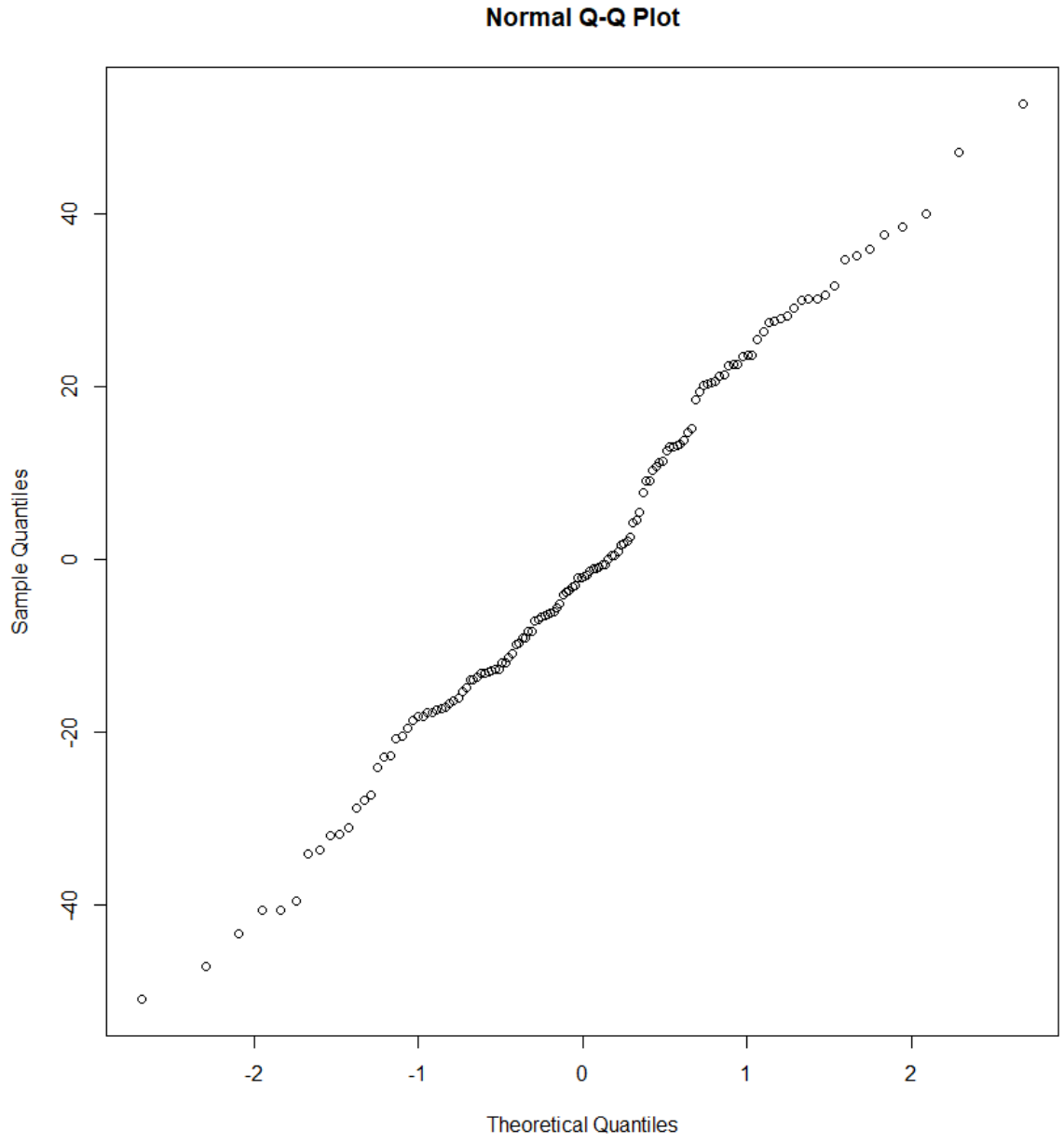

Figure 5.5 Q-Q plot of residuals indicating normality of response variable (aboveground carbon) of Shannon diversity and canopy height based linear mixed effect model (Table 5.4).

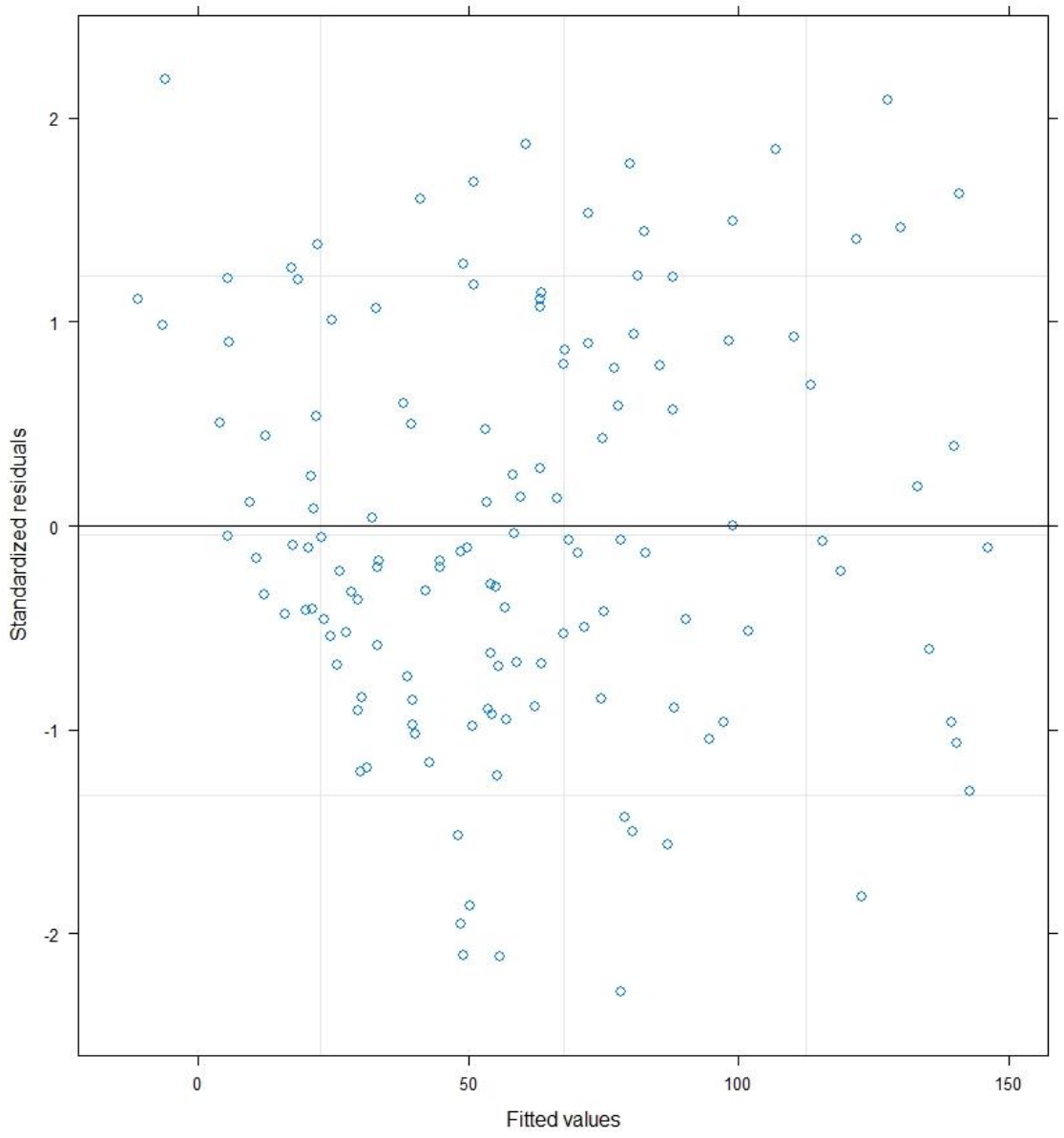

Figure 5.6 Fitted values versus standardized residuals of Shannnon diversity and canopy height-based model (test of homogeneity; Table 5.4).

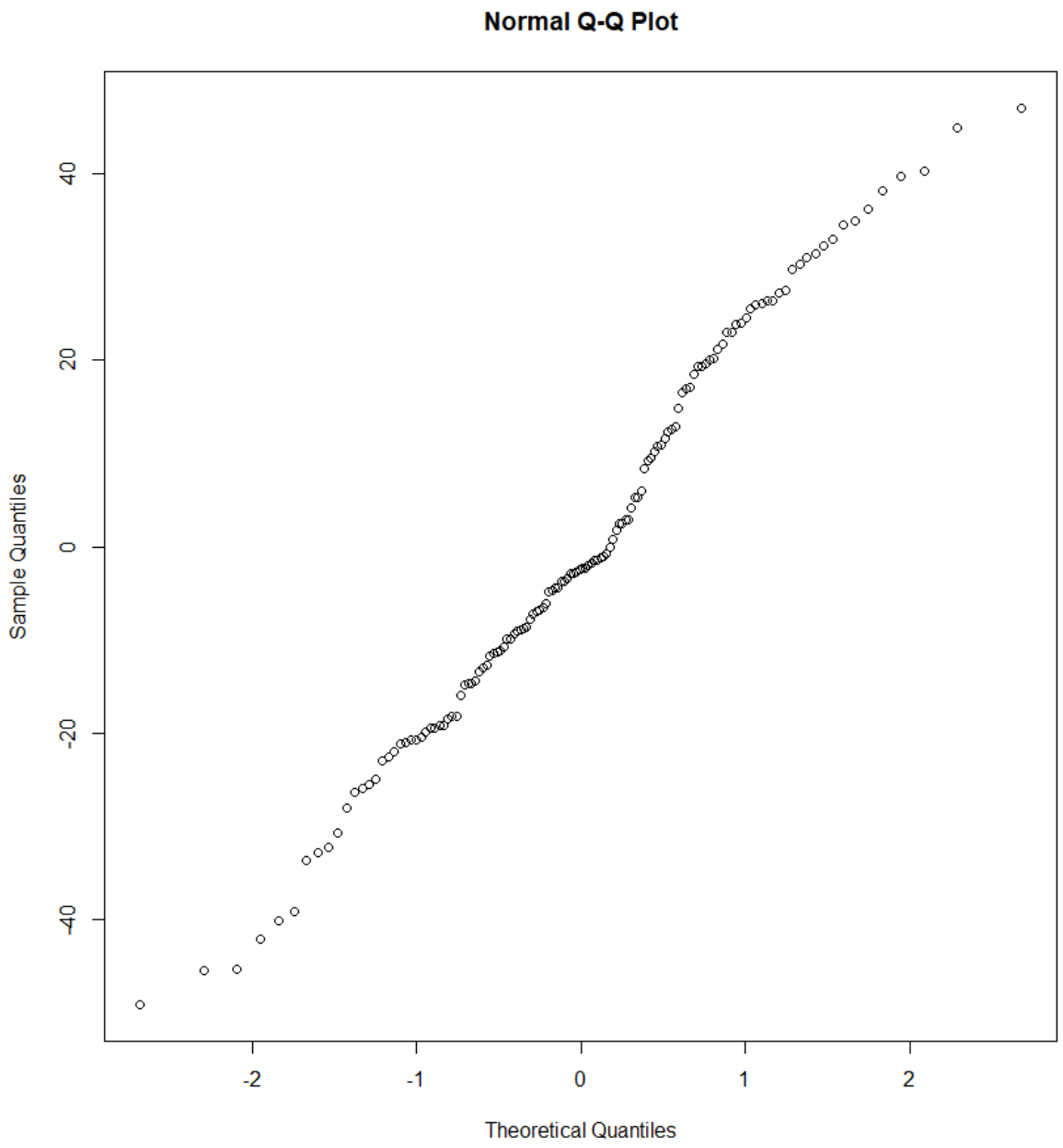

Figure 5.7 Q-Q plot of residuals indicating normality of response variable (aboveground carbon) of Pielou enveness and canopy height based linear mixed effect model (Table 5.4).

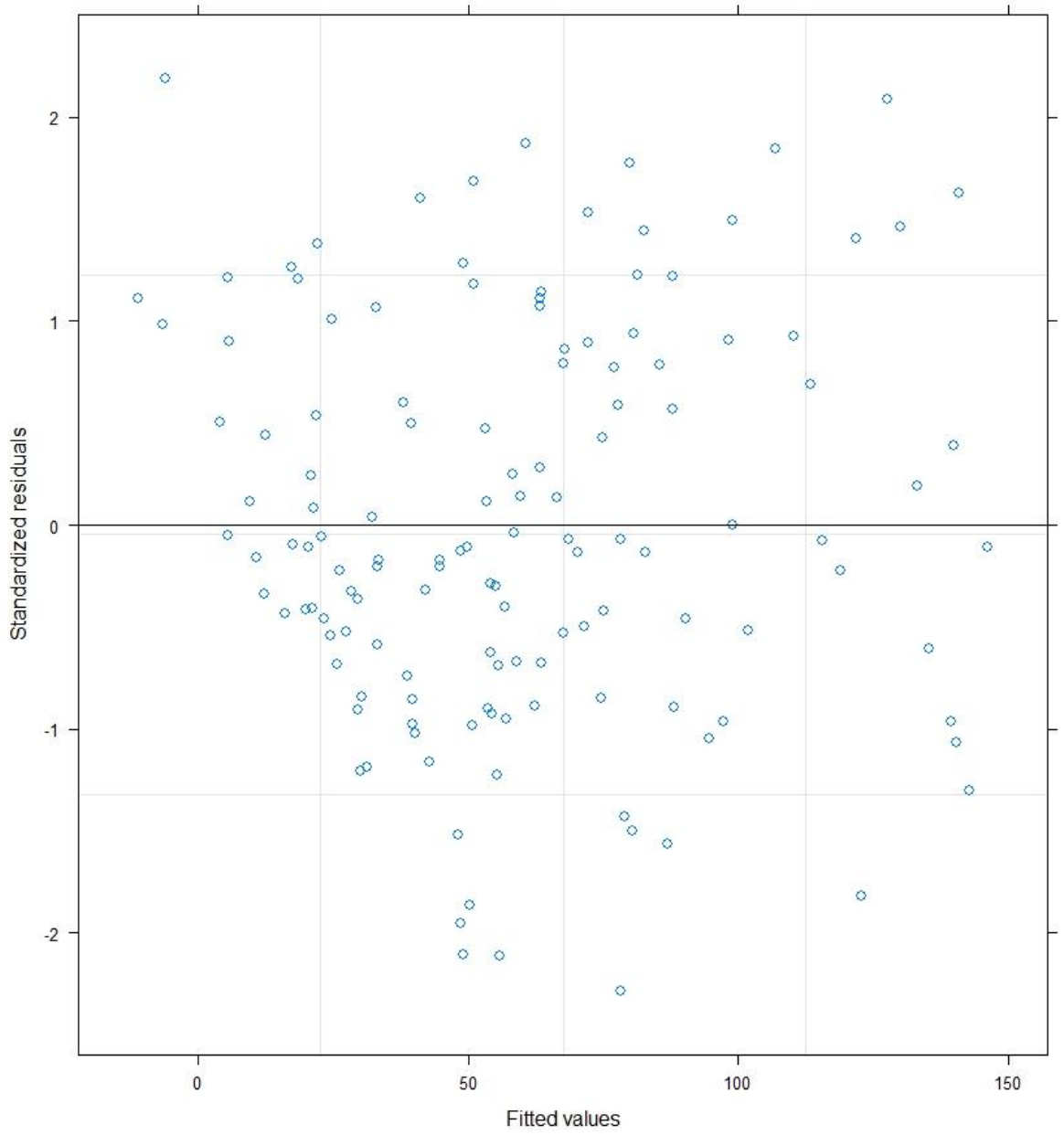

Figure 5.8 Fitted values versus standardized residuals of Pielou evenness and canopy height-based model (test of homogeneity; Table 5.4).

Chapter 6 General discussion

For halting global warming and biodiversity loss, the importance of protected area has been agreed by the scientific community and the policy makers. To evaluate protected area-based forest management approach, monitoring of biodiversity, forest stand structure and ecosystem function need to be explored. The SRF mangrove forest is a reserved forest where more than 50% of its total coverage is protected and from the reserved part of the forest only NTFPs are allowed to be harvested as timber harvest is forbidden from 1989. Thus, this thesis focused on estimation of horizontal variation in carbon stocks in SRF as it is a heterogeneous ecosystem where species zonation is prominent (Chapter 3), on evaluation of vegetation and forest canopy mapping with high resolution optical (WorldView2) and active imagery (TanDEM-X) because both of these forest parameters are important in assessment of ecosystem services such as biodiversity and carbon (Chapter 4), and on understanding of the relationship among tree diversity, forest structure and carbon storage, the key ecosystem processes which are important in the ecosystem based climate change mitigation and adaptation standpoint (Chapter 5).

In Chapter 3, I found that ecosystem carbon stock across the SRF was heterogeneous depending on vegetation type and ecological zonation based on salinity. Among the 10-vegetation types, the *H. fomes* dominant vegetation type had higher carbon stock while *E. agallocha-C. decandera* dominant forest had the least carbon stock. This variation was due to aboveground structure as I found carbon stock was strongly correlated with size of the trees (height) and basal area (Figs. 3.7 and 3.8). So, vegetation types with higher canopy height, larger tree diameter and thus more basal area, contain more ecosystem carbon. In each natural forest there are some key or indicator species which regulates the ecosystem process and thereby affects the carbon storage capacity. In SRF *H. fomes* is the main indicator species which is the tallest tree species (Fig. 4.4) and have large diameter (except *A. officinalis* and *S. apetala*). Thus, carbon stock becomes lower depending on vegetation type with fewer or no *H. fomes*. In terms of salinity, the fresh water zone showed the highest ecosystem carbon stock followed by moderate and strong salinity zones. Salinity was found to enhance belowground carbon stock as revealed by the lowest proportion of belowground carbon stock (57.2 %) with respect to ecosystem carbon in fresh water zone and by the highest (71.9 %) in strong salinity zone. The results also reveal that no matter whether the mangroves are tall or dwarf, significant amount of carbon is stored into the sediment.

As carbon stocks varied depending on species composition or functional type that is common in mangrove ecosystem, the so-called zonation, a high-resolution vegetation map

would contribute to accurate estimation of carbon stock in the spatial stand point. Thus, for developing high-resolution vegetation map, I used WorldView2 (WV2) and TanDEM-X (TDX) imagery as a pioneer study in SRF in Chapter 4. I focus on SEWS as a pilot study site because of its proximity to the three salinity zones which is one of the major determining factors of species composition in SRF. A total of 13 layers (All eight bands of WV2, four Normalized Difference Vegetation Indices and TDX based canopy height) were used for classifying land cover type following the Iterative Self-Organizing Data Analysis Technique Algorithm. I could not find any difference in vegetation or species identification WV2 with or without TDX data combination as in both cases similar overall accuracy, the Kappa Coefficient (WV2-TDX: 89.89% and 0.89, and WV2: 89.33% and 0.88) and change statistics (Table 4.2, 4.3 and 4.1) were found. Therefore, the WV2 image bands and their derivatives (different indices-NDVI) can separate mangrove communities without inclusion of height layer. However, in vegetation classification, height information may be effective if the whole SRF is considered because height difference is prominent in SRF from seaward (Southern) to landwards (Northern) and Eastern to Western depending on salinity and freshwater flow. The combination of different layers in my study separated tree vegetation types at a species level which cover almost 50 % of total area of SEWS (along with six other vegetation types as mixed stand which composed of two or more species: *H. fomes* (45%), *E. agallocha* (3 %), *S. apetala* (1.47%)). I found *H. fomes* as the most dominant which contrasted with the field-based study and had higher mean canopy height (12.30 m) than other eight mangrove types. In remote sensing-based biodiversity monitoring, both species composition and canopy structure are essential biodiversity variables or indicators set by CBD. Thus, the WV2 image can be effective in mangrove biodiversity indicators monitoring. I observed a clear zonation that initiated from canal or river bank to inland areas which is contrasted to the field-based study. Thus, high resolution optical imagery can overcome the spatial limitation of field-based study on spatial distribution and species composition. As I indicated, further field study is needed to check the zonation and unveil responsible factor for these zonation by laying out spatially distributed plots which would represented to total areas of SRF.

Quantification of the relationship between biodiversity and ecosystem function such as carbon stock is important in both ecological and policy formulation perspective (Cavanaugh et al., 2014; Ferreira et al., 2012; Mensah et al., 2016). Though this emerging research has been studied much in grassland and in terrestrial ecosystems (Ferreira et al., 2012), studies in the most carbon rich mangrove forests (Donato et al., 2011) address a key knowledge gap regarding that relationship (Ferreira et al., 2012); such as in Sundarbans Reserved Forest,

Bangladesh. Here I found that overstory diversity was less as two dominant species *H. fomes* and *E. agallocha* represented 94 % of total individuals. Though mangrove tree diversity is poor in SRF, I found that diversity (Shannon) and canopy height positively influence live aboveground carbon (AGC) stocks, which indicates mangrove with higher species diversity have higher carbon storage. Thus, my findings suggest that carbon stock in mangrove ecosystem is regulated by both niche complementarity and selection effects. Therefore, conservation of mangrove biodiversity would ensure climate change mitigation and adaptation because they can sequestrate atmospheric carbon at a higher rate and transport it to sediment which makes mangrove as store house of carbon and provide safeguard against tidal surge and cyclone.

Overall findings of my thesis would contribute to ecology, forest management and international conservation and climate change mitigation approach. Almost 90 % of the mangrove countries (mostly developing countries) lead global conservation and climate change mitigation approaches such REDD+, CBD, Kyoto Protocol, and SDG where they need to report biannually their update on conservation status such as forest cover and carbon change with spatial and temporal distribution of forest species as the biodiversity indicator. The accurate and cost-effective monitoring approach would be appreciated of the above-mentioned conservation and mitigation strategy. As I was able to separate dominant vegetation at species level and other vegetation at two or multiple species mixed stand using WV2 based forest vegetation classification, this method can be applied to whole SRF and other mangroves globally. This approach will contribute directly to REDD+ in terms of monitoring of deforestation and forest degradation as I also separated mangrove from non-mangrove and to CBD in monitoring essential biodiversity variables. On the other hand, the TDX based forest canopy height can be applied to height based allometry for spatial mapping biomass and carbon stock distribution across the whole SRF and similar method can be applied to other mangroves which ultimately help in policy making of REDD+ and CBD of Mangrove dwelling countries.

The positive correlation between mangrove biodiversity and carbon stock suggests that mangrove biodiversity conservation has direct benefit to climate change mitigation. Thus, my study finding suggests that a participatory REDD+ program in mangrove forests would create a triple win situation where conservation of mangrove biodiversity would ensure climate change mitigation and livelihoods support for adjacent forest dependent community from the non-timber forest products including fishery, and carbon credit.

As I found that carbon stocks in SRF varied depending on ecological zonation which is regulated by salinity and freshwater flow, the upstream freshwater from the Ganges river

system plays an important role in carbon sequestration in the Sundarbans. The total coverage of Ganga basin is 1,080,000 km^2 which spans through India (79%), Nepal (14%), Bangladesh (4%) and China (3%) (Rahman and Rahaman, 2017). Among the four countries, Bangladesh is the most downstream. Recently, Rahman and Rahman (2017), found that compared to pre-Farakka Barrage period (1935–1975), in post-Farakka Barrage period (1976–2015), the maximum, average and minimum discharges reduced around 22, 48 and 72%, respectively, in dry season (January–May). This reduction of freshwater due to Farakka Barrage, the south-western region of Bangladesh has been suffering from environmental harm through disruption to fisheries, forestry, agriculture, navigation and salinity intrusion towards inland (Rahman and Rahaman, 2017). Thus, not only the SRF but also Indian Sundarbans are degrading gradually due to this freshwater reduction and thereby affecting carbon stock capacity of the Sundarbans; the cause of top dying of *H. fomes*, most dominant tree species in Sundarbans was also reported as salinity change (Iftekhar and Islam, 2004; Mitra et al., 2011; MOEF, 2010; Rahman and Rahaman, 2017). Therefore, a regional treaty among India, Bangladesh, Nepal and China is urgently needed on upstream freshwater sharing which should be in favor of sufficient environmental flow in SRF and unified Sundarbans for better forest health and environment.

References

Adam, E., Mutanga, O., Rugege, D., 2010. Multispectral and hyperspectral remote sensing for identification and mapping of wetland vegetation: a review. Wetl. Ecol. Manag. 18, 281–296. https://doi.org/10.1007/s11273-009-9169-z

Adame, M.F., Kauffman, J.B., Medina, I., Gamboa, J.N., Torres, O., Caamal, J.P., Reza, M., Herrera-Silveira, J.A., 2013. Carbon Stocks of Tropical Coastal Wetlands within the Karstic Landscape of the Mexican Caribbean. PLOS ONE 8, e56569. https://doi.org/10.1371/journal.pone.0056569

Ahmed, I., Iqbal, Z., 2011. Sundarbans carbon inventory (2010) a comparison with 1997 inventory. SAARC J 1, 59–72.

Alongi, D.M., 2012. Carbon sequestration in mangrove forests. Carbon Manag. 3, 313–322. https://doi.org/10.4155/cmt.12.20

Alongi, D.M., 2008. Mangrove forests: Resilience, protection from tsunamis, and responses to global climate change. Estuar. Coast. Shelf Sci. 76, 1–13. https://doi.org/10.1016/j.ecss.2007.08.024

Anderson, K., Bows, A., 2011. Beyond 'dangerous' climate change: emission scenarios for a new world. Philos. Trans. R. Soc. Lond. Math. Phys. Eng. Sci. 369, 20–44. https://doi.org/10.1098/rsta.2010.0290

Aslan, A., Rahman, A.F., Warren, M.W., Robeson, S.M., 2016. Mapping spatial distribution and biomass of coastal wetland vegetation in Indonesian Papua by combining active and passive remotely sensed data. Remote Sens. Environ. 183, 65–81. https://doi.org/10.1016/j.rse.2016.04.026

Atwood, T.B., Connolly, R.M., Almahasheer, H., Carnell, P.E., Duarte, C.M., Lewis, C.J.E., Irigoien, X., Kelleway, J.J., Lavery, P.S., Macreadie, P.I., Serrano, O., Sanders, C.J., Santos, I., Steven, A.D.L., Lovelock, C.E., 2017. Global patterns in mangrove soil carbon stocks and losses. Nat. Clim. Change 7, 523–528. https://doi.org/10.1038/nclimate3326

Aziz, A., Paul, A., 2015. Bangladesh Sundarbans: Present Status of the Environment and Biota. Diversity 7, 242–269. https://doi.org/10.3390/d7030242

Aziz, M.A., Tollington, S., Barlow, A., Goodrich, J., Shamsuddoha, M., Islam, M.A., Groombridge, J.J., 2017. Investigating patterns of tiger and prey poaching in the Bangladesh Sundarbans: Implications for improved management. Glob. Ecol. Conserv. 9, 70–81. https://doi.org/10.1016/j.gecco.2016.12.001

Baker, T.R., Phillips, O.L., Malhi, Y., Almeida, S., Arroyo, L., Di Fiore, A., Erwin, T., Killeen, T.J., Laurance, S.G., Laurance, W.F., 2004. Variation in wood density determines spatial patterns inAmazonian forest biomass. Glob. Change Biol. 10, 545–562.

Ball, M., 1998. Mangrove species richness in relation to salinity and waterlogging: a case study along the Adelaide River floodplain, northern Australia. Glob. Ecol. Biogeogr. Lett. 7, 73–82. https://doi.org/10.1111/j.1466-8238.1998.00282.x

Ball, M.C., 2002. Interactive effects of salinity and irradiance on growth: implications for mangrove forest structure along salinity gradients. Trees 16, 126–139. https://doi.org/10.1007/s00468-002-0169-3

Balzter, H., Rowland, C.S., Saich, P., 2007. Forest canopy height and carbon estimation at Monks Wood National Nature Reserve, UK, using dual-wavelength SAR interferometry. Remote Sens. Environ. 108, 224–239. https://doi.org/10.1016/j.rse.2006.11.014

BFD, 2018a. খুলনা অঞ্চল - Forest Department-Government of the People\'s Republic of Bangladesh. URLhttp%3A%2F%2Fwww.bforest.gov.bd%2Fsite%2Fview%2Fofficer_list_category%2F%25E0%25A6%2596%25E0%25A7%2581%25E0%25A6%25B2%25E0%25A6%25A8%25E0%25A6%25BE%2520%25E0%25A6%2585%25E0%25A6%259E%25E0%25A7%258D%25E0%25A6%259A%25E0%25A6%25B2 (accessed 5.30.18).

BFD, 2018b. Wildlife-Sanctuary - Forest Department-Government of the People\'s Republic of Bangladesh. http%3A%2F%2Fwww.bforest.gov.bd%2Fsite%2Fpage%2Ff619019f-14cd-481a-86f4-1d5b4ae40515%2FWildlife-Sanctuary (accessed 5.30.18).

Blasco, F., Aizpuru, M., Gers, C., 2001. Depletion of the mangroves of Continental Asia. Wetl. Ecol. Manag. 9, 255–266. https://doi.org/10.1023/A:1011169025815

Bouillon, S., Frankignoulle, M., Dehairs, F., Velimirov, B., Eiler, A., Abril, G., Etcheber, H., Borges, A.V., 2003. Inorganic and organic carbon biogeochemistry in the Gautami Godavari estuary (Andhra Pradesh, India) during pre-monsoon: The local impact of extensive mangrove forests. Glob. Biogeochem. Cycles 17.

Brown, J.K., 1971. A planar intersect method for sampling fuel volume and surface area. For. Sci. 17, 96–102.

Cahoon, D.R., 2006. A review of major storm impacts on coastal wetland elevations. Estuaries Coasts 29, 889–898.

Cavanaugh, K.C., Gosnell, J.S., Davis, S.L., Ahumada, J., Boundja, P., Clark, D.B., Mugerwa, B., Jansen, P.A., O'Brien, T.G., Rovero, F., Sheil, D., Vasquez, R., Andelman, S., 2014. Carbon storage in tropical forests correlates with taxonomic diversity and functional dominance on a global scale: Biodiversity and aboveground carbon storage. Glob. Ecol. Biogeogr. 23, 563–573. https://doi.org/10.1111/geb.12143

CBD, 2010. Strategic Plan for Biodiversity 2011-2020, including Aichi Biodiversity Targets [WWW Document]. URL https://www.cbd.int/sp/default.shtml (accessed 5.3.18).

Cerón-Bretón, R., Cerón-Bretón, J., Sánchez-Junco, R., Damián-Hernández, D., Guerra-Santos, J., Muriel-Garcia, M., Cordova-Quiroz, A., 2011. Evaluation of carbon sequestration potential in mangrove forest at three estuarine sites in Campeche Mexico. Int J Energy Env. 5, 487–494.

Chaffey, D.R., Miller, F.R., Sandom, J.H., 1985. A Forest Inventory of the Sundarbans, Bangladesh. Overseas Development Administration, Land Resources Development Centre, Surrey, England.

Chauvaud, S., Bouchon, C., Maniere, R., 1998. Remote sensing techniques adapted to high resolution mapping of tropical coastal marine ecosystems (coral reefs, seagrass beds and mangrove). Int. J. Remote Sens. 19, 3625–3639. https://doi.org/10.1080/014311698213858

Chave, J., Andalo, C., Brown, S., Cairns, M.A., Chambers, J.Q., Eamus, D., Fölster, H., Fromard, F., Higuchi, N., Kira, T., Lescure, J.-P., Nelson, B.W., Ogawa, H., Puig, H., Riéra, B., Yamakura, T., 2005. Tree allometry and improved estimation of carbon stocks and balance in tropical forests. Oecologia 145, 87–99. https://doi.org/10.1007/s00442-005-0100-x

Chave, J., Condit, R., Aguilar, S., Hernandez, A., Lao, S., Perez, R., 2004. Error propagation and scaling for tropical forest biomass estimates. Philos. Trans. R. Soc. B Biol. Sci. 359, 409–420.

Chave, J., Coomes, D., Jansen, S., Lewis, S.L., Swenson, N.G., Zanne, A.E., 2009. Towards a worldwide wood economics spectrum. Ecol. Lett. 12, 351–366. https://doi.org/10.1111/j.1461-0248.2009.01285.x

Congalton, R.G., 2001. Accuracy assessment and validation of remotely sensed and other spatial information. Int. J. Wildland Fire 10, 321–328. https://doi.org/10.1071/wf01031

Congalton, R.G., Green, K., 2009. Assessing the accuracy of remotely sensed data: principles and practices, 2. ed. ed. CRC Press, Boca Raton, Fla.

Cornforth, W.A., Fatoyinbo, T.E., Freemantle, T.P., Pettorelli, N., 2013. Advanced Land Observing Satellite Phased Array Type L-Band SAR (ALOS PALSAR) to Inform the Conservation of Mangroves: Sundarbans as a Case Study. Remote Sens. 5, 224–237. https://doi.org/10.3390/rs5010224

Crooks, S., Herr, D., Tamelander, J., Laffoley, D., Vandever, J., 2011. Mitigating Climate Change through Restoration and Management of Coastal Wetlands and Near-shore Marine Ecosystems 69.

Cruz, C.C.D., Mendoza, U.N., Queiroz, J.B., Berrêdo, J.F., Neto, S.V.D.C., Lara, R.J., 2013. Distribution of mangrove vegetation along inundation, phosphorus, and salinity gradients on the Bragança Peninsula in Northern Brazil. Plant Soil 370, 393–406. https://doi.org/10.1007/s11104-013-1619-y

Detwiler, R.P., Hall, C. a. S., 1988. Tropical Forests and the Global Carbon Cycle. Science 239, 42–47. https://doi.org/10.1126/science.239.4835.42

Dhodhi, M.K., Saghri, J.A., Ahmad, I., Ul-Mustafa, R., 1999. D-ISODATA: A Distributed Algorithm for Unsupervised Classification of Remotely Sensed Data on Network of Workstations. J. Parallel Distrib. Comput. 59, 280–301. https://doi.org/10.1006/jpdc.1999.1573

Diloksumpun, S., Sripraram, D., Puangchit, L., Wachrinrat, C., Teejuntuk, S., Pranchai, A., Chumsangsri, T., Lamsak, N., 2011. An assessment of stand structure and carbon storage of a mangrove forest in Thailand. IUFRO World Ser. Vol 29 28.

Donato, D.C., Kauffman, J.B., Murdiyarso, D., Kurnianto, S., Stidham, M., Kanninen, M., 2011. Mangroves among the most carbon-rich forests in the tropics. Nat. Geosci. 4, 293–297. https://doi.org/10.1038/ngeo1123

Duke, N.C., Meynecke, J.-O., Dittmann, S., Ellison, A.M., Anger, K., Berger, U., Cannicci, S., Diele, K., Ewel, K.C., Field, C.D., Koedam, N., Lee, S.Y., Marchand, C., Nordhaus, I., Dahdouh-Guebas, F., 2007. A World Without Mangroves? Science 317, 41–42. https://doi.org/10.1126/science.317.5834.41b

Eaton, R.M., 1990. Human settlement and colonization in the Sundarbans, 1200?1750. Agric. Hum. Values 7, 6–16. https://doi.org/10.1007/BF01530432

Ellison, A.M., Bank, M.S., Clinton, B.D., Colburn, E.A., Elliott, K., Ford, C.R., Foster, D.R., Kloeppel, B.D., Knoepp, J.D., Lovett, G.M., Mohan, J., Orwig, D.A., Rodenhouse, N.L., Sobczak, W.V., Stinson, K.A., Stone, J.K., Swan, C.M., Thompson, J., Holle, B.V., Webster, J.R., 2005. Loss of foundation species: consequences for the structure and dynamics of forested ecosystems. Front. Ecol. Environ. 3, 479–486. https://doi.org/10.1890/1540-9295(2005)003[0479:LOFSCF]2.0.CO;2

Ellison, A.M., Mukherjee, B.B., Karim, A., 2000. Testing patterns of zonation in mangroves: scale dependence and environmental correlates in the Sundarbans of Bangladesh. J. Ecol. 88, 813–824.

Ellison, J., Zouh, I., 2012. Vulnerability to Climate Change of Mangroves: Assessment from Cameroon, Central Africa. Biology 1, 617–638. https://doi.org/10.3390/biology1030617

Ellison, J.C., 2015. Vulnerability assessment of mangroves to climate change and sea-level rise impacts. Wetl. Ecol. Manag. 23, 115–137. https://doi.org/10.1007/s11273-014-9397-8

Emch, M., Peterson, M., 2006. Mangrove Forest Cover Change in the Bangladesh Sundarbans from 1989-2000: A Remote Sensing Approach. Geocarto Int. 21, 5–12. https://doi.org/10.1080/10106040608542368

Fatoyinbo, T., Feliciano, E.A., Lagomasino, D., Lee, S.K., Trettin, C., 2018. Estimating mangrove aboveground biomass from airborne LiDAR data: a case study from the Zambezi River delta. Environ. Res. Lett. 13, 025012. https://doi.org/10.1088/1748-9326/aa9f03

Fatoyinbo, T., Lagomasino, D., Simard, M., Lee, S.K., Feliciano, E.A., Trettin, C., 2017. High-resolution three-dimensional mapping of forest structure and aboveground biomass stocks in blue carbon ecosystems with airborne Lidar, TanDEM-X and WorldView Stereo. AGU Fall Meet. Abstr. 33.

Fatoyinbo, T.E., Simard, M., 2013. Height and biomass of mangroves in Africa from ICESat/GLAS and SRTM. Int. J. Remote Sens. 34, 668–681. https://doi.org/10.1080/01431161.2012.712224

Feliciano, E.A., Wdowinski, S., Potts, M.D., Lee, S.-K., Fatoyinbo, T.E., 2017. Estimating Mangrove Canopy Height and Above-Ground Biomass in the Everglades National Park with Airborne LiDAR and TanDEM-X Data. Remote Sens. 9, 702.

Ferreira, J., Gardner, T., Guariguata, M.R., Koh, L.P., Okabe, K., Pan, Y., Schmitt, C.B., Tylianakis, J.M., Barlow, J., Kapos, V., Kurz, W.A., Parrotta, J.A., Spalding, M., Van Vliet, N., 2012. Forest biodiversity, carbon and other ecosystem services: relationships and impacts of deforestation and forest degradation. International Union of Forest Research Organizations (IUFRO), Vienna, Austria.

Friess, D., 2016. Ecosystem Services and Disservices of Mangrove Forests: Insights from Historical Colonial Observations. Forests 7, 183. https://doi.org/10.3390/f7090183

Fromard, F., Puig, H., Mougin, E., Marty, G., Betoulle, J.L., Cadamuro, L., 1998. Structure, above-ground biomass and dynamics of mangrove ecosystems: new data from French Guiana. Oecologia 115, 39–53. https://doi.org/10.1007/s004420050489

Fujimoto, K., Imaya, A., Tabuchi, R., Kuramoto, S., Utsugi, H., Murofushi, T., 1999. Belowground carbon storage of Micronesian mangrove forests. Ecol. Res. 14, 409–413.

Ghosh, M.K., Kumar, L., Roy, C., 2016. Mapping Long-Term Changes in Mangrove Species Composition and Distribution in the Sundarbans. Forests 7, 305. https://doi.org/10.3390/f7120305

Giri, C., 2016. Observation and Monitoring of Mangrove Forests Using Remote Sensing: Opportunities and Challenges. Remote Sens. 8, 783. https://doi.org/10.3390/rs8090783
Giri, C., Ochieng, E., Tieszen, L.L., Zhu, Z., Singh, A., Loveland, T., Masek, J., Duke, N., 2011. Status and distribution of mangrove forests of the world using earth observation satellite data. Glob. Ecol. Biogeogr. 20, 154–159. https://doi.org/10.1111/j.1466-8238.2010.00584.x
Giri, C., Shrestha, S., 1996. Land cover mapping and monitoring from NOAA AVHRR data in Bangladesh. Int. J. Remote Sens. 17, 2749–2759. https://doi.org/10.1080/01431169608949105
Giri, C., Zhu, Z., Tieszen, L.L., Singh, A., Gillette, S., Kelmelis, J.A., 2008. Mangrove forest distributions and dynamics (1975–2005) of the tsunami-affected region of Asia. J. Biogeogr. 35, 519–528. https://doi.org/10.1111/j.1365-2699.2007.01806.x
Goodale, C.L., Apps, M.J., Birdsey, R.A., Field, C.B., Heath, L.S., Houghton, R.A., Jenkins, J.C., Kohlmaier, G.H., Kurz, W., Liu, S., Nabuurs, G.-J., Nilsson, S., Shvidenko, A.Z., 2002. Forest Carbon Sinks in the Northern Hemisphere. Ecol. Appl. 12, 891–899. https://doi.org/10.1890/1051-0761(2002)012[0891:FCSITN]2.0.CO;2
Gopal, B., Chauhan, M., 2006. Biodiversity and its conservation in the Sundarban Mangrove Ecosystem. Aquat. Sci. 68, 338–354. https://doi.org/10.1007/s00027-006-0868-8
Hamilton, S.E., Casey, D., 2016. Creation of a high spatio-temporal resolution global database of continuous mangrove forest cover for the 21st century (CGMFC-21): CGMFC-21. Glob. Ecol. Biogeogr. 25, 729–738. https://doi.org/10.1111/geb.12449
Hamilton, S.E., Friess, D.A., 2018. Global carbon stocks and potential emissions due to mangrove deforestation from 2000 to 2012. Nat. Clim. Change 8, 240–244. https://doi.org/10.1038/s41558-018-0090-4
Harmon, M.E., Sexton, J., 1996. Guidelines for measurements of woody detritus in forest ecosystems. US LTER Network Office Seattle (WA).
Harrison, M.E., Paoli, G.D., 2012. Managing the Risk of Biodiversity Leakage from Prioritising REDD+ in the Most Carbon-Rich Forests: The Case Study of Peat-Swamp Forests in Kalimantan, Indonesia. Trop. Conserv. Sci. 5, 426–433. https://doi.org/10.1177/194008291200500402
Heenkenda, M., Joyce, K., Maier, S., Bartolo, R., 2014. Mangrove Species Identification: Comparing WorldView-2 with Aerial Photographs. Remote Sens. 6, 6064–6088. https://doi.org/10.3390/rs6076064
Herold, M., van Groenestijn, A., Kooistra, L., Kalogirou, V., Arino, O., 2011. User Requirements documents: Land Cover CCI. Univ. Cathol. Louvain UCL-Geomat. Louvain--Neuve Belg.
Herr, D., von Unger, M., Laffoley, D., McGivern, A., 2017. Pathways for implementation of blue carbon initiatives. Aquat. Conserv. Mar. Freshw. Ecosyst. 27, 116–129. https://doi.org/10.1002/aqc.2793
Heumann, B.W., 2011. Satellite remote sensing of mangrove forests: Recent advances and future opportunities. Prog. Phys. Geogr. 35, 87–108. https://doi.org/10.1177/0309133310385371
Hossain, M., Siddique, M.R.H., Saha, S., Abdullah, S.M.R., 2015. Allometric models for biomass, nutrients and carbon stock in Excoecaria agallocha of the Sundarbans, Bangladesh. Wetl. Ecol. Manag. 23, 765–774. https://doi.org/10.1007/s11273-015-9419-1
Huq, N., Hugé, J., Boon, E., Gain, A.K., 2015. Climate Change Impacts in Agricultural Communities in Rural Areas of Coastal Bangladesh: A Tale of Many Stories. Sustainability 7, 8437–8460. https://doi.org/10.3390/su7078437
Iftekhar, M. s., Islam, M. r., 2004. Degeneration of Bangladesh's Sundarbans Mangroves: A Management Issue. Int. For. Rev. 6, 123–135. https://doi.org/10.1505/ifor.6.2.123.38390
Iftekhar, M., Saenger, P., 2008. Vegetation dynamics in the Bangladesh Sundarbans mangroves: a review of forest inventories. Wetl. Ecol. Manag. 16, 291–312.
Imai, N., Tanaka, A., Samejima, H., Sugau, J.B., Pereira, J.T., Titin, J., Kurniawan, Y., Kitayama, K., 2014. Tree community composition as an indicator in biodiversity monitoring of REDD+. For. Ecol. Manag. 313, 169–179. https://doi.org/10.1016/j.foreco.2013.10.041
Isbell, F., Craven, D., Connolly, J., Loreau, M., Schmid, B., Beierkuhnlein, C., Bezemer, T.M., Bonin, C., Bruelheide, H., Luca, E. de, Ebeling, A., Griffin, J.N., Guo, Q., Hautier, Y., Hector, A., Jentsch, A., Kreyling, J., Lanta, V., Manning, P., Meyer, S.T., Mori, A.S., Naeem, S., Niklaus, P.A., Polley, H.W., Reich, P.B., Roscher, C., Seabloom, E.W., Smith, M.D., Thakur, M.P.,

Tilman, D., Tracy, B.F., Putten, W.H. van der, Ruijven, J. van, Weigelt, A., Weisser, W.W., Wilsey, B., Eisenhauer, N., 2015. Biodiversity increases the resistance of ecosystem productivity to climate extremes. Nature 526, 574–577. https://doi.org/10.1038/nature15374
Islam, M., 2011. Biodiversity and livelihoods: A case study in Sundarbans Reserve.
Islam, M., Dey, A., Rahman, M., 2015. Effect of Tree Diversity on Soil Organic Carbon Content in the Homegarden Agroforestry System of North-Eastern Bangladesh. Small-Scale For. 14, 91–101. https://doi.org/10.1007/s11842-014-9275-5
Islam, M.J., Alam, M.S., Elahi, K.M., 1997. Remote sensing for change detection in the Sunderbands, Bangladesh. Geocarto Int. 12, 91–100. https://doi.org/10.1080/10106049709354601
Islam, S., Rahman, M., Chakma, S., 2014. Plant Diversity and Forest Structure of the Three Protected Areas (Wildlife Sanctuaries) of Bangladesh Sundarbans: Current Status and Management Strategies, in: Mangrove Ecosystems of Asia. Springer, New York, NY, pp. 127–152. https://doi.org/10.1007/978-1-4614-8582-7_7
IUFRO, 2009. IUFRO: The Report / Adaptation of Forests to Climate Change / Global Forest Expert Panels (GFEP) [WWW Document]. URL https://www.iufro.org/science/gfep/adaptaion-panel/the-report/ (accessed 5.31.18).
Jain, T.B., Fried, J.S., 2010. Field instructions for the annual inventory of California, Oregon, and Washington 2010: Supplement for: Fire effects and recovery study. US Dep. Agric. For. Serv. Pac. Northwest Res. Stn. For. Inventory Anal. Resour. Monit. Assess. Program 30 P.
Kamal, M., Phinn, S., 2011. Hyperspectral Data for Mangrove Species Mapping: A Comparison of Pixel-Based and Object-Based Approach. Remote Sens. 3, 2222–2242. https://doi.org/10.3390/rs3102222
Kamal, M., Phinn, S., Johansen, K., 2015. Object-Based Approach for Multi-Scale Mangrove Composition Mapping Using Multi-Resolution Image Datasets. Remote Sens. 7, 4753–4783. https://doi.org/10.3390/rs70404753
Karim, A., 1988. Environment factors and the distribution of mangroves in the Sundarbans with special reference to Sundric C. Heritiera fomes.
Karim, J., Karim, A., 1993. Effect of salinity on the growth of some mangrove plants in Bangladesh, in: Towards the Rational Use of High Salinity Tolerant Plants, Tasks for Vegetation Science. Springer, Dordrecht, pp. 187–192. https://doi.org/10.1007/978-94-011-1858-3_20
Kasawani, I., Kamaruzaman, J., Nurun-Nadhirah, M., 2007. Biological diversity assessment of Tok Bali mangrove forest, Kelantan, Malaysia. WSEAS Trans. Environ. Dev. 3, 37–44.
Kathiresan, K., Bingham, B.L., 2001. Biology of mangroves and mangrove Ecosystems. Adv. Mar. Biol. 40, 81–251. https://doi.org/10.1016/S0065-2881(01)40003-4
Kathiresan, K., Rajendran, N., 2005. Coastal mangrove forests mitigated tsunami. Estuar. Coast. Shelf Sci. 65, 601–606. https://doi.org/10.1016/j.ecss.2005.06.022
Kauffman, J.B., Cole, T.G., 2010. Micronesian Mangrove Forest Structure and Tree Responses to a Severe Typhoon. Wetlands 30, 1077–1084. https://doi.org/10.1007/s13157-010-0114-y
Kauffman, J.B., Heider, C., Cole, T.G., Dwire, K.A., Donato, D.C., 2011. Ecosystem carbon stocks of Micronesian mangrove forests. Wetlands 31, 343–352.
Kauffman, J.B., Heider, C., Norfolk, J., Payton, F., 2014. Carbon stocks of intact mangroves and carbon emissions arising from their conversion in the Dominican Republic. Ecol. Appl. 24, 518–527.
Kessler, M., Hertel, D., Jungkunst, H.F., Kluge, J., Abrahamczyk, S., Bos, M., Buchori, D., Gerold, G., Gradstein, S.R., Köhler, S., Leuschner, C., Moser, G., Pitopang, R., Saleh, S., Schulze, C.H., Sporn, S.G., Steffan-Dewenter, I., Tjitrosoedirdjo, S.S., Tscharntke, T., 2012. Can Joint Carbon and Biodiversity Management in Tropical Agroforestry Landscapes Be Optimized? PLoS ONE 7, e47192. https://doi.org/10.1371/journal.pone.0047192
Khan, M.N.I., Suwa, R., Hagihara, A., 2007. Carbon and nitrogen pools in a mangrove stand of <Emphasis Type="Italic">Kandelia obovata</Emphasis> (S., L.) Yong: vertical distribution in the soil–vegetation system. Wetl. Ecol. Manag. 15, 141–153. https://doi.org/10.1007/s11273-006-9020-8
Kirby, K.R., Potvin, C., 2007. Variation in carbon storage among tree species: Implications for the management of a small-scale carbon sink project. For. Ecol. Manag. 246, 208–221. https://doi.org/10.1016/j.foreco.2007.03.072

Kirui, B., Kairo, J., Skov, M., Mencuccini, M., Huxham, M., 2012. Effects of species richness, identity and environmental variables on growth in planted mangroves in Kenya. Mar. Ecol. Prog. Ser. 465, 1–10. https://doi.org/10.3354/meps09999

Klimesova, J., Latzel, V., de Bello, F., van Groenendael, J.M., 2008. Plant functional traits in studies of vegetation changes in response to grazing and mowing: towards a use of more specific traits. Preslia 80, 245–253.

Komiyama, A., Havanond, S., Srisawatt, W., Mochida, Y., Fujimoto, K., Ohnishi, T., Ishihara, S., Miyagi, T., 2000. Top/root biomass ratio of a secondary mangrove (Ceriops tagal (Perr.) CB Rob.) forest. For. Ecol. Manag. 139, 127–134.

Komiyama, A., Ong, J.E., Poungparn, S., 2008. Allometry, biomass, and productivity of mangrove forests: A review. Aquat. Bot. 89, 128–137.

Komiyama, A., Poungparn, S., Kato, S., 2005. Common allometric equations for estimating the tree weight of mangroves. J. Trop. Ecol. 21, 471–477. https://doi.org/10.1017/S0266467405002476

Kridiborworn, P., Chidthaisong, A., Yuttitham, M., Tripetchkul, S., 2012. Carbon sequestration by mangrove forest planted specifically for charcoal production in Yeesarn, Samut Songkram. J. Sustain. Energy Environ. 3, 87–92.

Kristensen, E., Bouillon, S., Dittmar, T., Marchand, C., 2008. Organic carbon dynamics in mangrove ecosystems: A review. Aquat. Bot., Mangrove Ecology – Applications in Forestry and Costal Zone Management 89, 201–219. https://doi.org/10.1016/j.aquabot.2007.12.005

Kuenzer, C., Bluemel, A., Gebhardt, S., Quoc, T.V., Dech, S., 2011. Remote Sensing of Mangrove Ecosystems: A Review. Remote Sens. 3, 878–928. https://doi.org/10.3390/rs3050878

Kuenzer, C., Ottinger, M., Wegmann, M., Guo, H., Wang, C., Zhang, J., Dech, S., Wikelski, M., 2014. Earth observation satellite sensors for biodiversity monitoring: potentials and bottlenecks. Int. J. Remote Sens. 35, 6599–6647. https://doi.org/10.1080/01431161.2014.964349

Laffoley, D., Grimsditch, G.D., 2009. The management of natural coastal carbon sinks. Iucn.

Lagomasino, D., Fatoyinbo, T., Lee, S., Feliciano, E., Trettin, C., Simard, M., 2016. A Comparison of Mangrove Canopy Height Using Multiple Independent Measurements from Land, Air, and Space. Remote Sens. 8, 327. https://doi.org/10.3390/rs8040327

Lagomasino, D., Fatoyinbo, T., Lee, S., Simard, M., 2015. High-resolution forest canopy height estimation in an African blue carbon ecosystem. Remote Sens. Ecol. Conserv. 1, 51–60. https://doi.org/10.1002/rse2.3

Lee, S.K., Fatoyinbo, T., Lagomasino, D., Osmanoglu, B., Feliciano, E., 2016. Ground-level digital terrain model (DTM) construction from TanDEM-X InSAR data and WorldView stereo-photogrammetric images, in: 2016 IEEE International Geoscience and Remote Sensing Symposium (IGARSS). Presented at the 2016 IEEE International Geoscience and Remote Sensing Symposium (IGARSS), pp. 6040–6042. https://doi.org/10.1109/IGARSS.2016.7730578

Lee, S.K., Fatoyinbo, T., Lagomasino, D., Osmanoglu, B., Simard, M., Trettin, C., Rahman, M., Ahmed, I., 2015. Large-scale mangrove canopy height map generation from TanDEM-X data by means of Pol-InSAR techniques, in: 2015 IEEE International Geoscience and Remote Sensing Symposium (IGARSS). Presented at the 2015 IEEE International Geoscience and Remote Sensing Symposium (IGARSS), pp. 2895–2898. https://doi.org/10.1109/IGARSS.2015.7326420

Lee, S.K., Fatoyinbo, T.E., 2015. TanDEM-X Pol-InSAR Inversion for Mangrove Canopy Height Estimation. IEEE J. Sel. Top. Appl. Earth Obs. Remote Sens. 8, 3608–3618. https://doi.org/10.1109/JSTARS.2015.2431646

Loucks, C., Barber-Meyer, S., Hossain, M.A.A., Barlow, A., Chowdhury, R.M., 2010. Sea level rise and tigers: predicted impacts to Bangladesh's Sundarbans mangroves: A letter. Clim. Change 98, 291–298. https://doi.org/10.1007/s10584-009-9761-5

MacDicken, K.G., 1997. A guide to monitoring carbon storage in forestry and agroforestry projects.

Machiwa, J.F., Hallberg, R.O., 2002. An empirical model of the fate of organic carbon in a mangrove forest partly affected by anthropogenic activity. Ecol. Model. 147, 69–83. https://doi.org/10.1016/S0304-3800(01)00407-0

Margalef, R., 1958. Information theory in biology. Gen. Syst. Yearb. 3, 36–71.

Mark Westoby, Daniel S. Falster, Angela T. Moles, Peter A. Vesk, Wright, and I.J., 2002. Plant Ecological Strategies: Some Leading Dimensions of Variation Between Species. Annu. Rev. Ecol. Syst. 33, 125–159. https://doi.org/10.1146/annurev.ecolsys.33.010802.150452

Martinez-Sanchez, J.L., Cabrales, L.C., 2012. Is there a relationship between floristic diversity and carbon stocks in tropical vegetation in Mexico? Afr. J. Agric. Res. 7, 2584–2591. https://doi.org/10.5897/AJAR11.599

Mattsson, E., Ostwald, M., Nissanka, S.P., Pushpakumara, D.K.N.G., 2015. Quantification of carbon stock and tree diversity of homegardens in a dry zone area of Moneragala district, Sri Lanka. Agrofor. Syst. 89, 435–445. https://doi.org/10.1007/s10457-014-9780-8

Mensah, S., Veldtman, R., Assogbadjo, A.E., Glèlè Kakaï, R., Seifert, T., 2016. Tree species diversity promotes aboveground carbon storage through functional diversity and functional dominance. Ecol. Evol. 6, 7546–7557. https://doi.org/10.1002/ece3.2525

Mitra, A., Sengupta, K., Banerjee, K., 2011. Standing biomass and carbon storage of above-ground structures in dominant mangrove trees in the Sundarbans. For. Ecol. Manag. 261, 1325–1335. https://doi.org/10.1016/j.foreco.2011.01.012

MOEF, 2010. Integrated Resources Management Plans for the Sundarbans. Ministry of Environment and Forests,Dhaka, Bangladesh.

Moles, A.T., Warton, D.I., Warman, L., Swenson, N.G., Laffan, S.W., Zanne, A.E., Pitman, A., Hemmings, F.A., Leishman, M.R., 2009. Global patterns in plant height. J. Ecol. 97, 923–932. https://doi.org/10.1111/j.1365-2745.2009.01526.x

Mondal, S.H., Debnath, P., 2017. Spatial and Temporal Changes of Sundarbans Reserve Forest in Bangladesh. Environ. Nat. Resour. J. 15, 51–61.

Murdiyarso, D., Donato, D., Kauffman, J.B., Kurnianto, S., Stidham, M., Kanninen, M., 2010. Carbon storage in mangrove and peatland ecosystems: a preliminary account from plots in Indonesia. Cent. Int. For. Res. https://doi.org/10.17528/cifor/003233

Murdiyarso, Daniel, Donato, D., Kauffman, J.B., Kurnianto, S., Stidham, M., Kanninen, M., 2010. Carbon storage in mangrove and peatland ecosystems: a preliminary account from plots in Indonesia. Center for International Forestry Research (CIFOR), Bogor, Indonesia.

Murray, J.P., Grenyer, R., Wunder, S., Raes, N., Jones, J.P.G., 2015. Spatial patterns of carbon, biodiversity, deforestation threat, and REDD+ projects in Indonesia. Conserv. Biol. 29, 1434–1445. https://doi.org/10.1111/cobi.12500

Nakagawa, S., Schielzeth, H., 2013. A general and simple method for obtaining R2 from generalized linear mixed-effects models. Methods Ecol. Evol. 4, 133–142. https://doi.org/10.1111/j.2041-210x.2012.00261.x

Neigh, C.S.R., Masek, J.G., Nickeson, J.E., 2013. High-Resolution Satellite Data Open for Government Research. Eos Trans. Am. Geophys. Union 94, 121–123. https://doi.org/10.1002/2013EO130002

Neukermans, G., Dahdouh-Guebas, F., Kairo, J.G., Koedam, N., 2008. Mangrove species and stand mapping in Gazi Bay (Kenya) using Quickbird satellite imagery. J. Spat. Sci. 53, 75–86.

O'Connor, B., Secades, C., Penner, J., Sonnenschein, R., Skidmore, A., Burgess, N.D., Hutton, J.M., 2015. Earth observation as a tool for tracking progress towards the Aichi Biodiversity Targets. Remote Sens. Ecol. Conserv. 1, 19–28. https://doi.org/10.1002/rse2.4

Pachauri, R.K., Reisinger, A., 2007. Climate change 2007 synthesis report: summary for policymakers. IPCC Secretariat.

Page, S.E., Siegert, F., Rieley, J.O., Boehm, H.-D.V., Jaya, A., Limin, S., 2002. The amount of carbon released from peat and forest fires in Indonesia during 1997. Nature 420, 61.

Pandit, P.K., 2013. Past Management History of Mangrove Forests of Sundarbans.

Pearson, T., 2005. Sourcebook for Land Use, Land-Use Change and Forestry Projects 64.

Pendleton, L., Donato, D.C., Murray, B.C., Crooks, S., Jenkins, W.A., Sifleet, S., Craft, C., Fourqurean, J.W., Kauffman, J.B., Marbà, N., Megonigal, P., Pidgeon, E., Herr, D., Gordon, D., Baldera, A., 2012. Estimating Global "Blue Carbon" Emissions from Conversion and Degradation of Vegetated Coastal Ecosystems. PLoS ONE 7, e43542. https://doi.org/10.1371/journal.pone.0043542

Penman, J., Gytarsky, M., Hiraishi, T., Krug, T., Kruger, D., Pipatti, R., Buendia, L., Miwa, K., Ngara, T., Tanabe, K., Wagner, F., 2003. Good practice guidance for land use, land-use change and forestry. Good Pract. Guid. Land Use Land-Use Change For.

Pereira, H.M., Ferrier, S., Walters, M., Geller, G.N., Jongman, R.H.G., Scholes, R.J., Bruford, M.W., Brummitt, N., Butchart, S.H.M., Cardoso, A.C., Coops, N.C., Dulloo, E., Faith, D.P., Freyhof, J., Gregory, R.D., Heip, C., Höft, R., Hurtt, G., Jetz, W., Karp, D.S., McGeoch, M.A., Obura, D., Onoda, Y., Pettorelli, N., Reyers, B., Sayre, R., Scharlemann, J.P.W., Stuart, S.N., Turak, E., Walpole, M., Wegmann, M., 2013. Essential Biodiversity Variables. Science 339, 277–278. https://doi.org/10.1126/science.1229931

Petrou, Z.I., Manakos, I., Stathaki, T., 2015. Remote sensing for biodiversity monitoring: a review of methods for biodiversity indicator extraction and assessment of progress towards international targets. Biodivers. Conserv. 24, 2333–2363. https://doi.org/10.1007/s10531-015-0947-z

Phelps, J., Webb, E.L., Adams, W.M., 2012. Biodiversity co-benefits of policies to reduce forest-carbon emissions. Nat. Clim. Change 2, 497–503. https://doi.org/10.1038/nclimate1462

Phelps, J., Webb, E.L., Koh, L.P., 2011. Risky business: an uncertain future for biodiversity conservation finance through REDD+: Financial risks of REDD+. Conserv. Lett. 4, 88–94. https://doi.org/10.1111/j.1755-263X.2010.00155.x

Pielou, E.C., 1969. An introduction to mathematical ecology. Wiley-Interscience.

Poorter, L., Sande, M. van der, Thompson, J., Arets, E., Alarcón, A., Álvarez-Sánchez, J., Ascarrunz, N., Balvanera, P., Barajas-Guzmán, G., Boit, A., 2015. Diversity enhances carbon storage in tropical forests. Glob. Ecol. Biogeogr. 24, 1314–1328.

R Core Team, 2018. R: a language and environment for statistical computing. R Foundation for Statistical Computing, Vienna, Austria [WWW Document]. URL https://www.r-project.org/ (accessed 4.28.18).

R Core Team, 2014. R: The R Project for Statistical Computing [WWW Document]. URL https://www.r-project.org/ (accessed 5.31.18).

Rahman, M.M., Kabir, M.E., Ahmed, I., 2017. Protected Areas for Climate Change Mitigation and Livelihood Option: A Case Study of the Bangladesh Sundarbans Mangrove Forest, in: Participatory Mangrove Management in a Changing Climate, Disaster Risk Reduction. Springer, Tokyo, pp. 119–136. https://doi.org/10.1007/978-4-431-56481-2_8

Rahman, M.M., Kabir, M.E., Jahir Uddin Akon, A.S.M., Ando, K., 2015. High carbon stocks in roadside plantations under participatory management in Bangladesh. Glob. Ecol. Conserv. 3, 412–423. https://doi.org/10.1016/j.gecco.2015.01.011

Rahman, M.M., Khan, M.N.I., Hoque, A.K.F., Ahmed, I., 2015. Carbon stock in the Sundarbans mangrove forest: spatial variations in vegetation types and salinity zones. Wetl. Ecol. Manag. 23, 269–283. https://doi.org/10.1007/s11273-014-9379-x

Rahman, M.M., Rahaman, M.M., 2017. Impacts of Farakka barrage on hydrological flow of Ganges river and environment in Bangladesh. Sustain. Water Resour. Manag. 1–14. https://doi.org/10.1007/s40899-017-0163-y

Rahman, M.S., Hossain, G.M., Khan, S.A., Uddin, S.N., 2015. An annotated checklist of the vascular plants of Sundarban Mangrove Forest of Bangladesh. Bangladesh J. Plant Taxon. 22, 17–41. https://doi.org/10.3329/bjpt.v22i1.23862

Roy, A.K.D., Alam, K., Gow, J., 2012. A review of the role of property rights and forest policies in the management of the Sundarbans Mangrove Forest in Bangladesh. For. Policy Econ. 15, 46–53. https://doi.org/10.1016/j.forpol.2011.08.009

Ruiz-Jaen, M.C., Potvin, C., 2011. Can we predict carbon stocks in tropical ecosystems from tree diversity? Comparing species and functional diversity in a plantation and a natural forest. New Phytol. 189, 978–987. https://doi.org/10.1111/j.1469-8137.2010.03501.x

Ruiz-Jaen, M.C., Potvin, C., 2010. Tree Diversity Explains Variation in Ecosystem Function in a Neotropical Forest in Panama. Biotropica 42, 638–646. https://doi.org/10.1111/j.1744-7429.2010.00631.x

Schnitzer, S.A., DeWalt, S.J., Chave, J., 2006. Censusing and measuring lianas: a quantitative comparison of the common methods. Biotropica 38, 581–591.

SDG, 2015. Sustainable Development Goals: 17 Goals to Transform Our World [WWW Document]. URL https://www.un.org/sustainabledevelopment/ (accessed 5.3.18).

Seidensticker, J., Hai, M.A., 1983. The Sundarbans wildlife management plan: conservation in the Bangladesh coastal zone.
Shannon, C.E., 1948. A mathematical theory of communication. Bell Syst. Tech. J. 27, 379–423. https://doi.org/10.1002/j.1538-7305.1948.tb01338.x
Sharma, C.M., Baduni, N.P., Gairola, S., Ghildiyal, S.K., Suyal, S., 2010. Tree diversity and carbon stocks of some major forest types of Garhwal Himalaya, India. For. Ecol. Manag. 260, 2170–2179. https://doi.org/10.1016/j.foreco.2010.09.014
Siddiqi, N.A., 2001. Mangrove forestry in Bangladesh. Institute of Forestry & Environmental Sciences, University of Chittagong.
Siikamaki, J., Sanchirico, J.N., Jardine, S.L., 2012. Global economic potential for reducing carbon dioxide emissions from mangrove loss. Proc. Natl. Acad. Sci. 109, 14369–14374. https://doi.org/10.1073/pnas.1200519109
Smith, Christopher W., 1983. Soil survey of Islands of Yap Federated States of Micronesia [Trust Territory of Pacific Islands].
Smith, Christopher W, 1983. Soil survey of islands of Palau, Republic of Palau.
Stocker, T.F., Qin, D., Plattner, G.-K., Alexander, L.V., Allen, S.K., Bindoff, N.L., Bréon, F.-M., Church, J.A., Cubasch, U., Emori, S., 2013. Technical summary, in: Climate Change 2013: The Physical Science Basis. Contribution of Working Group I to the Fifth Assessment Report of the Intergovernmental Panel on Climate Change. Cambridge University Press, pp. 33–115.
Thant, Y.M., Kanzaki, M., Than, M.M., 2010. Mitigation Effects of Forests as a Natural Shelter in the Cyclone Nargis in Myanmar. Asian J. Environ. Disaster Manag. AJEDM - Focus. -Act. Risk Reduct. Asia 02, 179. https://doi.org/10.3850/S1793924009000169
Thomas, N., Lucas, R., Bunting, P., Hardy, A., Rosenqvist, A., Simard, M., 2017a. Distribution and drivers of global mangrove forest change, 1996–2010. PLOS ONE 12, e0179302. https://doi.org/10.1371/journal.pone.0179302
Thomas, N., Lucas, R., Bunting, P., Hardy, A., Rosenqvist, A., Simard, M., 2017b. Distribution and drivers of global mangrove forest change, 1996–2010. PLOS ONE 12, e0179302. https://doi.org/10.1371/journal.pone.0179302
Tilman, D., Isbell, F., Cowles, J.M., 2014. Biodiversity and Ecosystem Functioning. Annu. Rev. Ecol. Evol. Syst. 45, 471–493. https://doi.org/10.1146/annurev-ecolsys-120213-091917
Trettin, C.C., Stringer, C.E., Zarnoch, S.J., 2016. Composition, biomass and structure of mangroves within the Zambezi River Delta. Wetl. Ecol. Manag. 24, 173–186. https://doi.org/10.1007/s11273-015-9465-8
Turnhout, E., Gupta, A., Weatherley-Singh, J., Vijge, M.J., de Koning, J., Visseren-Hamakers, I.J., Herold, M., Lederer, M., 2017. Envisioning REDD+ in a post-Paris era: between evolving expectations and current practice: Envisioning REDD+ in a post-Paris era. Wiley Interdiscip. Rev. Clim. Change 8, e425. https://doi.org/10.1002/wcc.425
Twilley, R.R., Chen, R., 1998. A water budget and hydrology model of a basin mangrove forest in Rookery Bay, Florida. Mar. Freshw. Res. 49, 309–323. https://doi.org/10.1071/mf97220
Uddin, M.S., de Ruyter van Steveninck, E., Stuip, M., Shah, M.A.R., 2013. Economic valuation of provisioning and cultural services of a protected mangrove ecosystem: A case study on Sundarbans Reserve Forest, Bangladesh. Ecosyst. Serv. 5, 88–93. https://doi.org/10.1016/j.ecoser.2013.07.002
van Ewijk, K.Y., Randin, C.F., Treitz, P.M., Scott, N.A., 2014. Predicting fine-scale tree species abundance patterns using biotic variables derived from LiDAR and high spatial resolution imagery. Remote Sens. Environ. 150, 120–131. https://doi.org/10.1016/j.rse.2014.04.026
Van Wagner, C., 1968. The line intersect method in forest fuel sampling. For. Sci. 14, 20–26.
Wahid, S.M., Babel, M.S., Bhuiyan, A.R., 2007. Hydrologic monitoring and analysis in the Sundarbans mangrove ecosystem, Bangladesh. J. Hydrol. 332, 381–395. https://doi.org/10.1016/j.jhydrol.2006.07.016
Wang, G., Guan, D., Zhang, Q., Peart, M.R., Chen, Y., Peng, Y., Ling, X., 2014. Spatial patterns of biomass and soil attributes in an estuarine mangrove forest (Yingluo Bay, South China). Eur. J. For. Res. 133, 993–1005. https://doi.org/10.1007/s10342-014-0817-3

Wang, L., Sousa, W.P., Gong, P., Biging, G.S., 2004a. Comparison of IKONOS and QuickBird images for mapping mangrove species on the Caribbean coast of Panama. Remote Sens. Environ. 91, 432–440. https://doi.org/10.1016/j.rse.2004.04.005

Ward, R.D., Friess, D.A., Day, R.H., MacKenzie, R.A., 2016. Impacts of climate change on mangrove ecosystems: a region by region overview. Ecosyst. Health Sustain. 2. https://doi.org/10.1002/ehs2.1211

Werf, G.R. van der, Morton, D.C., DeFries, R.S., Olivier, J.G.J., Kasibhatla, P.S., Jackson, R.B., Collatz, G.J., Randerson, J.T., 2009. CO_2 emissions from forest loss [WWW Document]. Nat. Geosci. https://doi.org/10.1038/ngeo671

Westoby, M., 1998. A leaf-height-seed (LHS) plant ecology strategy scheme. Plant Soil 199, 213–227. https://doi.org/10.1023/A:1004327224729

Woodroffe, C.D., Rogers, K., McKee, K.L., Lovelock, C.E., Mendelssohn, I.A., Saintilan, N., 2016. Mangrove Sedimentation and Response to Relative Sea-Level Rise. Annu. Rev. Mar. Sci. 8, 243–266. https://doi.org/10.1146/annurev-marine-122414-034025

Woodwell, G.M., Hobbie, J., Houghton, R., Melillo, J., Moore, B., Peterson, B., Shaver, G., 1983. Global deforestation: contribution to atmospheric carbon dioxide. Science 222, 1081–1086.

Yakub, M., Omar Ali, M., Bhattacharjee, D.K., 1972. Strength properties of some Bangladesh timber species. Govt. of the People's Republic of Bangladesh, Forest Research Institute, Chittagong.

Yu, L., Gong, P., 2012. Google Earth as a virtual globe tool for Earth science applications at the global scale: progress and perspectives. Int. J. Remote Sens. 33, 3966–3986. https://doi.org/10.1080/01431161.2011.636081

Yu, X., Hyyppä, J., Karjalainen, M., Nurminen, K., Karila, K., Vastaranta, M., Kankare, V., Kaartinen, H., Holopainen, M., Honkavaara, E., Kukko, A., Jaakkola, A., Liang, X., Wang, Y., Hyyppä, H., Katoh, M., 2015. Comparison of Laser and Stereo Optical, SAR and InSAR Point Clouds from Air- and Space-Borne Sources in the Retrieval of Forest Inventory Attributes. Remote Sens. 7, 15933–15954. https://doi.org/10.3390/rs71215809

Zanne, A.E., Lopez-Gonzalez, G., Coomes, D.A., Ilic, J., Jansen, S., Lewis, S.L., Miller, R.B., Swenson, N.G., Wiemann, M.C., Chave, J., 2009. Data from: Towards a worldwide wood economics spectrum. https://doi.org/10.5061/dryad.234

Zhang, H., John, R., Peng, Z., Yuan, J., Chu, C., Du, G., Zhou, S., 2012. The Relationship between Species Richness and Evenness in Plant Communities along a Successional Gradient: A Study from Sub-Alpine Meadows of the Eastern Qinghai-Tibetan Plateau, China. PLoS ONE 7, e49024. https://doi.org/10.1371/journal.pone.0049024

Zhang, Y., Chen, H.Y.H., Reich, P.B., 2012. Forest productivity increases with evenness, species richness and trait variation: a global meta-analysis: *Diversity and productivity relationships*. J. Ecol. 100, 742–749. https://doi.org/10.1111/j.1365-2745.2011.01944.x

Zhang, Y., Chen, H.Y.H., Taylor, A.R., 2017. Positive species diversity and above-ground biomass relationships are ubiquitous across forest strata despite interference from overstorey trees. Funct. Ecol. 31, 419–426. https://doi.org/10.1111/1365-2435.12699

Zhang, Y., Duan, B., Xian, J., Korpelainen, H., Li, C., 2011. Links between plant diversity, carbon stocks and environmental factors along a successional gradient in a subalpine coniferous forest in Southwest China. For. Ecol. Manag. 262, 361–369. https://doi.org/10.1016/j.foreco.2011.03.042

Zhong, Y., Sun, Y., Xu, M., Zhang, Y., Wang, Y., Su, Z., 2017. Spatially destabilising effect of woody plant diversity on forest productivity in a subtropical mountain forest. Sci. Rep. 7, 9551. https://doi.org/10.1038/s41598-017-09922-7

Zhu, Y., Liu, K., Liu, L., Wang, S., Liu, H., 2015. Retrieval of Mangrove Aboveground Biomass at the Individual Species Level with WorldView-2 Images. Remote Sens. 7, 12192–12214. https://doi.org/10.3390/rs70912192

Acknowledgement

First of all, I am very grateful to almighty Allah for successfully completion of this thesis work.

I would like to express my sincere gratitude and profound appreciation to my honorable supervisor Professor Mamoru Kanzaki for his continuous supports, guidance, inspiration and thoughtful suggestions in completion of my Ph.D. thesis.

Besides my advisor, I am grateful to my reviewers Professor Akira Osawa and Professor Kauro Kitajima, for their meticulous review, thoughtful comments and suggestions which gave the thesis in an improved shape.

I really thank to the Ministry of Education, Culture, Sports, Science and Technology (MEXT) for funding my study in Japan and the Graduate School of Agriculture, Kyoto University for the fulfillment of my study. I am also thankful to United State Agency for International Aid (USAID) for funding in Sundarbans Reserved Forest Carbon Inventory and in my fellowship programs in NASA Goddard Space Flight Center.

My sincere thanks also go to my fellow colleagues, Dr. Lola E. Fatoyinbo Agueh, Dr. David Lagomasino, and Dr. Lee Seung Kuk Earth Sciences Remote Sensing, NASA Goddard Space Flight Center, Greenbelt, MD, USA for their technical support over the last two years and for making my life easy during my fellowship program. I would like to acknowledge Prof. A.K. Fazlul Hoque Prof. Enamul Kabir and Prof. Dr. Nabiul Islam Khan, Forestry and Wood Technology Discipline, Khulna University for their inspirations and suggestions.

I am very grateful to Integrated Protected Areas Co-management, USAID Bangladesh, and Bangladesh Forest Department for selecting me, as a team member of Sundarbans Reserved Forest Carbon Assessment and Forest Inventory-2009-2010 (SRF C Inventory-2009-2010) and for sharing the data for further studies. Special thanks to all the team members of SRF C Inventory-2009-2010 for their hard jobs for successful completion of the inventory work within five months. Special thanks to Imran Ahmad, Assistant Chief Conservator of Forest Bangladesh Forest Department, and Dr. Daniel Donato, Research Ecologist, USDA Forest Service for their valuable suggestions, encouragement and helping in data management.

Enormous gratitude to SilvaCarbon Bangladesh, US Forest Service International Program, USAID and Bangladesh Forest Department officials, especially, Md Ashraful Islam, Parsia Nargis, Elise deRiel, Henry Matiheu and Md. Zaheer Iqbal for their valuable support and suggestions during my fellowship programs activities in Bangladesh and NASA Goddard Space Flight Center.

I appreciate the supports and helps I received from all my friends and well-wishers here in Kyoto and my fellow lab mates at Laboratory of Forest Resources and Society and Laboratory of Environment and Tropical Forest Resources for making my life in Kyoto, Japan like a family member over the last three years.

Finally, but not last, my deepest gratitude goes to my beloved parents, brothers, sisters and all my well-wishers for their endless love, prayers, and encouragement. Most importantly, I am more than grateful to my wife Tasmia Nowrin for supporting me spiritually throughout writing this thesis and my life in general.